INFORMATION TO USERS

This reproduction was made from a copy of a manuscript sent to us for publication and microfilming. While the most advanced technology has been used to photograph and reproduce this manuscript, the quality of the reproduction is heavily dependent upon the quality of the material submitted. Pages in any manuscript may have indistinct print. In all cases the best available copy has been filmed.

The following explanation of techniques is provided to help clarify notations which may appear on this reproduction.

1. Manuscripts may not always be complete. When it is not possible to obtain missing pages, a note appears to indicate this.

2. When copyrighted materials are removed from the manuscript, a note appears to indicate this.

3. Oversize materials (maps, drawings, and charts) are photographed by sectioning the original, beginning at the upper left hand corner and continuing from left to right in equal sections with small overlaps. Each oversize page is also filmed as one exposure and is available, for an additional charge, as a standard 35mm slide or in black and white paper format.*

4. Most photographs reproduce acceptably on positive microfilm or microfiche but lack clarity on xerographic copies made from the microfilm. For an additional charge, all photographs are available in black and white standard 35mm slide format.*

***For more information about black and white slides or enlarged paper reproductions, please contact the Dissertations Customer Services Department.**

U·M·I Dissertation Information Service

University Microfilms International
A Bell & Howell Information Company
300 N. Zeeb Road, Ann Arbor, Michigan 48106

Syed, Danyal Barkat

COMPARISON BETWEEN YEAST OROTATE - AND HYPOXANTHINE/GUANINE-PHOSPHORIBOSYLTRANSFERASE ACTIVITIES: NMR STUDIES OF THE CONFORMATIONS OF FREE AND BOUND 5'-PHOSPHORIBOSYL - ALPHA - 1 - PYROPHOSPHATE. KINETIC INHIBITION STUDIES WITH CHROMIUM(III) PYROPHOSPHATE

City University of New York PH.D. 1986

PLEASE NOTE:

In all cases this material has been filmed in the best possible way from the available copy. Problems encountered with this document have been identified here with a check mark __✓__.

1. Glossy photographs or pages _____
2. Colored illustrations, paper or print _____
3. Photographs with dark background _____
4. Illustrations are poor copy _____
5. Pages with black marks, not original copy _____
6. Print shows through as there is text on both sides of page _____
7. Indistinct, broken or small print on several pages __✓__
8. Print exceeds margin requirements _____
9. Tightly bound copy with print lost in spine _____
10. Computer printout pages with indistinct print _____
11. Page(s) _____ lacking when material received, and not available from school or author.
12. Page(s) _____ seem to be missing in numbering only as text follows.
13. Two pages numbered _____. Text follows.
14. Curling and wrinkled pages _____
15. Dissertation contains pages with print at a slant, filmed as received _____
16. Other _____

_____

_____

Comparison Between Yeast Orotate - and Hypoxanthine/Guanine-Phosphoribosyltransferase Activities: NMR Studies of The Conformations of Free and Bound 5'-Phosphoribosyl - α - 1 - Pyrophosphate. Kinetic Inhibition Studies with Cr(III) Pyrophosphate.

by

DANYAL B. SYED

A dissertation submitted to the Graduate Faculty in Biochemistry in partial fulfillment of the requirements for the degree of Doctor of Philosophy, The City University of New York.

1986

This manuscript has been read and accepted for the Graduate Faculty in Biochemistry in satisfaction of the dissertation requirement for the degree of Doctor of Philosophy.

February 14, 1986
Date

Chair of Examing Committee

February 14, 1986
Date

Executive Officer

L. Davenport

Supervisory Committee

The City University of New York

ABSTRACT

Comparison Between Yeast Orotate and Hypoxanthine/Guanine Phosphoribosyltransferase Activities: NMR Studies of the Conformations of Free and Bound Phosphoribosyl Pyrophosphate. Kinetic Inhibitions Studies with Cr(III) Pyrophosphate.

By

Danyal B. Syed

Advisor: Dr. Donald L. Sloan

Both the orotate phosphoribosyltransferase (OPRTase) and the hypoxanthine/guanine phosphoribosyltransferase (HGPRTase) activities from yeast have been well characterized in our laboratory. The kinetic and metal ion activation studies carried out on these enzymes thus far have contributed a great deal towards the understanding of underlying mechanisms. Although M(II)-PRibPP has been established to be the true substrate for both of these enzymes, the two activities differ in their kinetic mechanism by which the phosphoribosyl transfer reaction occurs with the appropriate base. This difference in kinetic mechanisms led me to believe that the M(II)-PRibPP might have a different conformation on the active sites of these enzymes as compared to its conformation in solution. This thesis describes the elucidation of Mn(II)-PRibPP conformations free in solution as well as bound to OPRTase and HGPRTase from yeast using ^{1}H and ^{31}P magnetic relaxation rate measurements. The eight PRibPP metal-to-nucleus distances determined were used to resolve the conformation of the binary Mn(II)-PRibPP, ternary OPRTase-Mn(II)-

PRibPP and HGPRTase-Mn(II)-PRibPP complexes. In the case of the binary, Mn(II)-PRibPP complex, all the phosphates interact with the metal ion. The α - and β -phosphates were observed to be directly co-ordinated, in a bidentate fashion, while 5'-PO_4 might be co-ordinated via axial oxygen. In this conformation the β-position of the C-1 carbon of ribose is essentially unavailable for on-line substitutions. In the case of the OPRTase-bound Mn(II)-PRibPP, the Mn(II)-to- α and to- β - phosphate interactions were still defined as bidentate but could also occur via axial oxygen. The enzyme-bound ribose ring still exhibited a desired 2'-endo puckered conformation but was further away from the metal ion, as the 5'-phosphate lost its inner sphere axial co-ordination on OPRTase. This new position resulted in an increase of 0.8 $\mathring{A}$ in the metal ion to ribose distance (as measured from the center of the ring). In the case of the HGPRTase-Mn(II)-PRibPP complex, the α - and β - phosphates also remained bidentate. However, the 5'-phosphate metal distance more closely resembled the distance of Mn(II)-PRibPP than did this distance on OPRTase. Moreover, the calculated 5'-phosphate metal ion distance was consistent with a highly distorted direct co-ordination. The ribose ring of HGPRTase-bound PRibPP was also observed to position itself further away from the metal ion by a distance of 0.7 $\mathring{A}$. The new PRibPP conformation thus created would seem to allow for on-line displacement at the HGPRTase active site.

Also described in this dissertation are the inhibition studies carried out on these enzyme activities with Cr(III)PP_i and Na(I)PP_i in the presence of 1-2mM Mg(II) ion. These studies have revealed that Cr(III)PP_i is a substrate for the reverse reaction catalyzed by OPRTase but only in the presence of Mg(II) ion, suggesting that there is a requirement

for a divalent metal ion other than that complexed to PP_i and/or PRibPP. $Cr(III)PP_i$ exhibited mixed-type inhibition for the OPRTase catalyzed forward reaction, whereas the forward reaction catalyzed by HGPRTase was not inhibited, indicating that for HGPRTase the $Cr(III)PP_i$ may not bind or bind very loosely. Based upon the elucidated conformations of PRibPP when bound to these enzymes, upon inhibition studies with $Cr(III)PP_i$ and $Na(I)PP_i$ in presence of Mg(II) and upon previous kinetic and metal activation studies, I propose that one of the difference between the HGPRTase and OPRTase catalyzed reactions is how these enzymes make use of several metal-ions at their active sites to perform aspects of the catalysis.

During my unsuccessful attempt to prepare the Cr(III)-PRibPP complex, I have characterized the degradation products of PRibPP at acidic pH in presence of Cr(III) ion.

أَنَّ اللّٰهَ يَعْلَمُ مَا فِي السَّمٰوٰتِ وَمَا فِي الْأَرْضِ ط

المجادلة ع
پارہ ۲۸
سورۃ ۵۸

"Allah knowth all whatever is in heavens and whatever is in earth."

Chapter: 28

Verse: 58

Al Quraan

A C K N O W L E D G E M E N T S

This dissertation work is dedicated to the sweet memory of my mother, Munir Sultana, who died of cancer on January 31, 1978.

I am thankful to the members of my thesis committee, Dr. Sharon Cosloy, Dr. Lesley Davenport, Dr. Morton Glantz, Dr. Horst Schulz and Dr. William Sweeney for their cooperation and guidance throughout the course of this work. I express my gratitude to Dr. Denise Frechet for her help in the performance of NMR experiments.

I would also like to thank Olivia Mojar for her help in sodium and potassium determination on samples of Cr(III)PP_i by flame photometry and her constant encouragement, and to Susan Hess, Linda Ali, Aybar D. Batista, and Cong Yan for their valuable suggestions. I extend my special thanks to Roslyn Strauss for lending me purified orotate phosphoribosyltransferase (OPRTase) for use in NMR experiments and also letting me use some of the programs for analyzing kinetic data developed by her, to Robert Ashton for also providing purified OPRTase and for writing a program for the T_1 determination on his computer and letting me use it, and to Daisy Mojar for typing this manuscript.

I appreciate with great sense of gratitude the patience exhibited by my wife and my daughters and for their encouragement which helped me to complete this work successfully.

Finally, I would like to thank my mentor, Dr. Donald L. Sloan for his unsurpassed guidance, patience, persistence, perseverance, support and encouragement that he has shown during this work.

TABLE OF CONTENTS

TABLE OF CONTENTS

LIST OF TABLES

LIST OF FIGURES

LIST OF FIGURES

BACKGROUND

A living system in its entirety as well as at the cellular level is a highly improbable entity regulating chemical processes at a steady state position far removed from equilibrium (Zubay, 1983). In this regulation, concentrations of enzymes, their substrates and products as well as activators and inhibitors are very important. A living system, complex as it appears, is unique in preserving simplicity in having a common substrate for different metabolic reactions that are similar by their nature. So, if adenosine triphosphate (ATP) is a common substrate for kinases in phosphoryl transfer reactions, then 5'-phosphoribosyl α-1-pyrophosphate (PRibPP) serves the same role in phosphoribosyl transfer reactions catalyzed by phosphoribosyltransferases (PRTases). This commonness of a substrate in these reactions is well preserved throughout evolution. In order for such a compound to be apportioned through these various metabolic pathways, it is necessary that its intracellular concentration be closely regulated.

PRibPP was first discovered by Kornberg et al., (1955a). It is an essential substrate in the synthesis of purine, pyrimidine and pyridine nucleotides. Fox, et al., (1971) and Becker, et al., (1979) have shown that PRibPP plays a critical role in the de novo synthesis of purines in man. The synthesis of PRibPP is catalyzed by PRibPP synthetase (E.C. 2.7.6.1) in a reaction (given below) involving ATP and ribose-5'-phosphate and requires Mg(II) and inorganic phosphate.

$$\text{Ribose-5-Phosphate} + \text{ATP} \rightleftharpoons \text{PRibPP} + \text{AMP} \qquad (1)$$

In intact cells, increased availability of PRibPP correlates with higher levels of de novo purine synthesis (Brosh, et al., 1976; Bashkin, et al., 1978 and Becker, 1976) and decreased availability of PRibPP with lower levels of de novo purine synthesis (Kelley, et al., 1970 and Bagnara, et al., 1974). The rates of de novo and salvage purine synthesis decrease by approximately 80% and 60% respectively when normal human lymphoblasts are starved for an essential amino acid (Boss and Erbe, 1982). Amino acid starvation decreased the intracellular PRibPP and ribose-5'-phosphate concentrations by approximately 40% but neither the specific activities of PRibPP synthetase and glutamine amidophosphoribosyltransferase nor the intracellular concentration of purine nucleotides and inorganic phosphate (P_i) changed significantly (Boss and Erbe, 1982). In mutant cells having either higher PRibPP synthetase activity or hypoxanthine:guanine phosphoribosyltransferase (HGPRTase) deficiency, intracellular PRibPP concentrations decreased by less than 15% during amino acid starvation and de novo purine synthesis decreased less than in normal cells. These and similar other observations made by Boss (1984) suggest that amino acid starvation decreases purine synthesis by decreasing the generation of PRibPP from glucose. Ribose-5'-phosphate, the precursor of PRibPP, has also been proposed to be an important factor in controlling the rates of de novo purine synthesis (Becker, 1976 and Becker, et al., 1979). Pilz, et al., (1984) have now demonstrated that endogenous ribose reutilization for purine synthesis is important when either glucose availability is limited or synthesis is stimulated. They also showed that in the absence of glucose, exogenous purine nucleotide when included in the medium restored the intracellular concentration of ribose-5'-phosphate and purine nucleotides

to almost 100% and rates of purine synthesis to 50-75% to those of 10mM glucose. When peripheral blood lymphocytes were activated by phytohemagglutinin, the production of ribose-5'-PO_4 increased, resulting in the enhanced production of PRibPP and increased rates of de novo purine synthesis. From their recent studies on amino acid starved human lymphoblasts, Pilz and Boss (1985) have concluded that the non-oxidative pentose phosphate pathway is the major source of phosphoribosylpyrophosphate for purine nucleotide synthesis (Fig. 1). Their conclusion does not exclude the possibility that increasing the carbon flow through oxidative pentose phosphate pathway can increase the PRibPP concentration and rates of purine synthesis (Raivio, et al., 1981; Yeh and Phang, 1983). On the other hand, parameters like the NADP/NADPH ratio as well as fructose 2, 6 bi-phosphate level, that independently regulate the carbon flow through the two pentose phosphate shunts, may determine the extent of contribution by each path to PRibPP synthesis (Eggleston and Krebs, 1974; Blackmore and Shuman, 1982). The NADP/NADPH ratio may be affected by the pathway leading to the synthesis of NAD through the use of nicotinate phosphoribosyltransferase or one of the other pyridine PRTases. Therefore, common pathways must control mechanisms of NAD and purine nucleotides biosynthesis.

PRibPP DEGRADATION

Phosphoribosyltransferases degrade PRibPP. These enzymes are widely distributed in nature and catalyze the transfer of the ribose-5'-phosphate moiety of PRibPP to a nitrogenous base. In the de novo synthesis of purine nucleotides, the nitrogen base is either the amide of glutamine of ammonia (Hartman, 1963). Free bases serve as nitrogen donors in reactions leading to the synthesis of pyrimidine nucleotides

Figure 1. Synthesis of PRibPP by the oxidative and non-oxidative pentose phosphate pathways. Glucose-6-phosphate may be converted to PRibPP by either the oxidative or non-oxidative pentose phosphate pathway. When it is converted by the oxidative pentose phosphate pathway the carbon atom in position 1 is lost as CO_2

(From Boss and Pilz, 1985)

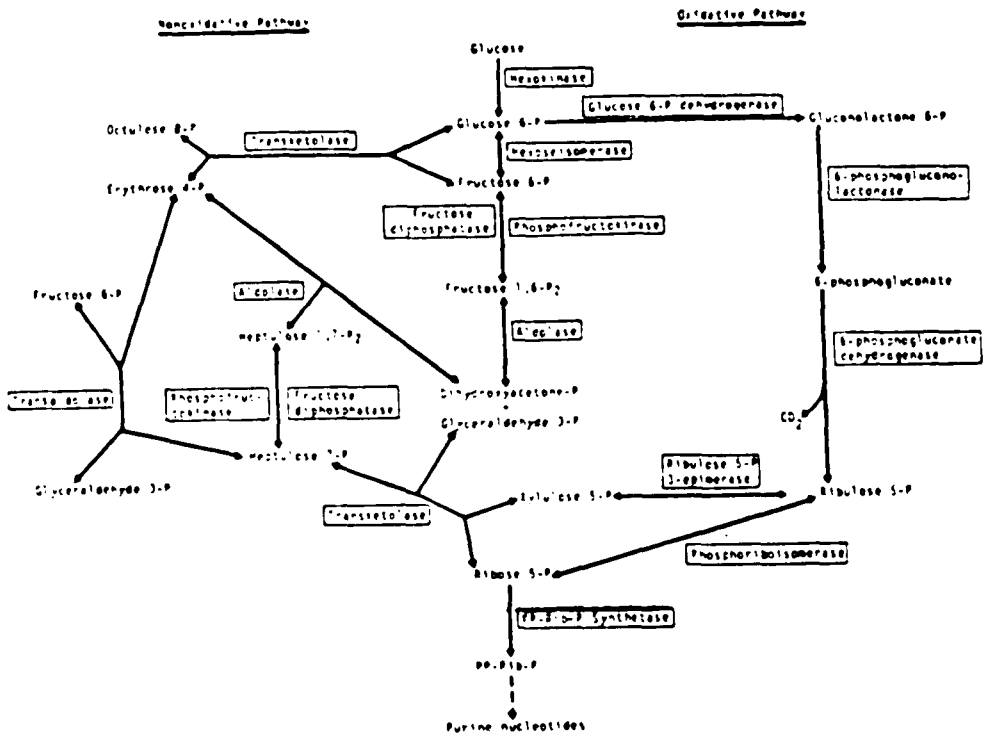
Oxidative Pathway
Glucose
Hexokinase
Glucose 6-P
Glucose 6-P dehydrogenase
Gluconolactone 6-P
Octulose 8-P
Transketolase
Hexoseisomerase
Fructose 6-P
Erythrose 4-P
6-phosphogluconolactonase
Fructose diphosphatase
Phosphofructokinase
Fructose 1,6-P2
6-phosphogluconate
Aldolase
Fructose 6-P
Heptulose 1,7-P2
6-phosphogluconate dehydrogenase
Dihydroxyacetone-P
Glyceraldehyde 3-P
CO2
Heptulose 7-P
Ribulose 5-P 3-epimerase
Glyceraldehyde 3-P
Ribulose 5-P
Transketolase
Ribose 5-P
Phosphoribosomerase
Purine nucleotides

(Kornberg, et al., 1955) and purine nucleotides using the salvage pathway (Korn, et al., 1955). In addition, nicotinic acid or quinolinic acid serves as the nitrogen base for NAD synthesis [Preiss, et al., 1958; Nishizuka and Hayaishi, 1963), anthranilate for tryptophan synthesis (Crowly, 1964) and ATP for histidine synthesis (Wegman, et al., 1965). All of the above reactions are shown in Figure 2 and can be represented by a general equation given below:

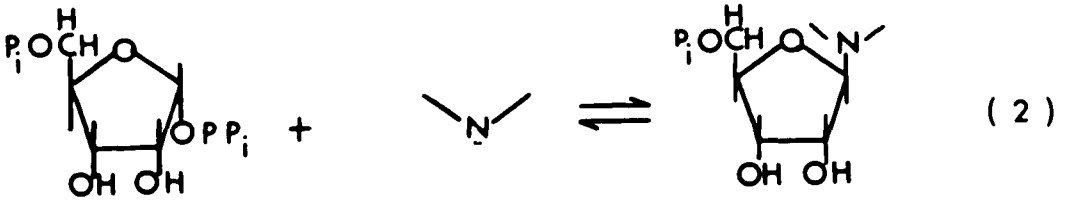

(2)

Each of the phosphoribosyltransferase and the PRibPP amidotransferases (ATase) have characteristics which are unique and other characteristics which are shared by these enzymes as a class. A wealth of information on the kinetics, genetics, biochemical and other aspects of these enzymes from plethora of sources has been gathered and is reviewed briefly in the following pages.

DISORDERS OF PRTase IN MAN

The importance of phosphoribosyltransfer enzymes and PRibPP metabolism in the normal functioning of living cells can be realized by the disorders that result in man when these reactions are not normal. It is now fairly well understood that abnormally high uric acid levels in

Figure 2. Summary of the reactions in which PRibPP (in center of circle) serves as key substrate. These reactions are catalyzed by many PRTase and amidotransferase. Lined along the outside of the circle are the second substrates for these reactions. Numbers on arrows represent the individual enzymes as follows:

1. Nicotinate phosphoribosyltransferase
2. Quinolinate phosphoribosyltransferase
3. Nicotinamide phosphoribosyltransferase
4. Hypoxanthine:Guanine phosphoribosyltransferase
5. Adenine phosphoribosyltransferase
6. Glutamine phosphoribosyltransferase
7. ATP phosphoribosyltransferase
8. Anthranilate phosphoribosyltransferase
9. Uridine (Uracil) phosphoribosyltransferase
10. Orotate phosphoribosyltransferase

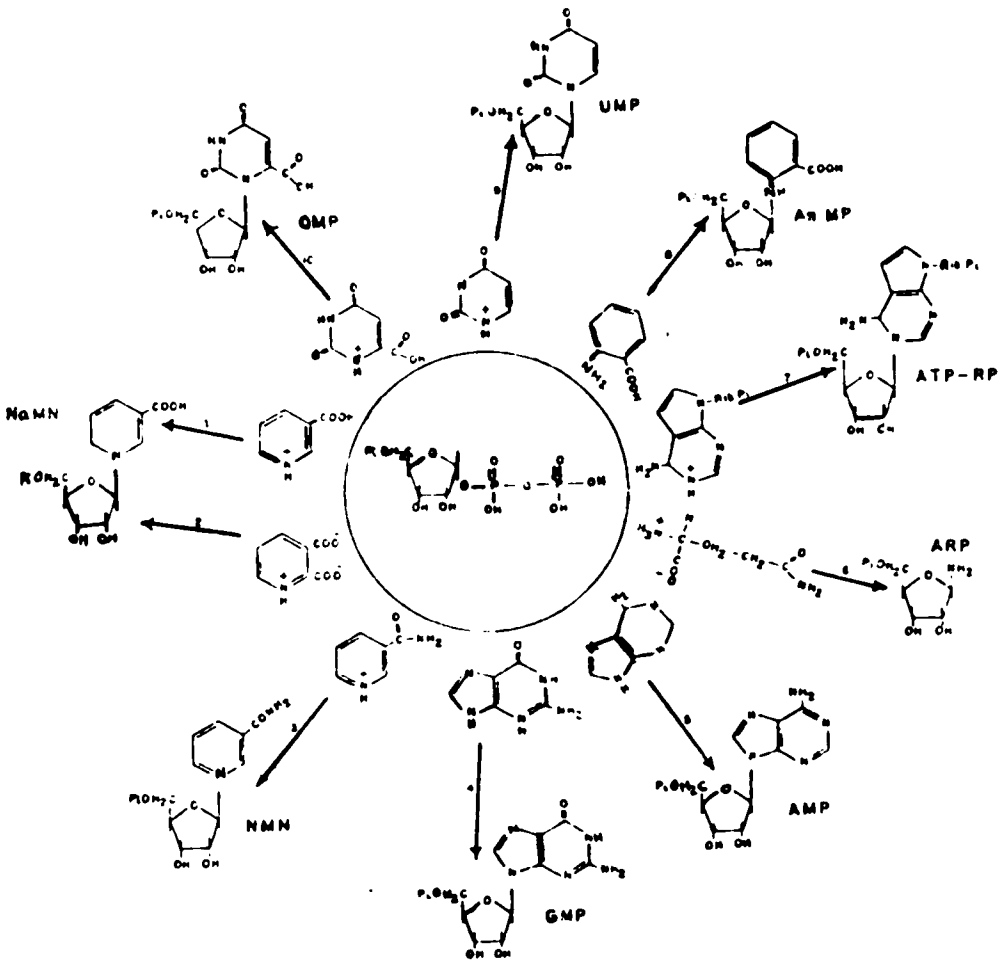
UMP
OMP
AnMP
ATP-RP
NaMN
ARP
NMN
AMP
GMP

blood are due to many factors. The enzymes PRibPP synthetase, PRibPP amidotransferase and HGPRTase have all been implicated for hyperuricemia and gout (Seegmiller, et al., 1967). Hyperuricemia has been shown to be due to an increased rate of de novo purine biosynthesis brought about by an increase in PRibPP amidotransferase activity. This may be the result of either an abnormal PRibPP amidotransferase itself or an increased level of PRibPP cellular pool which activates ATase activity. A partial HGPRTase deficiency (residual activity 30% of normal) as well as PRibPP synthetase hyperactivity enhances the availability of PRibPP which in turn stimulates de novo purine synthesis (Boer, et al., 1976) resulting in overproduction of uric acid and thus hyperuricemia (Seegmiller, et al., 1976). A complete deficiency of HGPRTase (residual activity less than 1%), on the other hand leads to the Lesch-Nyhan syndrome, a serious metabolic disorder characterized by spasticity, mental retardation, megaloblastic bones and compulsive self mutilation tendencies (Lesch and Nyhan, 1964). It has been demonstrated that adenine phosphoribosyltransferase (APRTase) levels increase in patients with higher concentrations of PRibPP and with HGPRTase deficiency. This is understandable since APRTase is responsible for the salvage synthesis of adenosine monophosphate (Fox and Kelley, 1971). However, higher levels of APRTase activity in erythrocytes of normal newborn infants have been observed in addition (Borden, et al., 1974). Deficiencies in APRTase activity have been observed in patients with gout and hyperuricemia (Debarre, et al., 1974). Interestingly, 2, 8 dihydroxyadenine urolithiasis is characteristic of patients with severe APRTase deficiency (Van Ackar and Simmonds, et al., 1977). The 2, 8 dihydroxyadenine in these patients is produced from accumulated adenine by the

action of xanthine oxidase (E.C. 1.2.3.2.) even though adenine is a poor substrate of this latter enzyme.

Deficiencies of orotate phosphoribosyltransferase (OPRTase) and orotate decarboxylase (ODCase) activities are characteristics of orotic aciduria, a potentially lethal inborn error of pyrimidine metabolism in man. Two variant forms of disease have been described: one having the deficiency of both OPRTase and ODCase (Type I) and other lacking ODCase while exhibiting elevated levels of OPRTase, (Type II) (Worth, et al., 1974). This disorder manifests itself as severe anemia, retardation and excessive orotic acid in urine (Smith, et al., 1972). Increased orotic acid secretion has been observed during drug treatment (Fox, et al., 1971), human pregnancy (Wood and O'Sullivan, 1973) and in some of the combined immunodeficiency disorders (Mills, et al., 1979). Malayappa, et al., (1985) have examined the excretion levels of orotic acid during the starvation and refeeding of normal men, as a marker of the pyrimidine pathway. They observed that orotic acid excretion levels decreased significantly during starvation and increased during refeeding. Orotic acid has been shown to reduce uric acid formation in gouty patients (Delbarre and Auscher, 1963). Elevated levels of PRibPP have been observed to enhance OPRTase activity. Thus, the pyridine, pyrimidine and purine nucleotide biosynthetic pathways are closely related and affected by PRibPP intracellular concentration.

Gershon and Fox (1974) have observed that administration of megadoses of nicotinic acid produced hyperuricemia without affecting uric acid levels in urine. They also observed that increasing the levels of nicotinic acid which stimulated NAD synthesis, decreases

PRibPP concentration in human erythrocytes. However, de novo purine synthesis is stimulated by nicotinamide in rat liver and kidney probably via production of PRibPP from ribose-5'-phosphate through the activation of the hexose monophosphate shunt (Shuster and Abraham, 1959). On the other hand, quinolinic acid, another pyridine base, has been hypothetically linked to neurodegenerative disorders such as Huntington's disease and epilepsy. Foster, et al., (1985) have observed that quinolinate phosphoribosyltransferase (QPRTase) activity is higher in the caudate (the tail end of medulla oblongata), in HD post mortem patients. Although the Km values for both quinolinic acid and PRibPP were similar in HD and normal caudate, the Vmax values in HD caudate were elevated. This suggests that QPRTase activity increases in response to specific degenerative events. Further elucidation of underlying mechanism of this elevation in neuropathological conditions is needed.

All the above described findings have lead to the conclusion that common control mechanisms of pyridine, pyrimidine and purine nucleotides biosynthetic pathways must be involved.

GENETIC ASPECTS

The nucleotide sequences of most of the phosphoribosyltransferases and PRibPP synthetase genes from a variety of sources have been elucidated and the structural genes for these enzymes, particularly HGPRTase have been mapped on the x-chromosomes (Yen, et al., 1978; Caskey and Kruh, 1979; Mantsälä and Zalkin, 1984; Richardson, et al., 1983; Dush, et al., 1985). Some of these enzymes have been reported to exist in isozymic forms, eg. HGPRTase exists in isozymic forms in erythrocytes (Olson, et al., 1978), in hemolysates (Ghangas, et al., 1977), enterobacteria (Hochstadt

1978), yeast (Nagy, et al., 1977), hamster (Olsen, et al., 1974) and rabbit brain (Kameda, 1975). Four unique structural variants of human hypoxanthine:guanine phosphoribosyltransferase have now been isolated from unrelated patients who presented with gout and a partial deficiency of HGPRTase activity (Wilson, et al., 1981 and Wilson, et al., 1982). These mutant enzymes have been termed HGPRTase London, HGPRTase Toronto, HGPRTase Ann Arbor and HGPRTase Munich. The enzyme deficiency states associated with London, Toronto and Ann Arbor alleles are caused primarily by decreased concentrations of HGPRTase protein. The deficiency in HGPRTase activity associated with the Munich allele in contrast, results entirely from abnormalities from enzyme function. Steyn and Harley (1984) have reported yet another variant of HGPRTase, HGPRTase Capetown. In this later variant the decreased activity is associated with substrate inhibition by hypoxanthine and guanine. The substrate acts with enzyme PP_i complex to form a ternary enzyme PP_i hypoxanthine/guanine dead-end complex. The study of such variants has added to our understanding of the kinetic mechanism of this enzyme. On the other hand, the wealth of genetic knowledge that has accumulated over the past few years may help to correct genetic defects caused by the absence or decreased activity of these enzymes via genetic engineering techniques.

BIOCHEMICAL ASPECTS

A feature common to all the phosphoribosyltransferases and amidotransferases from different sources studied thus far, is the requirement for a divalent metal ion activator, most commonly magnesium ion for catalytic function. Different PRTases from different sources exhibit a wide range in molecular weights, Km values for PRibPP and Km values for nitrogenous

bases, as summarized in Table 1. Strictly speaking, one cannot really compare these results due to the fact that these enzymes are in different states of purity and are from different sources. Moreover, evolutionary factors may contribute to some of the structural and kinetic dissimilarities. However, even when a single source such as yeast is considered, these enzymes are strikingly different with respect to their Km values. Moreover, different PRTase catalyze their reactions through different kinetic mchanisms.

Earlier studies on HGPRTase from human erythrocytes, as reviewed by Ismande, et al., (1961), suggested a ping pong bi bi kinetic mechanism based on the parallel double reciprocal initial velocity patterns as well as on the initial burst of IMP formation upon the addition of hypoxanthine to an enzyme, pre-incubated with and then purified from PRibPP and Mg(II). Henderson, et al., (1968) proposed a sequential mechanism for the enzyme even though initial velocity double reciprocal plots were composed of sets of parallel lines. Their argument was that the K_i [PRibPP] is much smaller than Km [PRibPP] (the ratio of these two parameters = less than 0.1) which would result in an apparent parallel pattern of lines. Later, Krenitsky and Papaioannou (1969) re-examined the kinetics of human HGPRTase catalyzed reaction using purified preparation and similar conditions (optimum Mg(II) concentration) and obtained the same IMP formation burst and sets of parallel patterns of initial velocity double reciprocal plots, but the K_i[PRibPP]/Km[PRibPP] was determined to be greater than 0.1. This suggested to them that under the optimum Mg(II) concentration, PP_i departure precedes IMP synthesis. Giacomello and Salerno (1978) performed a detailed analysis of both the forward and reverse reactions catalyzed by human HGPRTase. They characterized

Table 1 Properties of Phosphoribosyl Transfer Enzymes

Enzyme	Km(uM) substrate	Km(uM) PRibPP	M.W.	Source	Reference
APRTase	20	150	40,000	E. Coli	Hochstadt (1971)
	140	6	34,000	Human	Thomas (1973)
	0.9	5	22,000	Rat Liver	Groth (1978)
	69	32	50,000	Yeast	Nagy (1977)
Anthranilate PRTase	8.3	6.7	87,000	Salmonella	Henderson (1970)
	-	-	67,000	Enterobacteria	Largen (1975)
ATP-PRTase	430	56	34,000	S. Typhimurium	Whitfield (1971)
	99	15	216,000	S. Typhimurium	Morton & Parsons (1976)
	-	-	67,000	E. Coli	Tebar (1978)
HGPRTase	0.52 (H)*	5.3	80,000	Hamster	Olsen & Milman (1974)
	1.1 (G)**	5.3	80,000	Hamster	Olsen & Milman (1974)
		55	81,000	Mammalian Liver	Hughes (1975) & Hagen (1973)
	7.7 (H)*	66	100,000	Human	Giacomello & Salerno (1978) Holden & Kelley (1978)

Table 1 (Continued) Properties of Phosphoribosyl Transfer Enzymes

Enzyme	Km(uM) substrate	Km(uM) PRibPP	M.W.	Source	Reference
HGPRTase	120 (H)*	200	-	Enterobacteria	Hochstadt (1978)
	2.5 (G)**	100	-	Enterobacteria	Hochstadt (1978)
	23 (H)*	50	51,000	Yeast	Schmidt (1979)
	18 (G)**	50	51,000	Yeast	Schmidt (1979)
Nicotinamide PRTase	2.6	35.7	-	Rat Liver	Dietrich (1972)
	-	3.8	-	Rat Erythrocytes	Lin (1972)
Nicotinate PRTase	0.5	5	86,000	Human	Niedel & Dietrich (1973)
	1.0	50	-	Beef Liver	Ismande & Handler (1961)
	1.85	7.7	-	Yeast	Kosaka (1977)
OPRTase	35	38	40,000	Yeast	Victor (1979)
	2	16	58,000	Ascites	Kavipurapu & Jones (1976)
	3.6	-	-	Hepatoma	Hoffman & Sweeney (1973)
Quinolinate PRTase	12	45	68,000	Castor Bean	Mann & Byerrum (1974)

Table 1 (Continued Properties of Phosphoribosyl Transfer Enzymes

Enzyme	Km(uM) substrate	Km(uM) PRibPP	M.W.	Source	Reference
Quinolinate PRTase	6	50	205,000	Mammalian Liver	Gholson (1964) & Iwai (1979)
	130	74	165,000	Pseudomonas	Packman & Jacobi (1967)
	133	111	220,000	Alcaligenes	Iwai (1979)
Xanthine PRTase	30	53	42,000	Streptococcus	Miller (1974)
Uracil PRTase	0.7	11	100,000	Pea Seedlings	Bressan (1978)
Amidotrans-ferase	1000	25	210,000	Chicken Liver	Hartman (1963)
	1000	60	200,000	Pigeon Liver	Rowe & Wyngaarden (1968)
	1000	100	95,000	Human Lymp.	Reem (1974)
	530	86	-	Rat Liver	Caskey (1964)
	1250	110	-	Yeast	Satyanarayana & Kaplan (1971)

*(H) = Hypoxanthine

**(G) = Guanine

the role of Mg(II) in these catalyses and formulated a kinetic model for pyrophosphorolysis in which Mg(II) complexes of IMP and PP_i associate with hypoxanthine in a rapid equilibrium random fashion whereas hypoxanthine and Mg(II) PRibPP dissociate from the enzyme in an ordered manner (Giacomello and Salerno, 1979). Employing more sensitive HPLC assay procedure and alternate substrate kinetic analysis, Ali and Sloan (1982) determined that the pure HGPRTase from yeast catalyzes the formation of both IMP and GMP through the use of an ordered bi bi kinetic mechanism and that guanine is a highly preferred substrate over hypoxanthine in the forward reaction. They observed an exchange of label between ^{32}[P] pyrophosphate and PRibPP only, but not between ^{14}[C] hypoxanthine or guanine and their nucleotides (IMP and GMP) suggesting that HGPRTase may exist in part as a phosphoribosyl-enzyme complex in the presence of PRibPP.

Orotate phosphoribosyltransferase co-purifies with orotate decarboxylase from all mammalian tissues and it is now generally believed that OPRTase and ODCase co-exist as a single protein (McClard, et al., 1980). Wild and Belser (1977) have partially purified OPRTase and ODCase as a complex from S. Marcescens. They observed that when separated from the complex, the OPRTase activity was reduced. Upon recombining with ODCase, the original activity was recovered. In the yeast, however, OPRTase and ODCase activities can be separated and studied independently. Umezu, et al. (1971) have purified OPRTase to homogeneity. Based on the initial rate measurements and product inhibition studies of both the forward phosphoribosyl transfer and the reverse pyrophosphorolysis reactions, in the presence of excess magnesium ion, Victor, et al., (1979a) characterized the yeast OPRTase kinetic mechanism to be bi bi ping

pong as illustrated below:

$$E + PRibPP \rightleftharpoons E\text{-}RibP + Pyrophosphate \quad (3)$$

$$E\text{-}RibP + Orotate \rightleftharpoons E + OMP \quad (4)$$

Both of these half reactions require magnesium ion as determined by the label exchange between ^{14}[C]-orotic acid and OMP and between ^{32}[p]-PP_i and PRibPP in the presence and absence of metal ion. The main objection to a ping pong mechanism for PRTase enzymes is the stereochemical argument that double displacement mechanisms usually result in retention of configuration in the products, and phosphoribosyltransferases lead to inversion of configuration (Brashear and Parsons, 1975). Kaneti, et al., (1970) have utilized stereochemical considerations alone to propose an SN_2 mechanism for OPRTase. A ping pong mechanism for this enzyme from yeast has been implicated by Victor, et al., (1979) and these authors proposed a mechanism more complicated than double displacement, namely the formation of carbonium ion intermediate. The isotopic studies of Goitein and his colleagues (1978) also favor the carbonium ion formation by which OMP is formed in yeast.

The nicotinate phosphoribosyltransferase (NaPRTase) catalyzed reaction differs from the OPRTase and HGPRTase reactions in two respects. Nicotinate mononucleotide (NaMN) formation requires ATP and is irreversible, possibly because of the concomittant ATP hydrolysis. In addition, the enzyme does not appear to catalyze reversible bond cleavage between pyrophosphate and the ribose portion of PRibPP in the absence of nicotinic

acid to form a nicotinate-PRTase intermediate. Alternatively, the enzyme may not release PP_i subsequent to the breaking of this bond. Kosaka, et al., (1977), from their initial velocity and product inhibition studies on yeast NaPRTase enzyme and employing computer modeling, proposed sequential addition of substrates to the enzyme as the preferred kinetic mechanism. Hanna, et al., (1983) proposed an ordered uni uni bi ter ping pong kinetic mechanism with the following sequence of events. 1) ATP binds to a distinct site on nicotinate PRTase which leads to the phosphorylation of this site and the release of the product ADP. 2) The phosphorylated nicotinate PRTase then binds PRibPP and nicotinate sequentially at a second site leading to the formation of NaMN and PP_i and to the breaking of the phosphate-enzyme bond. 3) Three products are then released with NaMN and PP_i released randomly prior to the dissociation of phosphate.

METAL ACTIVATION STUDIES

As pointed out earlier, divalent metal ion activators such as magnesium ion or manganese ion are required for all phosphoribosyltransferase-catalyzed reactions (Musick, 1981). Since PRibPP, the common substrate for all of these enzymes, is known to form tight complexes with magnesium ion (Morton and Parson, 1976; Thompson, et al., 1978; Smithers and O'Sullivan, 1982) and Mn(II) (Victor, et al., 1979b) it is generally assumed that these complexes are the true substrates for the PRTase-catalyzed reactions. This was also revealed by the studies of Berlin (1969) and Hochstadt and Stadtman (1971) with adenine phosphoribosyltransferase from Escherichia coli, by studies of Krenitsky, et al., (1969) and Giacomello and Salerno (1978) on HGPRTase from rabbit brain and human erythrocytes respectively, by studies of Kavipurapu & Jones (1976) on OPRTase from ascites, by the work of Morton and Parsons (1976) on ATP phosphoribosyltransferase

from Salmonella typhimurium and from the studies of Henderson, et al., (1970) on the anthranilate synthetase - anthranilate phosphoribosyltransferase complex from Salmonella typhimurium. However, other substrate and metal ion ligations are known to occur as well (Victor, et al., 1979b and Giacomello and Salerno, 1978; Dodin, et al., 1982). Formations of metal ion complexes with enzymes themselves are also known to occur (Kosaka, et al., 1977 and Victor, et al., 1979b). Ali and Sloan (1983) have defined a mechanism through which metal ions activate nucleotide formation by HGPRTase from yeast. 1) A complex is formed between HGPRTase and metal ion. 2) This form of the enzyme then can bind the substrate PRibPP and a second metal ion (in either order) or can bind a metal-PRibPP complex. 3) Thereafter hypoxanthine or guanine binds and products are formed. On the other hand, metal ion activation studies done on OPRTase revealed a biphasic nature for Mg(II) and Mn(II) activation (Victor, et al., 1979b). The interpretation of these results was resolved in terms of an enzyme-metal ion complex and a metal free enzyme both of which catalyze the reaction but at different rates. To conclude, one can easily generalize that the mechanisms of metal ion activation may also differ among the PRTases.

RATIONALE

Although the kinetic and metal ion activation studies carried out on these enzymes thus far have contributed a great deal towards the understanding of underlying mechanisms, no direct information is available on the geometries or the structures of these metal-substrate complexes free in solution and enzyme-bound. In the present work, we present the studies carried out to characterize the interaction of Mn(II) complexes of PRibPP free in solution and bound to HGPRTase and OPRTase from yeast

using ^{1}H and ^{31}P magnetic relaxation rate measurements. This method, which was introduced in 1967 (Mildvan, et al.), is a standard technique for characterizing the conformations of enzyme-bound co-factors and substrates in solution, yielding results similar to those obtained by crystallographic studies (Schultz & Schirmer, 1974; Mildvan and Cohn, 1970; Mildvan, et al., 1976; Sloan and Mildvan, 1974 and 1976). This knowledge of conformations and arrangements of substrates at the active sites then can yield valuable clues to the mechanism of enzymic action (Mildvan, 1974). The choice of yeast OPRTase and yeast HGPRTase was made in order to have these studies carried out on representative phosphoribosyltransferases from pyrimidine and purine pathways from the same source. Both of these enzymes have been purified and well characterized in our laboratory (Victor, et al., 1979a and 1979b; Ali and Sloan, 1982 and 1983) and therefore became our natural choice.

The second part of the work presented here deals with the effect of Cr(III)PP_i complex on the kinetics of these two enzymes and describes our attempt to prepare a Cr(III)PRibPP complex. Hunt and Plane (1954) have observed that the rate of exchange of inner sphere water ligands for Cr(III) is 2-5 x 10^{-6} sec^{-1} at 27°C, depending on the ionic strength. If one compares this rate with the inner sphere water ligands of Co(II), Ni(II), Mn(II) and Mg(II), one finds that the Cr(III) rate is many times slower (10^{10} - 10^{13} times). The chelates of Cr(III) dissociate slowly as well. Therefore, 1:1 complexes of Cr(III) and nucleotides have been prepared by many investigators and used either as substrates or dead-end inhibitors in the kinetic studies of various enzymes associated with phosphoryl transfer or pyrophosphorolytic reactions. All this work has been reviewed elsewhere (Cleland, 1982). Since PP_i is one of the pro-

ducts of the phosphoribosyltransferase catalyzed reactions, we expected Cr(III)PP_i to be either an inhibitor or a substrate for such reactions. We also hoped to determine if these complexes could be used in the future as probes to elucidate further the active site geometry by NMR relaxation rate measurements of ternary complexes such as Cr(III)PP_i - E - mononucleotide. We have shown also that one cannot prepare a Cr(III) -PRibPP complex by employing techniques used generally for preparing Cr(III)-nucleotide complexes (Cleland, 1982, 1979).

EXPERIMENTAL PROCEDURES

MATERIALS

Tetra sodium 5'-phosphoribosyl - α -1-pyrophosphate (PRibPP); $MnCl_2 \cdot 4H_2O$ and Trizma base were supplied by Sigma Chemical Company, where as Chelex 100, AG 50W X-4 H^+ form 100 - 200 mesh, Sephadex G-10, and AG1 X-4 Cl^- form resins for various column chromatographies were obtained from Bio-Rad Laboratories. Chromium chloride and sodium pyrophosphate were from Fisher Scientific Company. All other chemicals were analytical grade. Distilled water was further purified and deionized with a Gelman Water 1 apparatus for use in NMR experiments. This deionized water hereafter will be referred to as Water 1.

ENZYME PURIFICATIONS

HGPRTase was purified to apparent electrophoretic homegeneity from baker's yeast using the procedure of Ali and Sloan (1982). Three preparations of OPRTase were employed in this study. Two of which were homogenous by the criteria of gel electrophoresis and one of which was at least 95% pure. The OPRTase purification procedure has been described (Victor, et al., 1979a).

ENZYME ASSAY PROCEDURES

OPRTase was assayed spectrophotometrically using a Cary 15 recording spectrophotometer by a method previously described (Umezu, et al., 1971). The final concentrations of reactants in 1ml of total volume were 100uM PRibPP, 1-2mM $MgCl_2$, 150uM orotate, 20mM Tris pH 8.0 and known volume of the enzyme. HGPRTase was either assayed spectrophotometrically at 245 nm (Hill, 1979) in 100mM Tris pH 7.4 or by using a modification of the method of Flasks (1963) employing high performance

liquid chromatography as described by Ali and Sloan (1982). The assay mixture in the later case consisted of 100uM hypoxanthine, 200uM PRibPP, 1mM $MgCl_2$ in 20mM Tris buffer pH 8.0.

ELIMINATION OF PARAMAGNETIC AND OTHER TRACE METAL ION

All glassware was washed with distilled water, soaked for at least 5 hours in HNO_3, rinsed again with purified Water 1 and then re-rinsed with metal-free water. PRibPP was dissolved in metal-free 5mM Tris, pH 8.0 and pressure squeezed through a mini column of Chelex-100 previously equilibrated with metal-free 5mM, pH 8.0 buffer. The column was then washed with 0.5 -1ml aliquots of Water 1 three times to insure the removal of residual PRibPP from the column. Metal ion traces were removed from the enzyme sample and assay mixtures. The extent of removal of Mn(II) was monitored by observing the absence of nucleotide formation during the assay previously described (Umezu, et al., 1971; Ali and Sloan, 1982) in the presence of enzyme but no added metal.

Prior to the NMR spectroscopic studies water solvent was replaced by the desired percentage of D_2O using vacuum dialysis, as previously described (Slater, et al., 1972). The 5mm, 10mm and micro NMR tubes used in these experiments were either obtained from Wilmad Glass Company or were made at the City College glass blowing facility from precision-made glass tubing.

MAGNETIC RELAXATION MEASUREMENTS

The different proton resonance signals of PRibPP were assigned previously (Sloan, et al., unpublished) by comparing different peak heights, and by comparison with previously established resonances of sugar rings in nucleosides and nucleotides (Altona and Sundaralingam,

1973). The phosphorus resonances of PRibPP were assigned based on a comparison of proton decoupled and non-decoupled spectra (Sloan, et al., unpublished). These assignments are analogous with those reported by Smithers and O'Sullivan (1979).

Magnetic relaxation measurements of the longitudinal relaxation times (T_1) of phosphorus and the proton resonances of PRibPP were measured by employing an inversion recovery method at 161.82 MHz (phosphorus) and 400 MHz (proton) using JEOL GX-400 FT-NMR spectrometer at the CUNY NMR Facility at Hunter College. The temperature was maintained at 19°C ± 2°C with a nitrogen-flow temperature control. Proton decoupling was used to simplify the three phosphorus signals. The $1/T_1$ values for each individual peak were evaluated from three different plotting methods as follows: 1) Null point method. During a 180°/90° pulse sequence a time for each individual peak is reached when the net magnetization in the Z-direction is zero. At this time (τ null), equation 5

$$\tau_{null} = T_1 \ln (M_\infty - M_o) / M_\infty \qquad (5)$$

reduces to $\tau_{null} = T_1 \ln 2$, permitting an evaluation of T_1 from the null point (Mildvan and Gupta, 1978). The peak heights (M_z) were plotted vs. τ values and the null point was determined for each individual peak. T_1 was then calculated by dividing the null point by 0.693.
2) It is well known from the Bloch (1946) equations that the rate of decay of magnetization in the Z direction is

$$dM_z / dt = -(M_z - M_o) / T_1 \qquad (6)$$

where M_o is equal to the magnetization at equilibrium prior to the pulse sequence and is related to M_z as shown below (Equation 7). This inte-

$$M_z = M_o (1 - 2e^{-t} /T_1) \qquad (7)$$

gration may be expanded and related to the signal intensity as shown in Equation 8. The equation (8) is of the form $y = m_x + b$. Since I is

$$\ln (I_\infty - I_t) = \ln (I_\infty - I_0) e^{-t / T_1} \qquad (8)$$

(In eq. 8 I_∞ = intensity for $\tau \ggg T_1$ and I_t = intensity for a given τ)

observed in form of signal peak height, in the equation (8), peak heights, (m) can be substituted for I so that a plot of ln $(m_\infty - m_\tau)$ vs. τ will give a slope which is equal to $1/T_1$. 3) In this method, designed in our laboratory, values of $-\ln (m_\infty - m_\tau)/2m_\infty)$ are plotted vs. τ and the slope of the line is equal to $1/T_1$. We also used a program (developed by Robert Ashton) to determine values of $1/T_1$ using peak heights and τ values, which employed a procedure designed by Kowalewski, et al., (1977). T_1 values determined by all these plotting methods were averaged and mean values were used to calculate distances. T_2 values were determined from the line widths of each resonance by employing equations shown below. Equation 9a defines the relationship

$$\text{Width at half height} = \frac{(1 + \omega_i^2 T_1 T_2)^{1/2}}{T_2} \qquad (9)$$

between T_2 and line width at frequencies well below saturation ($\omega_1^2 \ll 1/T_1T_2$), π width at half peak height $= \frac{1}{T_2}$ (9a)

CALCULATION OF CORRELATION TIMES AND DISTANCES

Paramagnetic contributions to the longitudinal ($T_{1_P}^{-1}$) and transverse relaxation rates ($T_{2_P}^{-1}$) were calculated by subtracting the diamagnetic contribution as described by Mildvan and Cohn (1970). The diamagnetic corrections for the binary Mn(II)-PRibPP complex were made using the PRibPP relaxation rates in the absence of metal ion. For the ternary OPRTase-Mn(II)-PRibPP and HGPRTase-Mn(II)-PRibPP complexes, corrections were made using the OPRTase -PRibPP and HGPRTase-PRibPP solution in the absence of metal ion. The $T_{1_P}^{-1}$ were normalized by the concentration ratio (f) equal to [Mn(II)]/[PRibPP] as described by Luz and Mieboom (1964). The distances from the metal to the PRibPP nuclei were calculated using the dipolar term of the Solomon-Bloembergen equation (Solomon, 1955) where

$$r = C \left[f T_{1_P} \times f(\tau_c) \right]^{1/6} \qquad (10)$$

The parameter C is a collection of constants well defined for manganese ion in solution and is numerically equal to 601 and 812 for Mn(II)-Phosphorus and Mn(II)-Proton interactions respectively (Mildvan and Engle, 1972). The $fT_{1_P}^{-1}$ values in the case of enzyme-bound PRibPP are in the limit of fast exchange (Mildvan and Engle, 1972). The correlation

function $f(\tau c)$ is given by

$$f(\tau_c) = \frac{3\tau_c}{1 + \omega_i^2 \tau_c^2} + \frac{7\tau_c}{1 + \omega_s^2 \tau_c^2} \qquad (11)$$

in which τc is the correlation time for dipolar interaction, ωi is the nuclear precession frequency and ωS is the electron precession frequency. A τc value of 3×10^{-10} for Mn(II) systems free in solution was used to calculate $f(\tau c)$ and Mn(II)-PRibPP (in solution) distances. The τc values for enzyme-bound Mn(II)PRibPP were estimated from extrapolated T_{1_P}/T_{2_P} values that had been measured over an enzyme concentration range and extrapolated to infinite enzyme. Thereafter, these values and the Ray and Mildvan equation was employed to evaluate τc.

$$\omega_i \tau_c = [3/2 (T_{1_P}/T_{2_P} - 7/6)]^{1/2} \qquad (12)$$

In instances where these plots were non-linear, both minimum and maximum T_{1_P}/T_{2_P} values were used to calculate τc values.

PREPARATION OF Cr(III)PP_i

Cr(III)PP_i was prepared by the method of Merrit, et al., (1981). The procedure is briefly described below. A 250ml sample of 250mM sodium pyrophosphate was adjusted to pH 4.0 with Dowex resin 50W X-2 in its hydrogen ion form. To this was added 250ml of 250mM $Cr[(H_2O)_4Cl_2]Cl$. The resulting solution was mixed completely and cooled to 10°C and the pH was adjusted to 5.3 with saturated $KHCO_3$. The solution was stirred for approximately 15-25 minutes at room temperature, filtered to remove unwanted polymers, cooled to 4°C, adjusted to pH 2.0 with 6N

HCl and loaded on to a 65 x 2 cm Dowex 50W X - 2 (H^+ ion), 100 - 200 mesh column previously washed with a large volume of deionized "Water-1" water. The column was also eluted with deionized water at 4°C. Cr(III)PP_i began eluting after 4-5 void volumes had passed through the column. After its elution, Cr(III)PP_i was concentrated by evaporation at 4°C over a period of 4-8 weeks. When scanned for absorbance maximas, the concentrated solution exhibited peaks at 425 nm and 595 nm as described by Merrit, et al. It was further characterized for chromium ion content by the method of Postmas and King (1955), for total and inorganic phosphates by methods of Ames and Dublin (1960) as well as Chen, et al., (1965) and for Na(I) and K(I) contents by flame photometry.

Cr(III)PP_i AS SUBSTRATE FOR OPRTase REVERSE REACTION

The enzyme sample used was chelexed by passing it through a Chelex 100 column as described for the NMR experiments, as were all the substrates except for Cr(III)PP_i. The assay mixture consisted of 50uM (OMP), varying concentrations of Cr(III)PP_i and 10ulof chelexed OPRTase and was made to 1.0ml total volume with 20mM Trizma buffer pH 8.0. To check if Cr(III)PP_i would serve as substrate in the presence of $MgCl_2$ only, the assay mixture was made 1mM with respect to $MgCl_2$. The change in absorbance (Δ A) per unit time was measured on a Cary 15 spectrophotometer at 295 nm.

EFFECTS OF SODIUM PYROPHOSPHATE AND Cr(III)PP_i ON OPRTase CATALYZED REACTIONS

To observe the effect of Cr(III)PP_i on the reverse reaction of OPRTase, the assay mixture (1.0ml total volume) consisted of 50uM OMP, 1000uM $MgCl_2$, 40ul of standardized OPRTase (10ul of enzyme was used

in a repeat experiment), varying concentrations of Na(I)PP_i at different fixed concentrations of Cr(III)PP_i. In the forward direction the assay mixture consisted of 150uM orotate, 1000uM $MgCl_2$, varying concentration of PRibPP at fixed concentrations of Na(I)PP_i or Cr(III)PP_i, 5.0ul of OPRTase and made to 1.0ml with Tris pH 8.0.

EFFECTS OF Na(I)PP_i AND Cr(III)PP_i ON HGPRTase FORWARD REACTIONS

In these studies the assay mixture consisted of 100uM hypoxanthine, 2000uM $MgCl_2$, 40ul of standardized HGPRTase, varying concentrations of PRibPP at fixed different concentrations of Na(I)PP_i and Cr(III)PP_i to a total volume of 1.0ml made with 100mM Tris buffer pH 7.4. The PRibPP concentration range selected was 25uM-200uM. The reaction was monitored on a Cary-15 spectrophotometer at 245 nm.

AN ATTEMPT TO MAKE THE Cr(III)PRibPP COMPLEX

The standard technique for making nucleotide-Cr(III) complexes consisted of adjusting the pH of a 20mM nucleotide solution to 4, mixing it with an equal volume of 20mM $CrCl_3 \cdot 6H_2O$ and then heating the resulting solution to 80°C for 15-20 minutes. PRibPP is quite sensitive to both temperature and pH. Therefore, prior to attempting to make a Cr(III)-PRibPP complex, we studied the effect of temperature and pH on PRibPP. Based on the results of these studies, we tried to make Cr(III)PRibPP by the following modified procedure of Cleland (1982). The pH of 25ml of 20mM PRibPP solution was adjusted with Dowex resin (50W X-2 H^+ form) to 5.5 ± 0.5. After removal of this resin by filtration, the PRibPP solution was mixed with 25ml of 20mM $CrCl_3 \cdot 6H_2O$. After stirring for about 4.5 minutes, the resulting solution was cooled to 4°C and pH was readjusted to 5.5 with saturated $KHCO_3$. The solution was then heated

to 30°C for about 25 minutes with occasional stirring in between, filtered to remove any unwanted precipitate, cooled to 4°C and adjusted the pH back to 5.5. The reaction mixture was then loaded on to a regenerated column of Dowex 50W X-4 (hydrogen ion form) and eluted with Water-1. Fractions of $\sim$ 8ml were collected. All fractions were checked for ribose by the orcinol test, for chromium and total phosphate by procedures previously mentioned. Fractions which were positive for ribose or Cr(III) or phosphate were assayed for their inhibitory effect on the OPRTase forward reaction. An inhibitory effect was observed for Fractions 9-13. These fractions were pooled and concentrated by lyophilization and subjected to Sephadex G-10 column chromatography using Water-1 as eluent. These fractions were also monitored for their inhibitory effect on the OPRTase forward activity. It was noted that the fractions exhibiting an inhibitory effect were colorless (indicating an absence of Cr(III)]. The fractions with green color did not inhibit the OPRTase forward activity. The colorless fractions were then pooled and concentrated again by lyophilization. This pooled material was then checked for its Cr(III) content and subjected to AG1 X-4 column chromatography. The new fractions from the AG1 X-4 column were assayed for total phosphate, acid labile PO_4, inorganic PO_4 and ribose. They were also tested for their OPRTase inhibitory effect. Surprisingly, the inhibitory effect was contained in one fraction which was negative for ribose, as well as for phosphates. The fractions that were positive for ribose or phosphate or both were further identified by ^{31}P NMR spectroscopy. Here ribose-1-PO_4, ribose-5'-phosphate and PRibPP itself were used as standards. From these experiments, we were able to identify the products of disintegration of PRibPP when incubated with $CrCl_3 \cdot 6H_2O$ even at

mild conditions of pH and temperature. We tried also to identify the material within the fraction exhibiting the inhibitory effect by different spectroscopic methods, but failed. This procedure was repeated and the inhibitory effect on OPRTase was checked at each step of the procedure to determine that the inhibitor was an artifact. Since the column I used was also employed for cytosine/cytidine arabinosides preparation and purification, a guess was made that cytidine might be the inhibitory culprit. Cytidine was therefore checked for its inhibitory effect also on the OPRTase forward reaction.

RESULTS

MAGNETIC RELAXATION RATES OF THE PROTONS OF PHOSPHORIBOSYL PYROPHOSPHATE

The longitudinal and transverse relaxation rates of the five resolved protons of PRibPP were measured at 400MHz. The peak assignments were done previously at 200MHz (Sloan, et al., unpublished) as shown in Figure 3 with chemical shifts centered at 5.5 (H_1), 4.14 (H_2) 3.97 (H_3), 3.91 (H_4) and 3.60 (H_5) ppm with respect to HDO being the reference at 4.45 ppm. As described under "Methods", longitudinal relaxation rates were determined by three different plotting methods. An example of how these methods were employed is depicted in Figure 4 for the C_1 proton of PRibPP at 10mM concentration in the presence of 250uM OPRTase. The calculated T_1 values thus determined for this proton were 1.1544 seconds by null point method, 1.0417 seconds from the slope of the plot of $\ln(m_\infty - m_\tau)$ vs. τ and 1.1333 seconds as obtained from the slope of the plot of $-\ln(m_\infty - m_\tau)/2m_\infty$ vs. τ. The corresponding T_1 value obtained for this proton using the three-parameter inversion recovery computer program was 1.1357 seconds. The mean average value thus calculated was 1.1162 (1.12) seconds with a standard deviation of ($\pm$0.05) seconds, giving a mean longitudinal relaxation rate of 8.96×10^{-1} sec.$^{-1}$. All T_1 and T_1^{-1} values were calculated in a similar manner and averaged for all experimental systems for both proton and phosphorus nuclei. Table 2 summarizes these values along with the T_2 and T_2^{-1} values determined by line widths measurements for the five protons of PRibPP. The average values of T_1^{-1} were then used to determine $T_{1_P}^{-1}$ and f $T_{1_P}^{-1}$ values. The resulting f $T_{1_P}^{-1}$ values were then used to calculate all distances from the paramagnetic probe. Mn(II)-to-proton

Figure 3

^{1}H NMR spectrum of PRibPP (10mM) in 5mM Tris pH 8.0 at 400 MHz in 99.97% D_2O. The peaks were resolved previously at 200 MHz (Sloan, D. L., unpublished). Here the peaks are centered at 5.5 (H_1), 4.14 (H_2), 3.97 (H_3), 3.91 (H_4) and 3.60 (H_5) ppm. HDO served as the reference resonance with a chemical shift centered at 4.45 ppm.

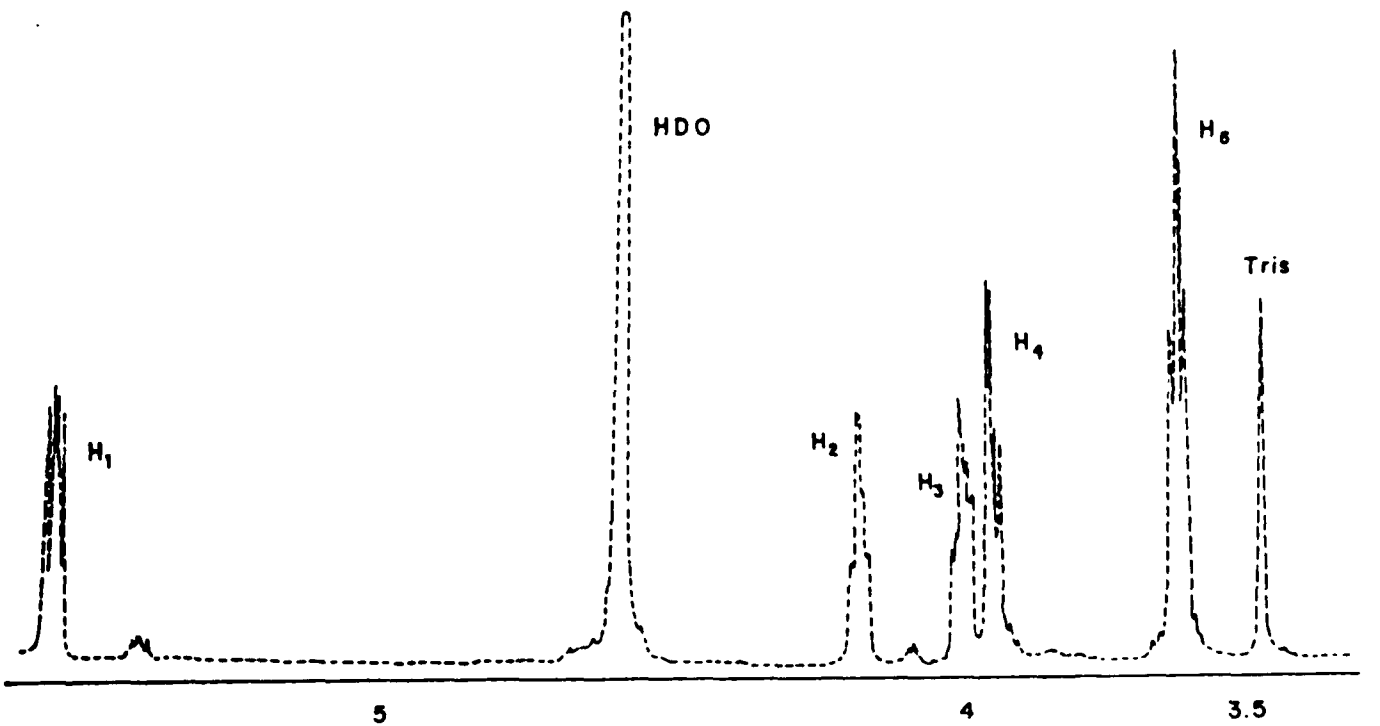

PPM

Figure 4

Sample Evaluation of a T_1. Each figure depicts a T_1 or T_1^{-1} determination for the C_1 proton of PRibPP (10mM) in the presence of 250uM OPRTase by a single plotting method. First, peak heights for this proton were measured from the spectra at different τ values. A) Null point method where peak heights (m) in millimeters (mm) are plotted vs. τ values. The null point thus obtained is divided by 0.693 to get the T_1 value. B) Plot of $\ln(m_\infty - m_\tau)$ vs. τ values where the - slope of the line gives the $1/T_1$ value. C) Plot of $\ln(m_\infty - m_\tau / 2m_\infty)$ vs. τ. Here the slope of the line yields a T_1^{-1} value. This figure is typical of many such figures generated to obtain the best T_1^{-1} values for different protons and phosphorus atoms of PRibPP when free in solution and bound to OPRTase and HGPRTase.

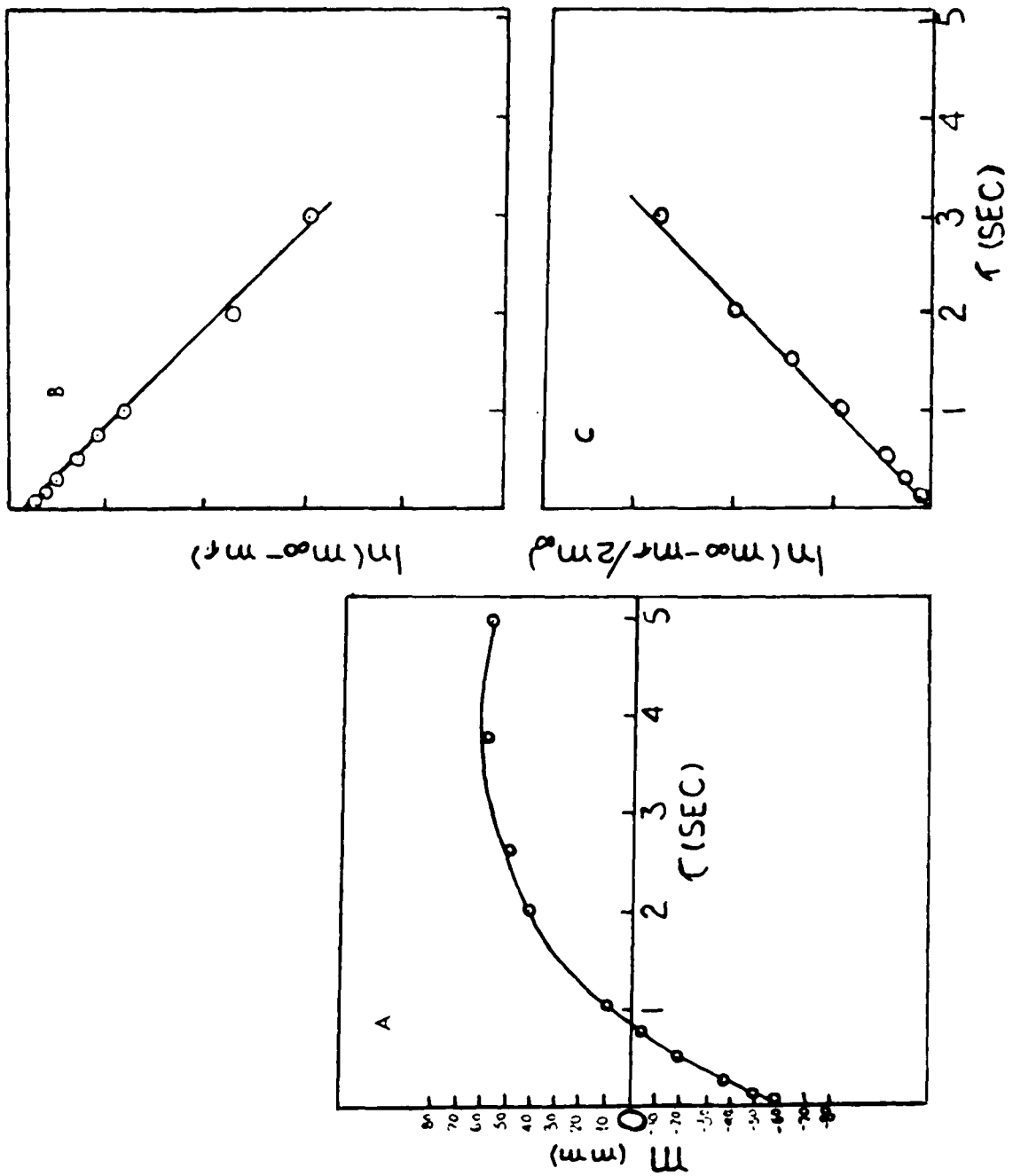
A
B
C
m (mm)
ln(m∞-mt)
ln(m∞-mt/2m∞)
t (SEC)
t (SEC)

Table 2: Comparison of T_1 and $\frac{1}{T_1}$ values determined by four different methods for the protons of PRibPP (10mM) in 5mM Tris pH 8.0 in the presence of 0.25mM OPRTase. T_2 and $\frac{1}{T_2}$ calculated from line widths at 1/2 height are also listed. The average value of $\frac{1}{T_1}$ were processed further and used to calculate Mn(II)-to-proton distances.

Proton	Null Pt. Method		-slope = $\frac{1}{T_1}$ from the plot of $\ln(m_\infty - m_\tau)$ vs.		slope = $\frac{1}{T_1}$ = $-\ln(m_\infty - m_\tau/2m_\infty)$		Computer Program		Mean Average		π (line width at 1/2 ht.) = $1/T_2$	
	T_1	$\frac{1}{T_1}$	T_1	$\frac{1}{T_1}$	T_1	$\frac{1}{T_1}$	T_1	$\frac{1}{T_1}$	T_1	$\frac{1}{T_1}$	T_2	$\frac{1}{T_2}$
	Sec	Sec^{-1}	Sec	Sec^{-1}	Sec	Sec^{-1}	Sec	Sec^{-1}	Sec	Sec^{-1}	Hz	Hz^{-1}
C_1	1.15	0.87	1.04	0.96	1.13	0.88	1.36	0.88	1.116	0.896	0.026	38.56
C_2	1.05	0.96	0.96	1.05	0.98	1.02	1.001	0.99	0.991	1.00	0.050	19.83
C_3	0.98	1.02	0.90	1.115	0.98	1.02	0.92	1.08	0.945	1.058	0.035	28.64
C_4	1.08	0.92	1.09	0.91	1.027	0.97	1.09	0.91	1.093	0.91	0.030	33.06
C_5	0.36	2.77	0.45	2.21	0.42	2.40	0.43	2.31	0.416	2.40	0.025	40.06

distances were calculated for the binary Mn(II)-PRibPP complex using a $f(\tau_c)$ value of 3.0×10^{-10}. The effects of Co(II) and Cr(III) ions on the relaxation rates of the protons of PRibPP were also observed. For these binary complexes, metal-to-proton distances were calculated using $f(\tau_c)$ values of 7×10^{-12} and 3.9×10^{-10} for Co(II) and Cr(III) respectively (Gupta, et al., 1976; Peterson and Gupta, 1979). The effects of these metal ions on the protons of PRibPP are listed in Table 3 in the form of $fT_{1_P}^{-1}$ values. The C values employed in the distance calculations were 812 for Mn(II) (Tinkham, et al., 1951), 900 ± 175 for Co(II) (Luz, et al., 1964) and 710 for Cr(III) (Peterson and Gupta, 1979). The relative metal-to-proton distances are shown in Table 8. The Cr(III)-to-proton distances are greater than those calculated for Mn(II)-to-proton and Co(II)-to-proton suggesting that it does not coordinate to any portion of PRibPP and that it would have been a poor paramagnetic reference point in the micromolar concentration range in resolving metal-to-proton and metal-to-phosphorus distances. Because Co(II) binds to but does not activate OPRTase catalysis (Victor, et al., 1979), Mn(II) was preferred as a paramagnetic probe for elucidating PRibPP-metal ion-enzyme conformations in this study. Figure 5 depicts the effects of increasing concentrations of Mn(II) on $T_{1_P}^{-1}$ values when Mn(II)-PRibPP is bound to OPRTase (Fig. 5A) or HGPRTase (Fig. 5B). The initial linearity of these plots indicates the binding of Mn(II) to PRibPP in a 1:1 ratio. This is not unexpected because the Mn(II) concentration is much smaller than the PRibPP concentration. Significant changes in the relative order and magnitudes were observed in $fT_{1_P}^{-1}$ values when Mn(II)-PRibPP is enzyme bound. These results are listed in Table 4 for a single Mn(II) concentration, and they indicate the occurence of conform-

Table 3: The Effect of Paramagnetic Metal Ions on the Longitudinal Relaxation Rates (400 MHz) of the Protons of PRibPP*

Experimental Conditions	Protons				
	1	2	3	4	5
10mM PRibPP 20uM Mn(II)	4612	2504	563	544	989
10mM PRibPP 20uM Co(II)	297	169	86	42	126
10mM PRibPP 20uM Cr(III)	102	62	42	61	225

*The $1/fT_{1_P}$ values were calculated from the average $1/T_1$ values obtained by three plotting methods for each proton.

Figure 5

Plots of the $T_{1_P}^{-1}$ values for the five protons of PRibPP vs. Mn(II) concentration for ternary complexes, PRibPP-Mn(II)-OPRTase (A) and PRibPP-Mn(II)-HGPRTase (B). In figure 5A ●–● ◑–◑ ◐–◐ ◒–◒ and ◓–◓ signify C_1, C_2, C_5, C_3 and C_4 protons. In 5B these circles represent C_1, C_2, C_3, C_4, and C_5, protons respectively.

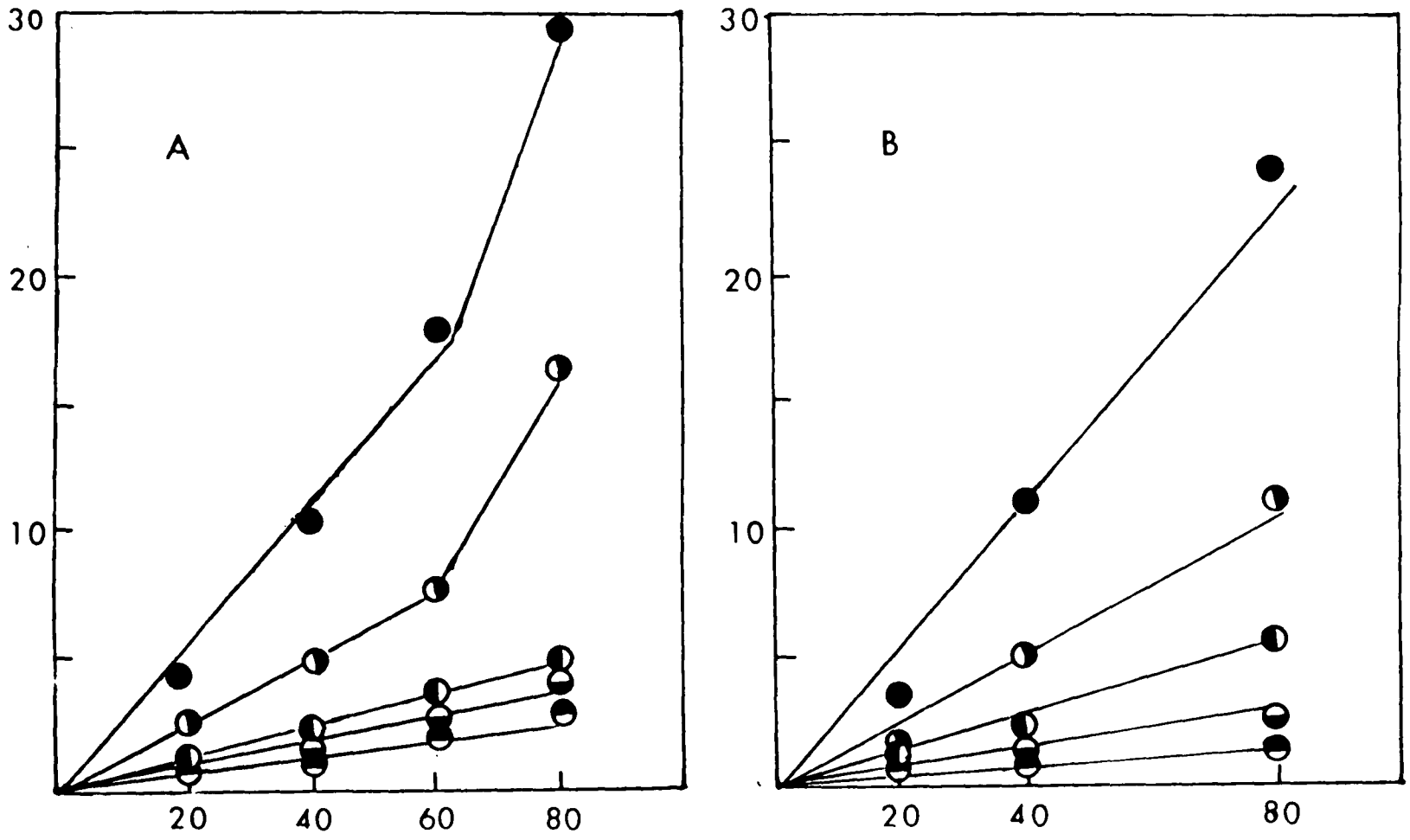
30
20
10
A
20
40
60
80
30
20
10
B
20
40
80
[Mn (II)] μM

Table 4: The Effects of Paramagnetic Mn(II) on the Longitudinal Relaxation Rates (400 MHz) of the Protons of PRibPP free in solution as well as in the presence of 250uM OPRTase and 664uM HGPRTase.*

Experimental Conditions	Protons				
	1	2	3	4	5
10mM PRibPP 20uM Mn(II)	4612	2504	563	544	989
10mM PRibPP 20uM Mn(II) 250uM OPRTase	2181	1122	293	325	415
10mM PRibPP 20uM Mn(II) 664uM HGPRTase	1751	769	453	253	121

*The $1/fT_{1_P}$ values were calculated from average $1/T_1$ values obtained by three different plotting methods for each proton.

ational adjustments of the metal ion-PRibPP bound to this enzyme. Upon decreasing the concentration of OPRTase at constant Mn(II) and PRibPP concentrations, increasing f $T_{1_P}^{-1}$ (Table 5) for all protons of PRibPP were observed. In the case of HGPRTase, all the protons of PRibPP upon dilution of the enzyme (at lower concentration of enzyme) exhibited a similar trend except for H_3 (see Table 6), in which case the f $T_{1_P}^{-1}$ value first decreases slightly on dilution and then increases slightly upon further decrease in the enzyme concentration. This suggests that conformational changes occur as the Mn(II)-PRibPP binds to both of these two enzymes.

The τ_c values to be used in distance calculations were determined by using extrapolated T_{1_P}/T_{2_P} ratios, obtained from the plots of T_{1_P}/T_{2_P} vs. $\frac{1}{[E]}$ shown in Figure 6 (OPRTase) and Figure 7 (HGPRTase). For most of the protons these plots were linear, but where they were non-linear, individual T_{1_P}/T_{2_P} ratios were used instead of extrapolated values. As is obvious in Figure 7, the H_3 proton of the PRibPP-Mn(II)-HGPRTase complex exhibited linearity in T_{1_P}/T_{2_P} plot but had a lower y-intercept value than allowed by the Ray and Mildvan equation(Equation 12). The individual T_{1_P}/T_{2_P} ratios obtained for this proton under these experimental condition also are not allowed by this theory. In this particular case a value calculated for the C_4 proton was used to calculate (τ_c). This is justified by the fact that these protons resonate at very close frequencies and are nearly in the same environment. $f(\tau_c)$ values were calculated from (τ_c) values thus obtained for individual protons for ternary PRibPP-Mn(II)-OPRTase and PRibPP-Mn(II)-HGPRTase complexes. τ_c and $f(\tau_c)$ values are depicted in Table 7. Thereafter, Mn(II)-to-proton distances of OPRTase-Mn(II)-PRibPP and HGPRTase-

Table 5: The Effects of Paramagnetic Mn(II) on the Longitudinal Relaxation Rates (400 MHz) of the Protons of PRibPP in the presence of OPRTase.*

Experimental Conditions	Protons				
	1	2	3	4	5
10mM PRibPP 20uM Mn(II) 250uM OPRTase	2181	1122	293	325	415
10mM PRibPP 40uM Mn(II) 250uM OPRTase	2615	1310	328	350	503
10mM PRibPP 60uM Mn(II) 250uM OPRTase	2989	1336	590	450	517
10mM PRibPP 80uM Mn(II) 250uM OPRTase	3720	2075	578	359	615
10mM PRibPP 80uM Mn(II) 125uM OPRTase	3795	2152	1435	539	1148
10mM PRibPP 80uM Mn(II) 62.5uM OPRTase	6900	2258	1608	1337	1518
Extrapolated**	2630	1995	525	229	479

*The $1/fT_{1_P}$ values were calculated from average $1/T_1$ values obtained by three different plotting methods for each proton.

**These values of $1/fT_{1_P}$ were obtained by extrapolating plots of the log $fT_{1_P}^{-1}$ vs. the reciprocal of the OPRTase concentration to infinite enzyme concentration.

Table 6: The Effects of Paramagnetic Mn(II) on the Longitudinal Relaxation Rates (400 MHz) of the Protons of PRibPP in the presence of HGPRTase.*

Experimental Conditions	Protons				
	1	2	3	4	5
10mM PRibPP 20uM Mn(II) 664uM HGPRTase	1751	769	453	253	121
10mM PRibPP 40uM Mn(II) 664uM HGPRTase	2776	1322	498	380	348
10mM PRibPP 80uM Mn(II) 664uM HGPRTase	3031	1411	746	323	238
10mM PRibPP 80uM Mn(II) 332uM HGPRTase	4169	2295	639	393	385
10mM PRibPP 80uM Mn(II) 166uM HGPRTase	4593	2884	694	460	756
Extrapolated**	2884	1230	708	302	166

*The $1/f T_{1_P}$ values were calculated from average $1/T_1$ values obtained by three different plotting methods.

**These values of $1/f T_{1_P}$ were obtained by extrapolating plots of the log of $1/f T_{1_P}$ vs. the reciprocal of HGPRTase concentration to infinite enzyme concentration.

Figure 6 Plots of T_{1_P}/T_{2_P} ratios vs. $[OPRTase]^{-1}$

T_{1_P}/T_{2_P} ratios are plotted vs. 1/OPRTase concentration for the different protons of PRibPP to obtain extrapolated T_{1_P}/T_{2_P} ratios, that were subsequently used to calculate τ_c values by employing the Ray Mildvan equation (Equation 12). The τ_c values thus obtained were used to calculate $f(\tau_c)$ values. ●—● , ⬢—⬢, ■—■ , ▲—▲ and ▼—▼, signify C_1, C_3, C_2, C_5 and C_4 protons of PRibPP respectively.

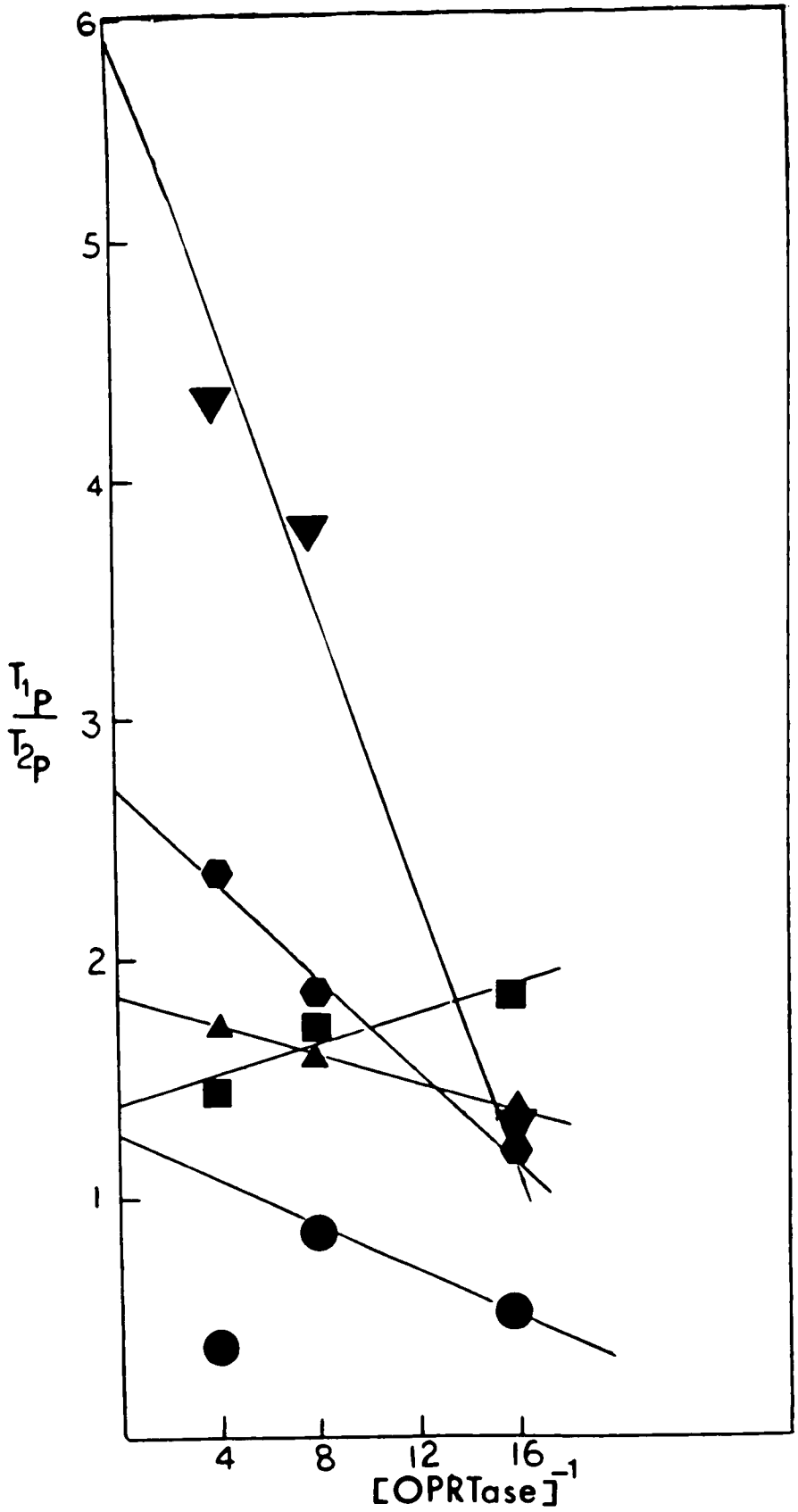
6
5
4
3
2
1
$\frac{T_{1P}}{T_{2P}}$
4
8
12
16
[OPRTase]$^{-1}$

Figure 7 Plots of T_{1_P}/T_{2_P} ratios vs. $[HGPRTase]^{-1}$

T_{1_P}/T_{2_P} ratios are plotted vs. 1/HGPRTase for the different protons of PRibPP in the PRibPP-Mn(II)-HGPRTase complex, to obtain extrapolated T_{1_P}/T_{2_P} values. The extrapolated T_{1_P}/T_{2_P} ratios thus obtained were used to calculate τ_c and then $f(\tau_c)$ values for these protons. Here C_1, C_2, C_3, C_4, and C_5 protons of PRibPP are represented by 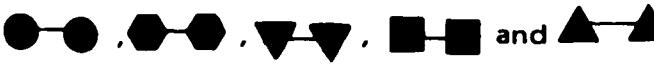 respectively.

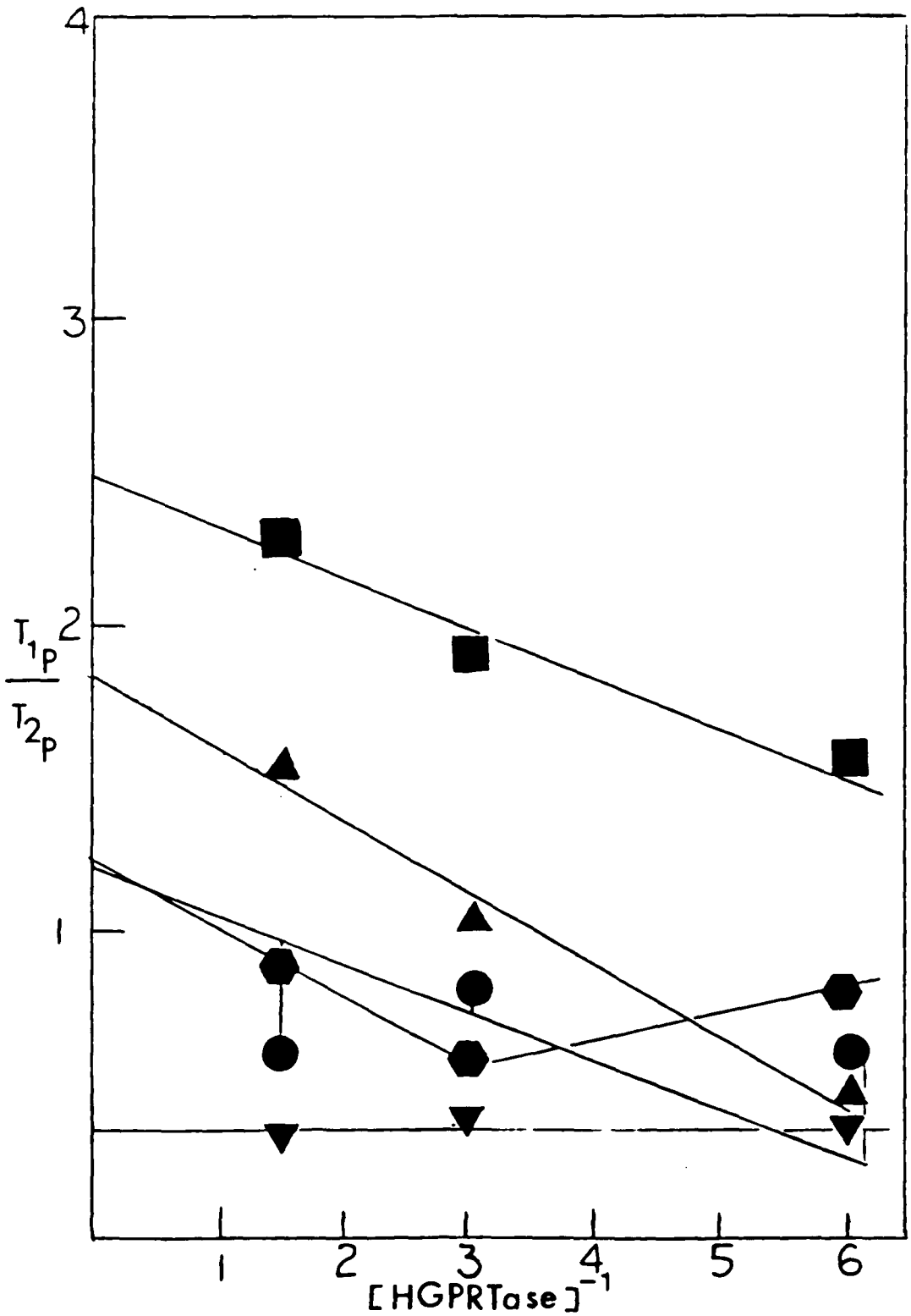
4
3
2
1
$\frac{T_{1p}}{T_{2p}}$
1
2
3
4
5
6
[HGPRTase]$^{-1}$

Table 7: * τ_c and $f(\tau_c)$ Values Calculated for Various Protons of PRibPP in the PRibPP-Mn(II)-OPRTase and PRibPP-Mn(II)-HGPRTase Complexes.

EXPERIMENTAL CONDITIONS		PROTONS					
		1	2	3	4	5	Mean of all Protons
PRibPP-Mn(II)-OPRTase	τ_c	0.9×10^{-10}	2.15×10^{-10}	6.0×10^{-10}	1.06×10^{-9}	3.94×10^{-10}	2.81×10^{-10}
	$f(\tau_c)$	2.6×10^{-10}	5.0×10^{-10}	5.51×10^{-10}	4.14×10^{-10}	9.47×10^{-10}	5.33×10^{-10}
PRibPP-Mn(II)-HGPRTase	τ_c	0.55×10^{-10}	1.01×10^{-10}	**5.58×10^{-10}	5.58×10^{-10}	3.87×10^{-10}	3.32×10^{-10}
	$f(\tau_c)$	1.64×10^{-10}	2.85×10^{-10}	**5.65×10^{-10}	5.65×10^{-10}	5.97×10^{-10}	4.35×10^{-10}

* values were determined from Equation (12) using extrapolated T_{1_P}/T_{2_P} ratios, obtained by plotting T_{1_P}/T_{2_P} ratios vs. $\frac{1}{[E]}$ to infinite enzyme concentration. The T_{1_P} values employed in these calculations were the average T_{1_P} values obtained by the different plotting methods.

**Extrapolated T_{1_P}/T_{2_P} ratio as well as individually determined T_{1_P}/T_{2_P} ratio for the C_3 proton in PRibPP-Mn(II)-HGPRTase complex was less than that dictated by Equation 12. Since C_3 and C_4 proton resonate at very close frequencies we used extrapolated T_{1_P}/T_{2_P} ratio of C_4 proton to calculate τ_c and $f(\tau_c)$ for both C_3 and C_4 protons, assuming that paramagnetic effects will be similar on these two protons and that these effects are governed by the same correlation time.

Table 8: Calculated Distances (in Å) Between the Protons of PRibPP and Various Metal Ions in Solution and PRibPP-Mn(II) Distances when Bound to OPRTase and HGPRTase.

EXPERIMENTAL CONDITIONS	PROTONS				
	1	2	3	4	5
10mM PRibPP 20uM Mn(II)*	5.0 ± 0.5	5.7 ± 0.2	7.3 ± 0.4	7.3 ± 0.3	6.4 ± 0.2
10mM PRibPP 20uM Co(II)**	4.8 ± 0.9	5.4 ± 0.9	7.0 ± 1.5	7.0 ± 1.2	5.8 ± 1.0
10mM PRibPP 20uM Cr(III)***	8.4 ± 0.9	9.6 ± 1.0	9.3 ± 1.0	7.8 ± 0.8	7.8 ± 0.8
OPRTase-Mn(II) PRibPP****	5.7 ± 1.3	6.7 ± 0.6	8.0 ± 0.4	8.7 ± 0.8	8.2 ± 0.9
HGPRTase-Mn(II) PRibPP****	5.2 ± 1.2	6.3 ± 1.3	7.5 ± 0.8	8.6 ± 0.8	9.6 ± 1.3

*An $f(\tau_c)$ value for Mn(II)-complexes in solution of 3.0×10^{-9} sec. was employed in these calculations.

**An $f(\tau_c)$ value for Co(II)-complexes in solution of 7.0×10^{-12} sec. was employed in these calculations.

***An $f(\tau_c)$ value for Cr(III)-complexes in solution of 3.9×10^{-10} sec. was employed in these calculations.

Table 8 (Continuation)

****Values of $f(\tau_c)$ for OPRTase and HGPRTase-bound Mn(II) complexes with PRibPP were determined by extrapolating a plot of the T_1 to T_2 ratios vs. the reciprocal of the enzyme concentration to infinite enzyme concentration. The extrapolated T_{1_P}/T_{2_P} values were then used to calculate τ_c and from it the $f(\tau_c)$ for the individual protons.

Mn(II)-PRibPP complexes were determined (Table 8) using C value of 812 and both individual and extrapolated $fT_{1_P}^{-1}$ values. Extrapolated $fT_{1_P}^{-1}$ values were obtained from the plots of log $fT_{1_P}^{-1}$ vs. [E] (Figure 8A and 8B). In every instance the proton-to-metal distances of OPRTase-Mn(II)-PRibPP and HGPRTase-Mn(II)-PRibPP exceed those of binary Mn(II)-PRibPP complex indicating a shift of metal ion away from the ribose ring upon formation of ternary enzyme Mn(II)-PRibPP complexes.

MAGNETIC RELAXATION OF THE PHOSPHORUS ATOMS OF PRibPP

The chemical shifts of the three phosphorus atoms of PRibPP were found to be similar to those of the 5'-phosphate group of ribose-5'-phosphate and the diphosphate portion of ADP under similar conditions of pH, with the 5'-PO_4 singlet, and the α -PO_4 and β -PO_4 doublets (Figure 9) positioned 5.1ppm, -4.4ppm and -10.7ppm upfield and downfield (-), respectively, from an orthophosphoric acid (85%) standard. The decoupled spectrum shown in Figure 9 is that of the tetra sodium salt of PRibPP in 5mM Tris buffer at pH 8.0. The chemical shifts that we observed differ slightly from those reported by Smithers and O'Sullivan (1982) by a shift of -1.4ppm which may be due to the environmental effect of Tris buffer on the phosphorus resonances at this pH. Figure 10 illustrates effect of increasing concentrations of Mn(II) on the relaxation rates of the phosphate resonances of PRibPP. This effect is directly proportional as expected. As shown in Table 9 for the binary Mn(II)-PRibPP complex, the added Mn(II) increased the normalized longitudinal relaxation rates. The magnitude of this increase is greater for the α - and β -phosphate groups than for the 5'-phosphate. As shown also in Table 9, $fT_{2_P}^{-1}$ is greater than $fT_{1_P}^{-1}$, indicating that $T_{1_P}^{-1}$ is not

Figures 8A and 8B

Plots of log $f T_{1_P}^{-1}$ vs. $\frac{1}{[E]}$ for the five protons of PRibPP in Tris pH 8.0 in presence of 80 μ molar - Mn(II). In both figures  represent C_1, C_2, C_3, C_4 and C_5 protons respectively. In figure 8A [E] is HGPRTase and in figure 8B [E] is OPRTase. The extrapolated values of $f T_{1_P}^{-1}$ obtained from these plots were used to calculate distance (r_c) for these protons from paramagnetic metal [Mn(II)] in PRibPP-Mn(II)-HGPRTase and PRibPP-Mn(II)-OPRTase complexes.

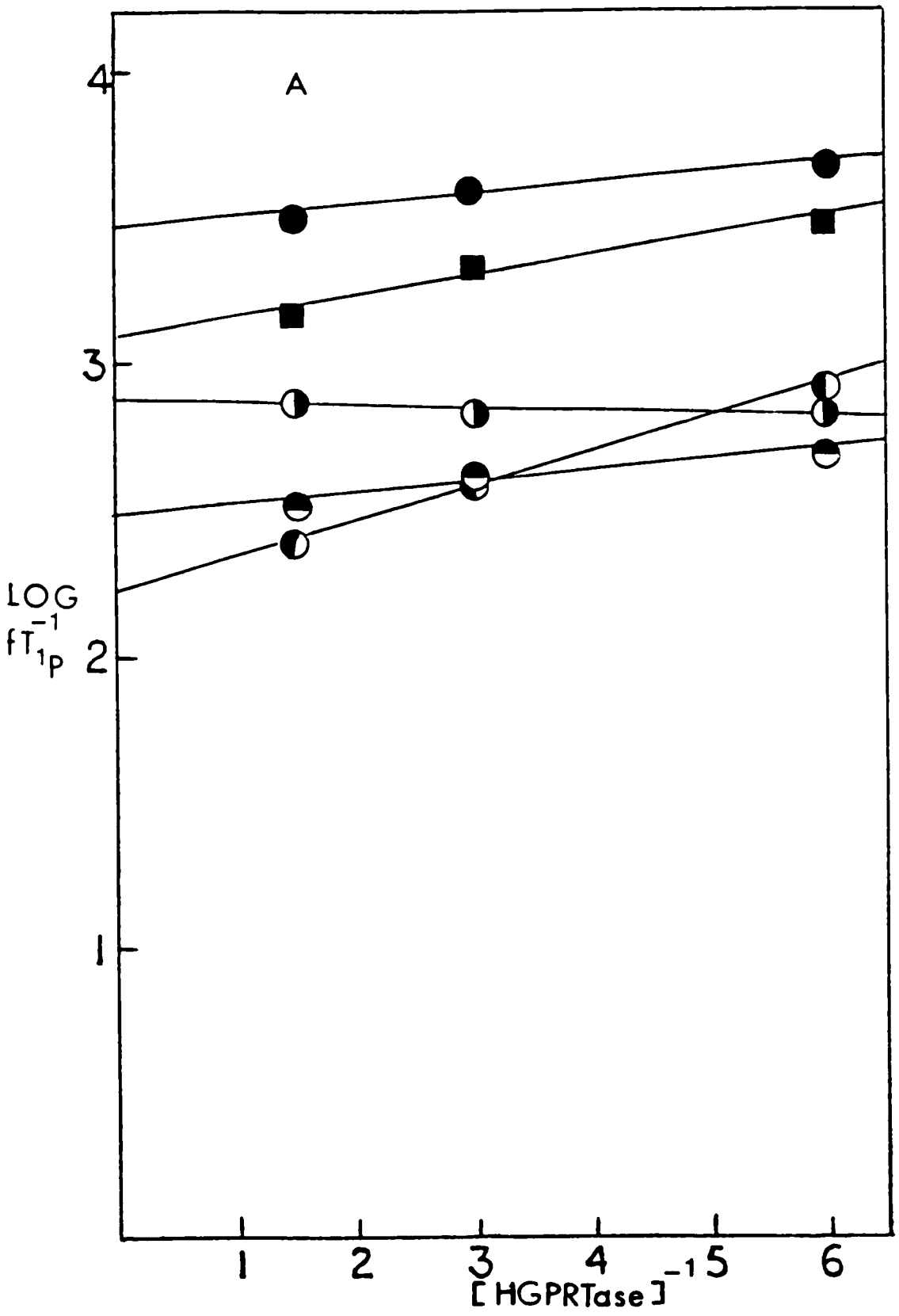
A
4
3
2
1
LOG
fT_{1P}^{-1}
1
2
3
4
5
6
$[HGPRTase]^{-1}$

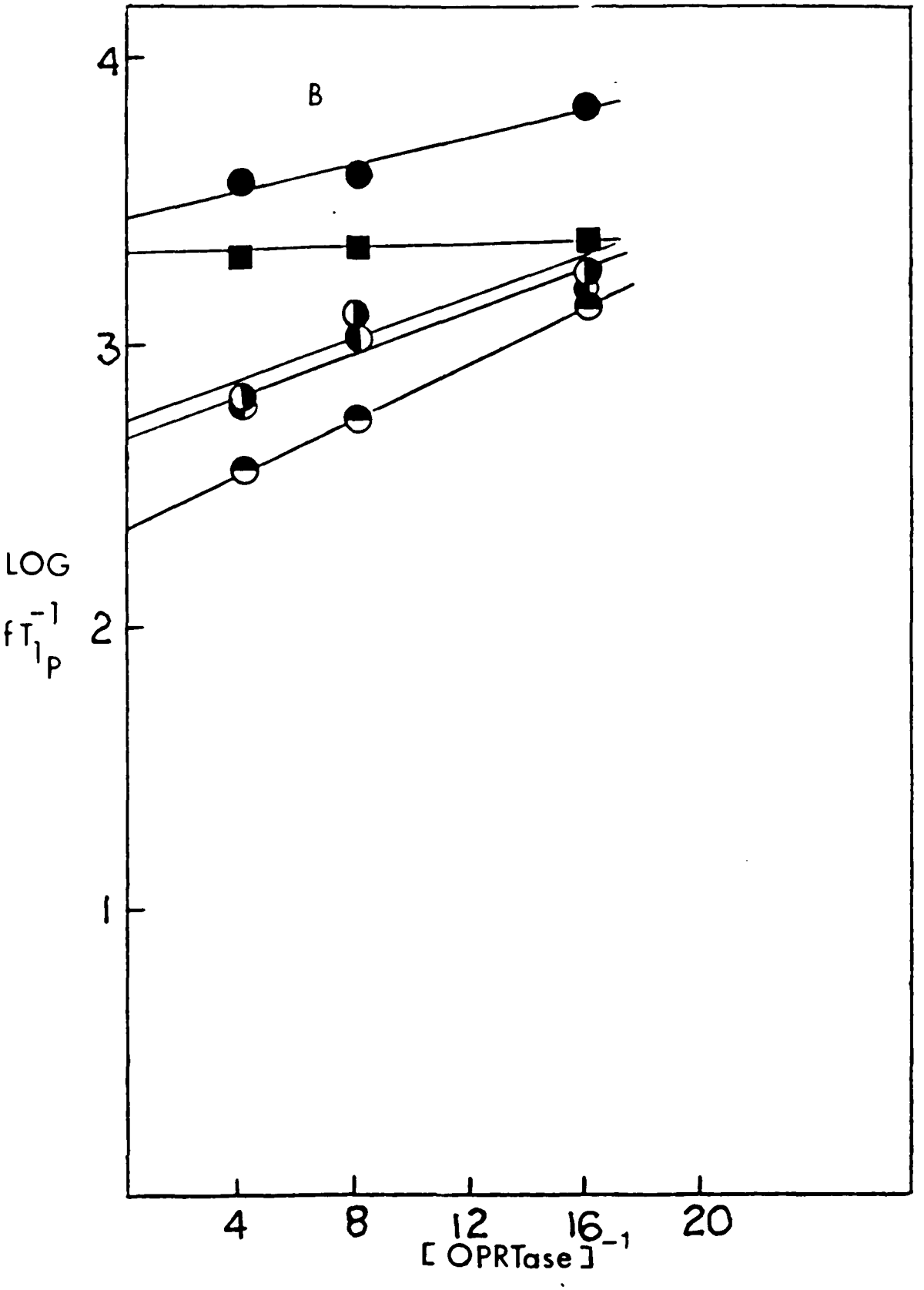
B
4
3
2
1
LOG
$fT_{1_P}^{-1}$
4
8
12
16
20
$[OPRTase]^{-1}$

Figure 9

^{31}P NMR spectrum of PRibPP (10mM) in 5mM Tris pH 8.0 at 161.82 MHz in 50% D_2O. The peaks were previously resolved (Sloan, unpublished; Smithers and O'Sullivan, 1982). Here the peaks are centered at 5.1 ppm, -4.4 ppm and -10.7 ppm from an orthophosphoric acid 85% standard.

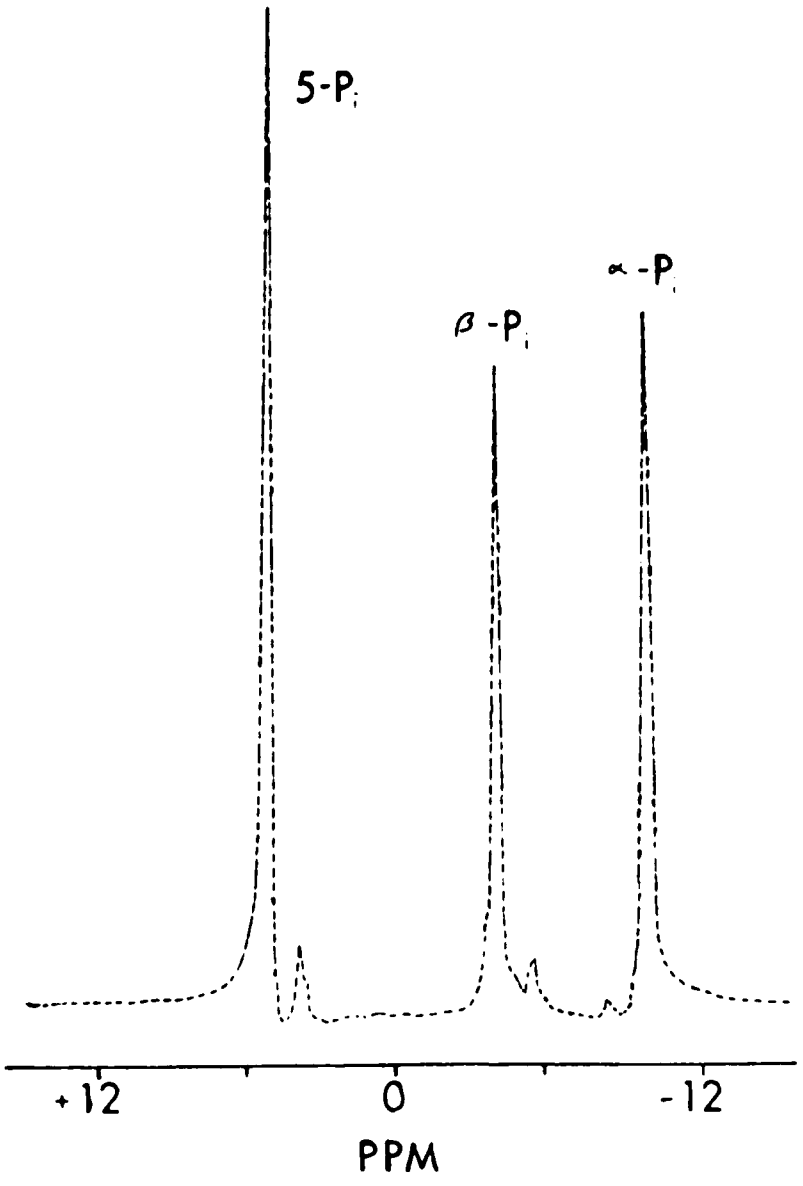
5-P$_i$
β-P$_i$
α-P$_i$
+12
0
-12
PPM

Figure 10

Plot of $T_{1_P}^{-1}$ values for three phosphates of PRibPP vs. Mn(II) concentration for binary complex PRibPP-Mn(II). In this figure ●—● , ◑—◑ , and ◐—◐ respresent 5'-phosphate, α -phosphate and β -phosphate respectively.

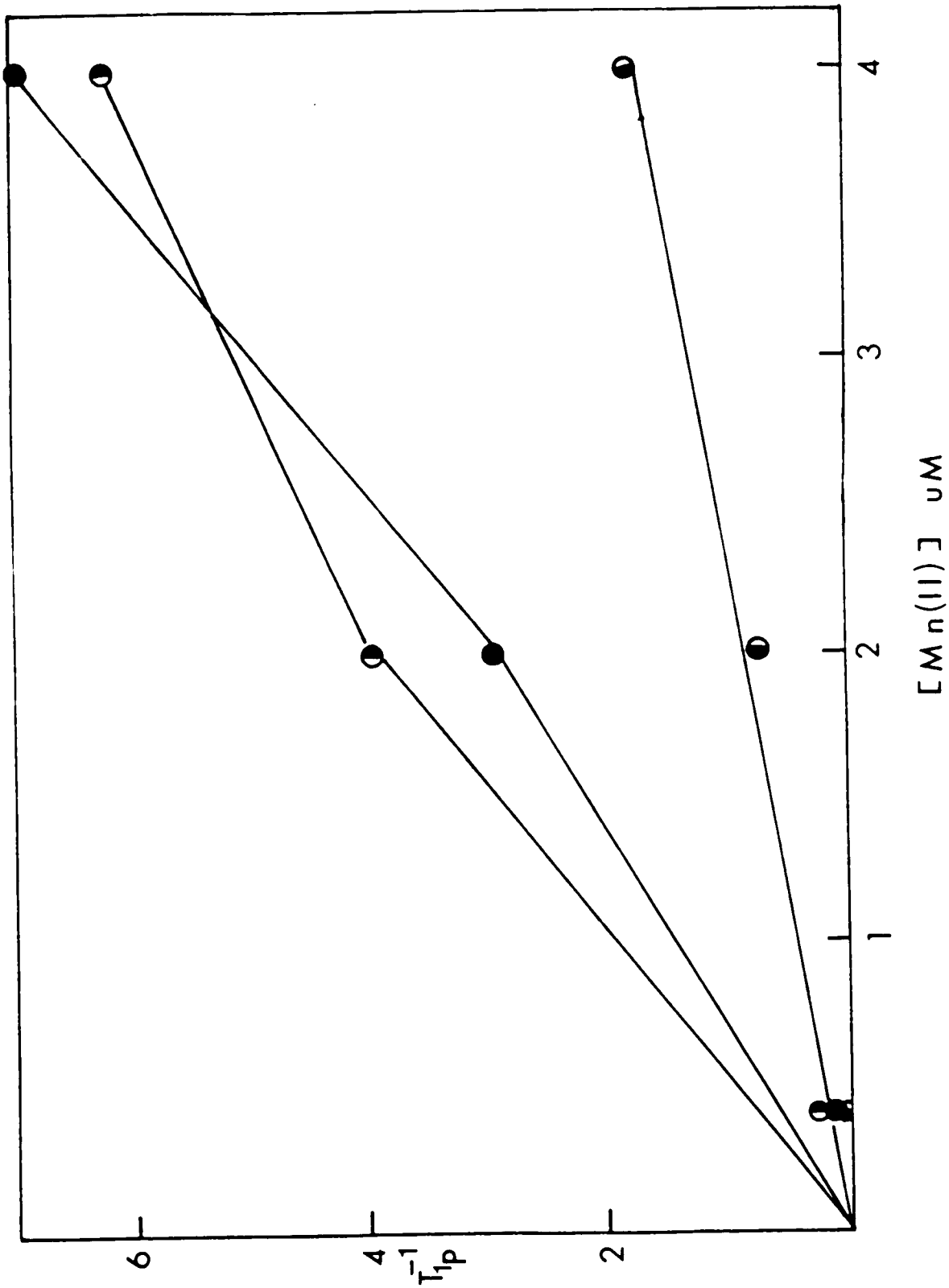
6
4
2
T_{1p}^{-1}
1
2
3
4
[Mn(II)] uM

Table 9: The Effects of Paramagnetic Mn(II) on the Longitudinal and Transverse Relaxation Rates of the Phosphorus Atoms of PRibPP in Solution and Bound to OPRTase and HGPRTase.

Experimental Conditions	$fT_{1_P}^{-1}$ ($\times 10^{-3}$)			$fT_{2_P}^{-1}$ ($\times 10^{-3}$)		
	5-P_i	-P_i	-P_i	5-P_i	-P_i	-P_i
10mM PRibPP (1/f = 25000) 0.4uM Mn(II)	1.5	3.9	1.9	128	295	321
10mM PRibPP (1/f = 5000) 2uM Mn(II)	3.5	14.8	15.5	231	303	270
10mM PRibPP (1/f = 2500) 4uM Mn(II)	4.7	17.6	15.5	167	280	266
10mM PRibPP (1/f = 2500) 4uM Mn(II) 241uM OPRTase	0.34	2.1	2.0	46	89	127
10mM PRibPP (1/f = 2500) 4uM Mn(II) 107uM OPRTase	0.39	2.4	2.3	61	70	86
10mM PRibPP (1/f = 2500) 4uM Mn(II) 53.5uM OPRTase	0.34	2.1	2.0	49	67	79
Extrapolated (OPRTase)***	0.36	2.1	2.4	-	-	-
10mM PRibPP 4uM Mn(II) 541uM HGPRTase	1.5	9.7	3.2	196	101	108
10mM PRibPP 4uM Mn(II) 271uM HGPRTase	1.6	6.9	5.0	285	123	149
10mM PRibPP 4uM Mn(II) 135.25uM HGPRTase	5.0	11.9	7.1	336	174	158
Extrapolated (HGPRTase)***	1.0	6.8	2.4	-	-	-

Table 9 : The Effects of Paramagnetic Mn(II) on the Longitudinal and Transverse Relaxation Rates of the Phosphorus Atoms of PribPP in Solution and Bound to OPRTase and HGPRTase.

(Continuation)

*The $f\,T_{1_P}^{-1}$ value of each phosphorus atom was calculated from average $1/T_1$ values obtained by three different plotting methods.

** $f\,T_{2_P}^{-1}$ values were calculated from $1/T_2$ values obtained by multiplying the line widths at ½ peak height by π .

***The values of $f\,T_{1_P}^{-1}$ were obtained by extrapolating plots of log $1/f\,T_{1_P}$ vs. the reciprocal of the respective enzyme concentration to infinite enzyme concentration.

exchange limited and may therefore be used to calculate interatomic distances (Mildvan and Cohn, 1966; Nowak and Mildvan, 1972). To test whether the rate of PRibPP exchange made any contribution to the observed relaxation rate (Equation 13), the fastest measured relaxation rate ($fT_{2_P}^{-1}$) of α -phosphate was used to set the lower limit of τm^{-1} to estimate the maximum contribution of τm to $fT_{1_P}^{-1}$. This calculated adjustment did not yield any significant change in $fT_{1_P}^{-1}$ values and therefore no resultant adjustment in Mn(II)-to-phosphorus distances was required.

$$fT_{1_P}^{-1} = \frac{1}{(T_{1_M} - \tau m)} \qquad (13)$$

Thus, the observed values of $fT_{1_P}^{-1}$ of phosphorus atoms of binary Mn(II)-PRibPP complex are essentially equal to their respective $T_{1_M}^{-1}$ values and thus an exchange contribution is negligible. A similar criterion was applied to the relaxation rates of the protons of binary and ternary complexes of PRibPP described earlier (vide infra) with same results.

Mn(II)-phosphorus distances for the binary Mn(II)-PRibPP complex were evaluated using a $f(\tau c)$ value of 3.0×10^{-10} as well as individually calculated values of $f(\tau c)$ based on T_{1_P}/T_{2_P} values using Equation 12 (Table 10). The distances reported in Table 11 are therefore mean averages of the calculated distances using these different $f(\tau c)$ values. These distances reveal that the α - and β -phosphate groups of PRibPP are directly co-ordinated to the metal ion in a bidentate manner whereas a distance of 4.0 ± 0.2 Å for 5'-phosphate disallows direct co-ordination.

In the presence of OPRTase and HGPRTase, extrapolation of the

Table 10: Calculated τ_c and $f(\tau_c)$ Values Derived from the Individual or Extrapolated T_{1_P}/T_{2_P} ratios of Phosphorus Atoms of PRibPP.

Experimental Conditions		5-P_i	β-P_i	α-P_i
PRibPP-Mn(2uM)	τ_c	8.43×10^{-9}	5.34×10^{-9}	4.09×10^{-9}
	$f(\tau_c)$	3.39×10^{-9}	5.25×10^{-10}	6.69×10^{-10}
PRibPP-Mn(4uM)	τ_c	7.0×10^{-9}	4.05×10^{-10}	4.43×10^{-9}
	$f(\tau_c)$	4.05×10^{-10}	5.24×10^{-10}	6.2×10^{-10}
PRibPP-Mn(II)-OPRTase	τ_c	15.5×10^{-9}	5.29×10^{-9}	6.23×10^{-9}
	$f(\tau_c)$	1.80×10^{-10}	5.29×10^{-10}	4.5×10^{-10}
	τ_c	12.6×10^{-9}		
	$f(\tau_c)$	2.28×10^{-10}		
	τ_c	10.4×10^{-9}		
	$f(\tau_c)$	2.75×10^{-10}		
PRibPP-Mn(II)-HGPRTase	τ_c	14.17×10^{-9}	3.57×10^{-9}	7.25×10^{-9}
	$f(\tau_c)$	2.03×10^{-10}	7.5×10^{-10}	3.92×10^{-10}
	τ_c	11.78×10^{-9}		
	$f(\tau_c)$	2.44×10^{-10}		

Table 11: Calculated Distances (in Å) Between the Phosphorus Atoms of PRibPP and Mn(II) in Solution and Bound to OPRTase and HGPRTase.

Experimental Conditions	Phosphorus		
	5'-P_i	β-P_i	α-P_i
PRibPP-Mn(II)*	4.0 ± 0.2	3.3 ± 0.2	3.2 ± 0.2
PRibPP-Mn(II)-OPRTase**	5.5 ± 0.2	4.3 ± 0.2	4.3 ± 0.2
PRibPP-Mn(II)-HGPRTase**	4.4 ± 0.5	3.8 ± 0.3	4.0 ± 0.3

*An $f(\tau_c)$ value for Mn(II) complexes in solution of 0.3×10^{-9} seconds as well as individually calculated $f(\tau_c)$ values from T_{1_P}-to-T_{2_P} ratios were employed in these calculations.

**Values of $f(\tau_c)$ for the OPRTase and HGPRTase-bound Mn(II) complexes of PRibPP were determined by extrapolating a plot of the T_{1_P}-to-T_{2_P} ratios vs. the reciprocal of the enzyme concentration. The extrapolated ratios were then used to calculate $f(\tau_c)$ values for individual phosphorus atoms.

Figures 11A and 11B

Plots of log $fT_{1_P}^{-1}$ vs. $\frac{1}{[E]}$ for the three phosphorus atoms of PRibPP in Tris pH 8.0 in the presence of 4.0uM Mn(II). In both figures ●—● , ◑—◑ and ◐—◖ represent the 5'-phosphate, β -phosphate and α -phosphate atoms respectively. In Figure 11A [E] is OPRTase and in Figure 11b [E] is HGPRTase. The extrapolated values of $fT_{1_P}^{-1}$ obtained from these plots were used to calculate distances (r) for these phosphorus nuclei from paramagnetic metal, Mn(II) in the PRibPP-Mn(II)-OPRTase and PRibPP-Mn(II)-HGPRTase complexes as described in the text.

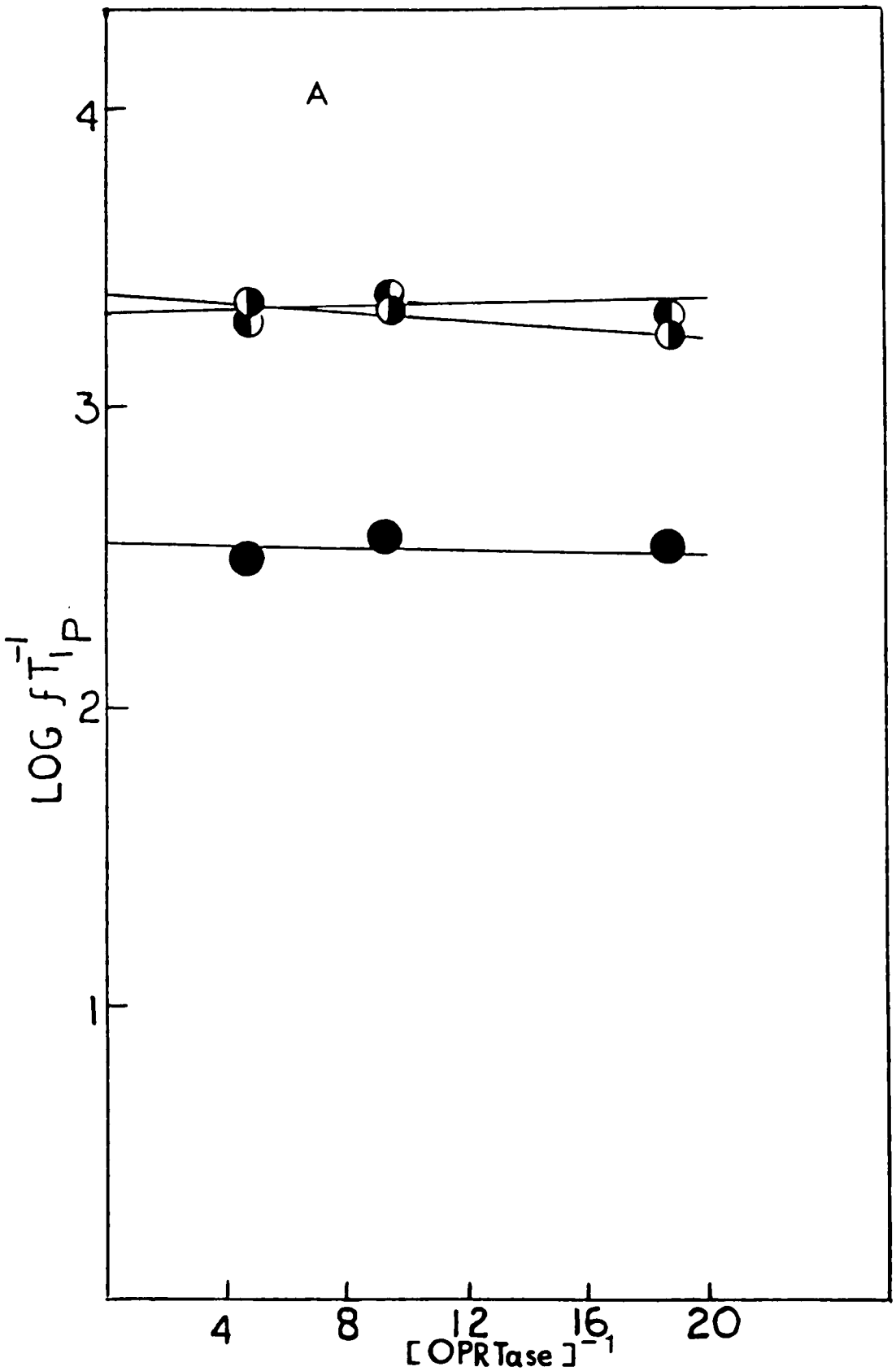
A
4
3
2
1
LOG fT^{-1}_{1P}
4
8
12
16
20
$[OPRTase]^{-1}$

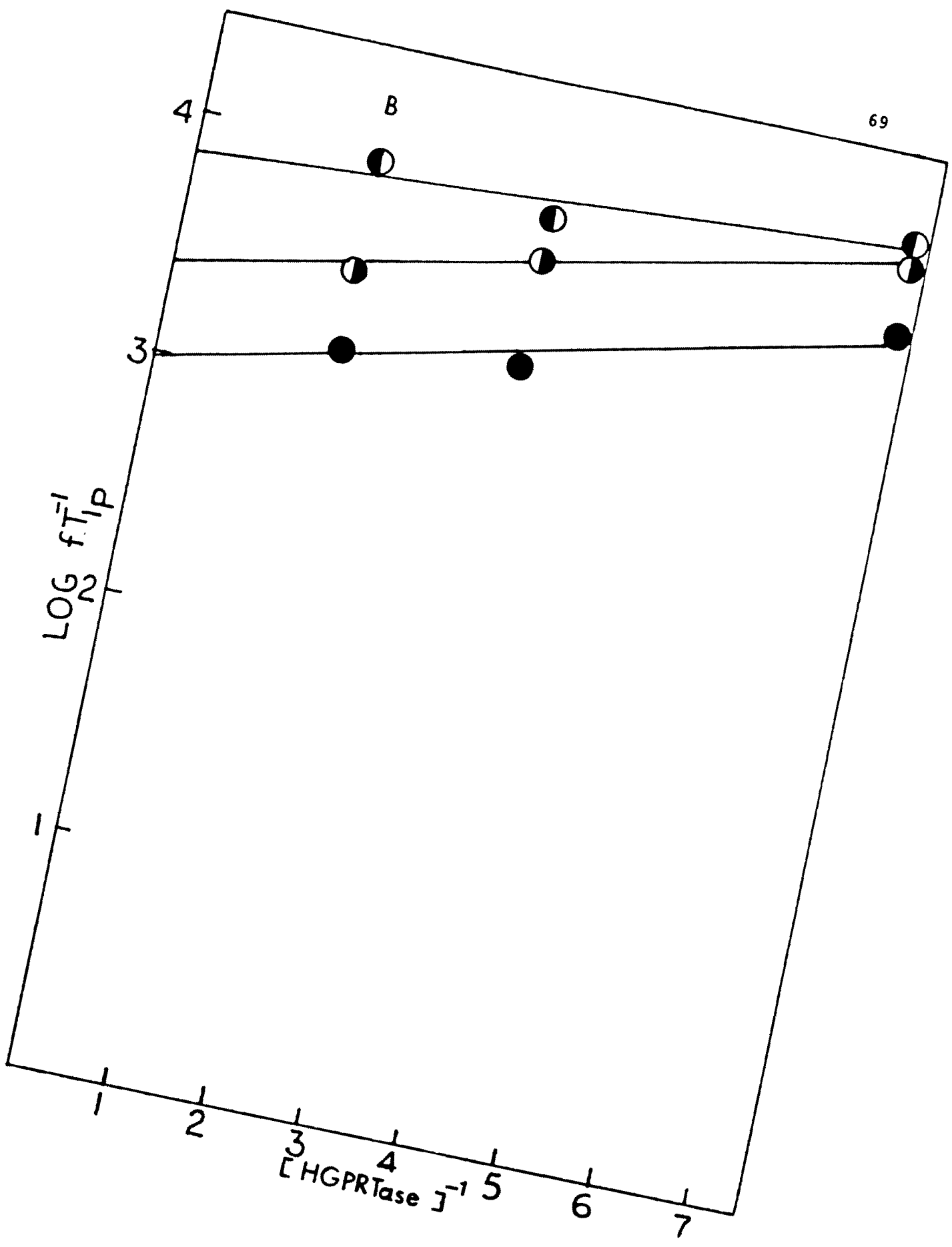
B
69
4
3
2
1
LOG $fT^{-1}_{1/2}$
1
2
3
4
5
6
7
[HGPRTase]$^{-1}$

$f T_{1_P}^{-1}$ values at three different concentrations of each enzyme to infinite enzyme concentration (Figure 11) yielded $f T_{1_P}^{-1}$ values for the ternary enzyme Mn(II)-PRibPP complexes (Table 9). Such extrapolations resulted in changes of $f T_{1_P}^{-1}$ values of 20% for OPRTase and 79% for HGPRTase from those directly measured at highest enzyme concentrations. Moreover, the values of $f T_{1_P}^{-1}$ are independent of OPRTase concentration perhaps because all of the Mn(II) resides at a tight metal binding site on this enzyme. In all cases the largest observed paramagnetic effect on the transverse relaxation rate ($T_{2_P}^{-1}$) is more than four fold greater than the observed values of $T_{1_P}^{-1}$ indicating as stated previously that $fT_{1_P}^{-1}$ values cannot be exchange-limited. Interestingly, the order of magnitude of $fT_{1_P}^{-1}$ for the three phosphates of PRibPP was $\beta \geq \alpha > 5$ P_i. This order remained the same even when the Mn(II)-PRibPP was enzyme bound, suggesting that metal always resided nearest to the pyrophosphate group. Upon binding to either enzyme the $f T_{1_P}^{-1}$ values of the phosphorus atoms of PRibPP decreased significantly, since the substrate motion is now governed by a different correlation time. The magnitude of this decrease was observed to be smaller for HGPRTase than for OPRTase, even though these enzymes are approximately the same size, indicating that the metal may be more tightly held by the pyrophosphate group of PRibPP on the HGPRTase active site than on OPRTase active site.

The calculation of Mn(II)-to-phosphorus distances requires an accurate determination of the correlation time (τ_c). In instances where the plots of T_{1_P} to T_{2_P} ratios vs. 1/enzyme concentration (Figure 12 A and B) were non-linear, maximum and minimum ratios of T_{1_P}/T_{2_P} were used to calculate τ_c and from it the $f(\tau_c)$. The extent of uncertainty in the distance calculations by making use of this range of τ_c values was

Figures 12A and 12B

T_{1_P}/T_{2_P} ratios are plotted vs. $\frac{1}{[E]}$ for different phosphorus nuclei of PRibPP-Mn(II)-OPRTase (12A) and PRibPP-Mn(II)-HGPRTase (12B) complexes, to obtain extrapolated T_{1_P}/T_{2_P} values. The extrapolated T_{1_P}/T_{2_P} values thus obtained were used to calculate τ_c and $f(\tau_c)$ values for these nuclei. In both figures, 5'-, α- and β- phosphate are represented by ●—● , ◑—◑ and ◐—◐ respectively.

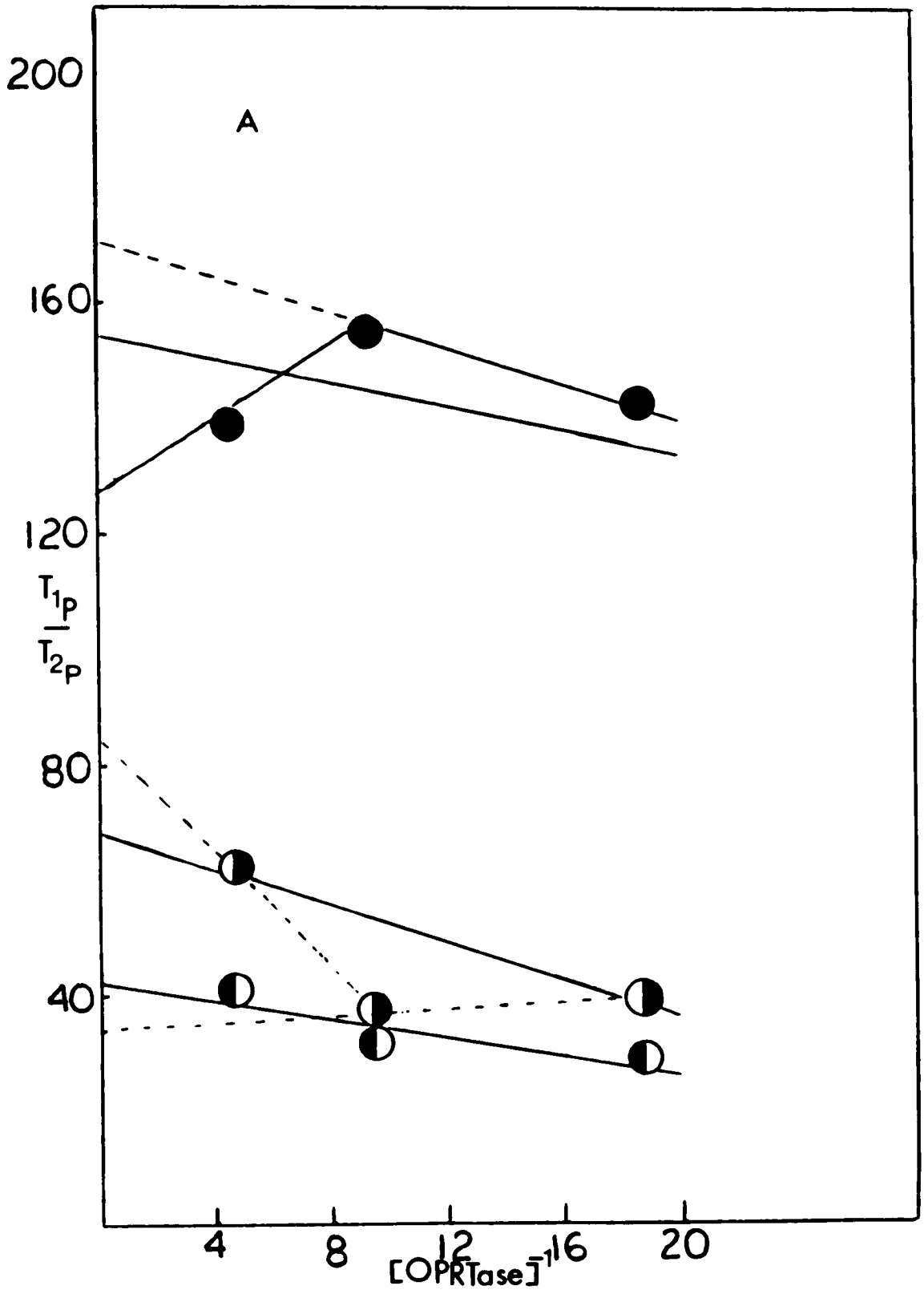
200
160
120
80
40
A
$\frac{T_{1P}}{T_{2P}}$
4
8
12
16
20
[OPRTase]$^{-1}$

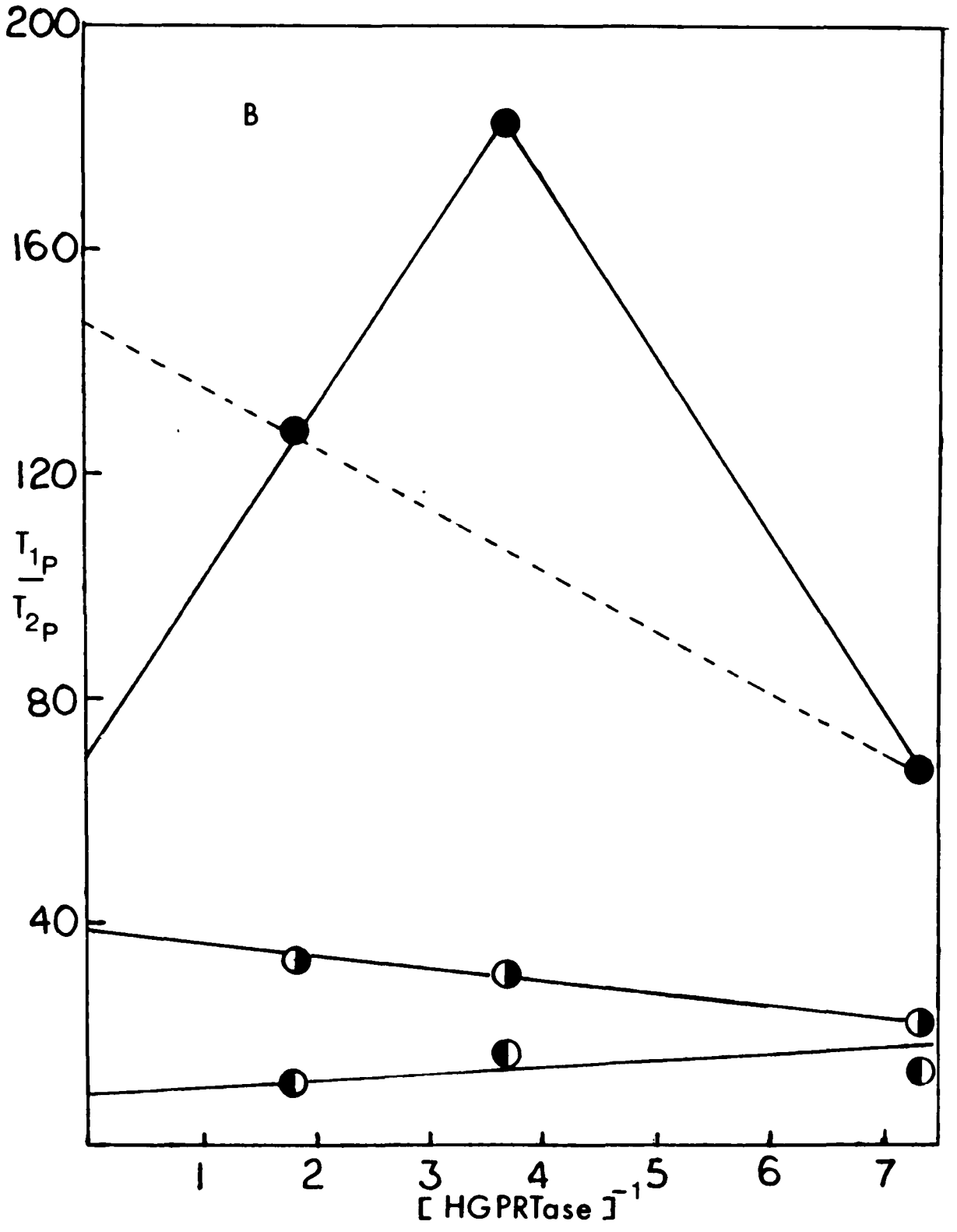
200
160
120
80
40
B
$\frac{T_{1P}}{T_{2P}}$
1
2
3
4
5
6
7
[HGPRTase]$^{-1}$

calculated to be less than 10%. Moreover, for the binary Mn(II)-PRibPP complex, individual T_{1_P}/T_{2_P} ratios were used to calculate τ_c to estimate the maximum error in the distance calculations which was also 10%. The various τ_c and $f(\tau_c)$ values thus calculated for the phosphorus atoms of PRibPP are listed in Table 10.

From crystallographic and metal binding studies reviewed elsewhere (Mildvan and Grisham, 1974; Mildvan, et al., 1973), the Mn(II)-to-phosphorus distance for an inner sphere monodentate complex of tetrahedral phosphate is 3.0 ± 0.2 Å. For an axial complex of a pentacoordinated phosphorus (i.e. a distorted inner sphere complex) the distance is 3.6 ± 0.2 Å. For Mn(II) chelated by an adjacent phosphate in a polyphosphate chain the distance would be 4.9 ± 0.4 Å, and for a secondary sphere complexation having another inner sphere ligand such as H_2O residing between the Mn(II) and phosphorus atom, the distance is 6.1 ± 0.5 Å. As noted previously for the binary Mn(II)-PRibPP complex, the r (distance) values (Table 11) indicated direct metal co-ordination to the α - and β -phosphates and perhaps a distorted inner sphere complexation for 5'-phosphate. In the ternary OPRTase-Mn(II)-PRibPP complex, the α -and β -phosphate distances of 4.3 ± 0.2 Å suggested that the inner sphere co-ordination is quite distorted whereas the distance of 5.5 ± 0.2 Å for the 5'-phosphate indicated that only second sphere co-ordination if any, might exist. Alternatively there may be a partial contribution to T_{1_P} by T_{1_M} under these conditions. In the case of the HGPRTase-bound Mn(II)-PRibPP, both the α-and β -phosphate distances (4.0 ± 0.3 and 3.8 ± 0.3 respectively) were indicative of distorted inner sphere co-ordination. The 5'-phosphate of HGPRTase-bound PRibPP-Mn(II) exhibited a distance suggestive of a highly distorted inner

sphere co-ordination or chelation to Mn(II) in a polyphosphate chain suggesting that metal ion might still interact with all three phosphorus atoms at the HGPRTase active site.

CONFORMATION OF Mn(II)-PRibPP FREE AND COMPLEXED WITH YEAST OPRTase AND HGPRTase

The eight PRibPP metal-to-nucleus distances (Tables 8 and 11) determined from the $f T_{1_P}^{-1}$ values were used to construct models for the conformation of the binary Mn(II)-PRibPP, ternary OPRTase-Mn(II)-PRibPP and ternary HGPRTase-Mn(II)-PRibPP complexes. The models which are shown in Figures 13A, 13B and 13C were constructed with as much staggering of phosphorus oxygen atoms and 2'-endo-puckering of ribose ring as the distances would allow. In the case of the binary Mn(II)-PRibPP complex, all of the phosphate atoms are positioned towards the metal ion. The α - and β -phosphates were directly co-ordinated to metal (bidentate co-ordination) whereas 5'-phosphate might be co-ordinated via a second sphere water interaction (Figure 13). In the case of OPRTase-bound PRibPP-Mn(II) complex, the Mn(II)-to-phosphorus interaction between α -and β -phosphates are still bidentate but could be via an axial oxygen atom. The enzyme bound ribose ring still could exhibit the desired 2'-endo configuration, but was positioned further away from the metal ion as the 5'-phosphate lost the ability to coordinate with metal ion on OPRTase. This resulted in an increase of 0.8 $\mathring{A}$ in the metal ion to ribose distance (as measured from the center of ribose ring). In the case of the HGPRTase-Mn(II)-PRibPP complex, the α- and β -phosphates also remained bidentate. However, the β -phosphate metal distance was less distorted (as determined by the extent of increase of the distances from 3 $\mathring{A}$) than this distance on OPRTase. The 5'-phos-

Figures 13A, 13B and 13C Conformations of Free and Bound PRibPP

The eight PRibPP metal to nuclei distances are depicted in Tables 8 and 11 were utilized to construct models for the conformations of binary Mn(II)-PRibPP (Figure 13A), ternary OPRTase-Mn(II)-PRibPP (Figure 13B) and ternary HGPRTase-Mn(II)-PRibPP (Figure 13C) complexes. These models as shown in these figures were constructed with as much staggering of phosphorus oxygen atoms and 2'-endo puckering of ribose ring as the distances would allow.

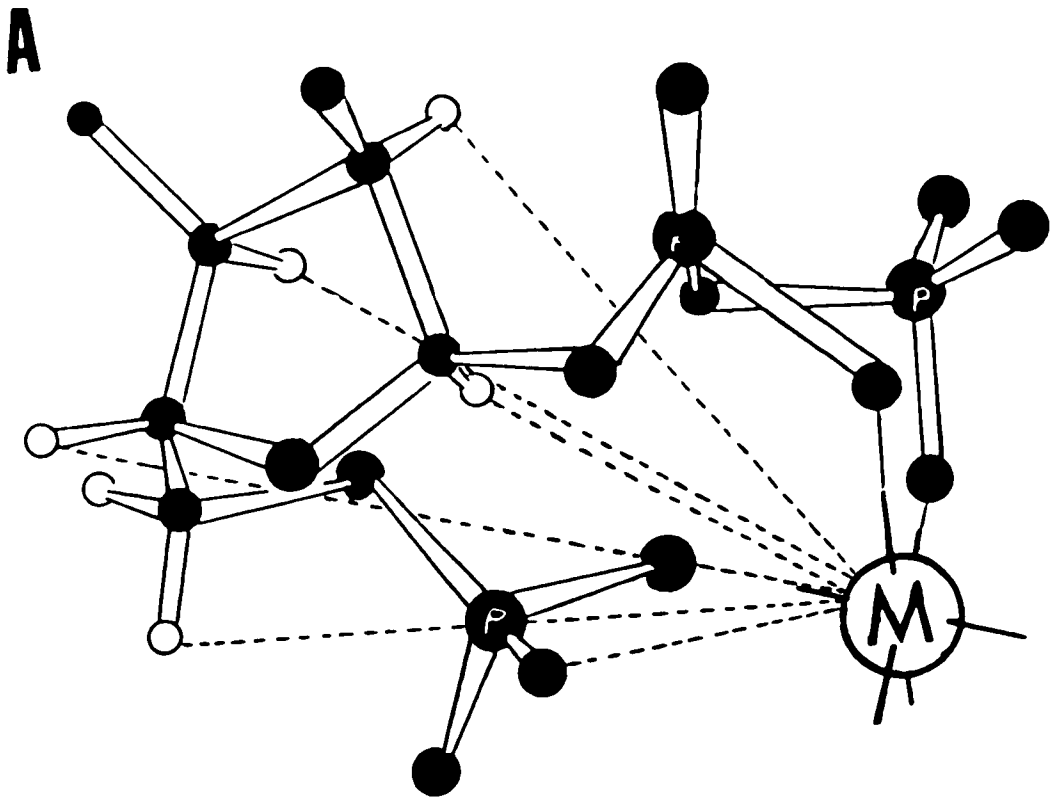
A
P
P
M

B

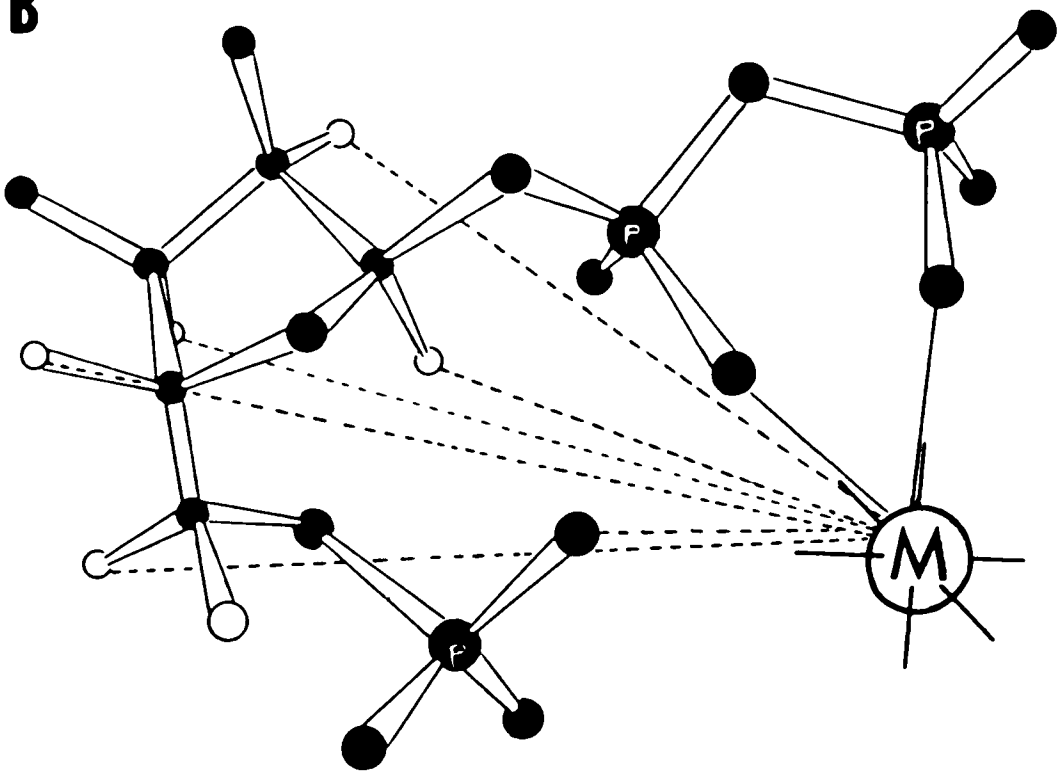

C

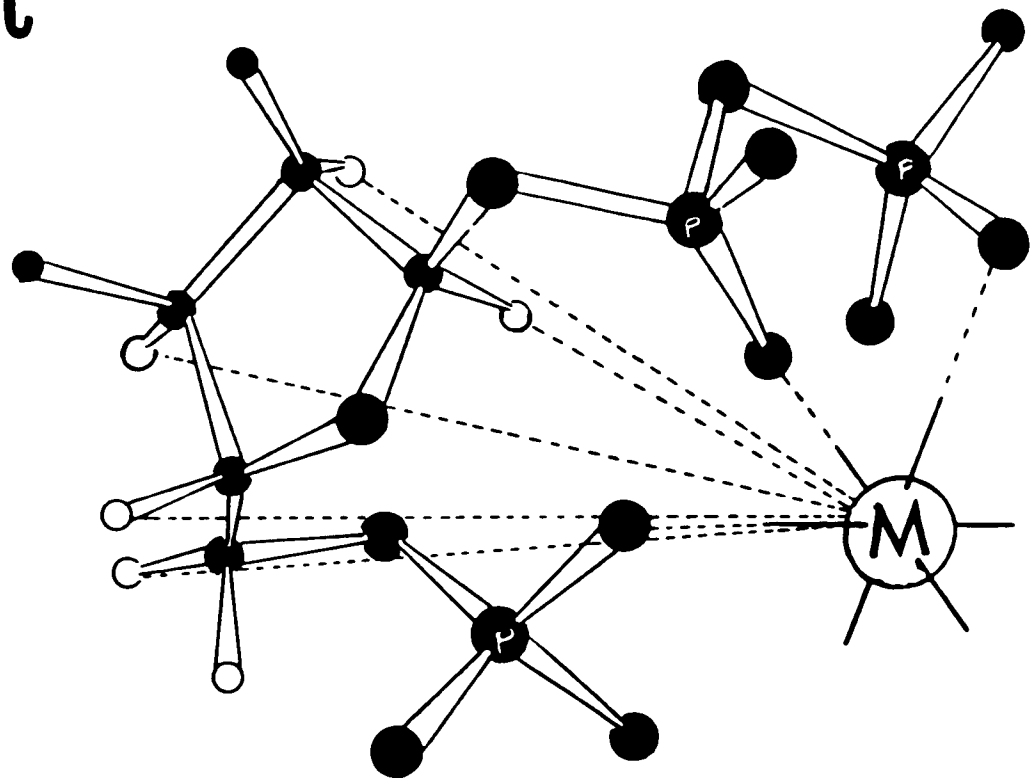

phate-metal ion distance was found to be consistent with a highly distorted direct co-ordination. The ribose ring of HGPRTase-bound PRibPP was also observed to be positioned further away from the metal by a distance of 0.7 Å. These subtle differences thus observed between the ternary enzyme complexes might explain in part the difference in the mechanism of action displayed by these enzymes, since the PRibPP conformation on HGPRTase allows most readily an on-line displacement of pyrophosphate at the C-1 ribose position.

INHIBITION STUDIES WITH Cr(III)PP_i AND Mg(II)PP_i

Characterization of Cr(III)PP_i. Cr(III)PP_i prepared by method of Merrit, et al., (1981) was characterized to be at least 97% pure. The inorganic PO_4 content was less than 0.5mM or 1.5 percent of total phosphate. Cr(III)PP_i ratio was determined to be 1:0.9. Na ion and K ion contents were neglegible (0 - 2 meq/l and 0 meq/l, respectively), as determined by flame photometry. When scanned for absorbance maxima, the Cr(III)PP_i thus prepared exhibited peaks at 425 nm and 595 nm in exact agreement with the observations of Merrit, et al., (1981).

Cr(III)PP_i as Substrate for the OPRTase Reverse Reaction. Cr(III)PP_i served as a substrate for the OPRTase reverse reaction but only in the presence of $MgCl_2$. Figure 14 depicts the resulting plot of $\frac{1}{V}$ vs. $\frac{1}{[Cr(III)PP_i]}$. The Vmax, as determined at the y-intercept, is 0.0114 (absorbance units/minute) with the Km value equal to 130 ± 20uM. In comparison, the Km of Na(I)PP_i for the same preparation of OPRTase was found to be 40 ± 4.0uM.

Effect of Cr(III)PP_i on the Reverse Activity of OPRTase. The results of the effect of Cr(III)PP_i on the reverse pyrophosphorolysis ac-

Figure 14

Double reciprocal plot of initial velocity (V) vs. varied concentration of Cr(III)PP_i. Besides Cr(III)PP_i the assay mixture consisted of 50uM orotidine monophosphate (OMP), 1000uM $MgCl_2$, 10ul of OPRTase made to 1.0ml with 20mM Tris buffer pH 8.0. Δ A/min was measured at 295 nm.

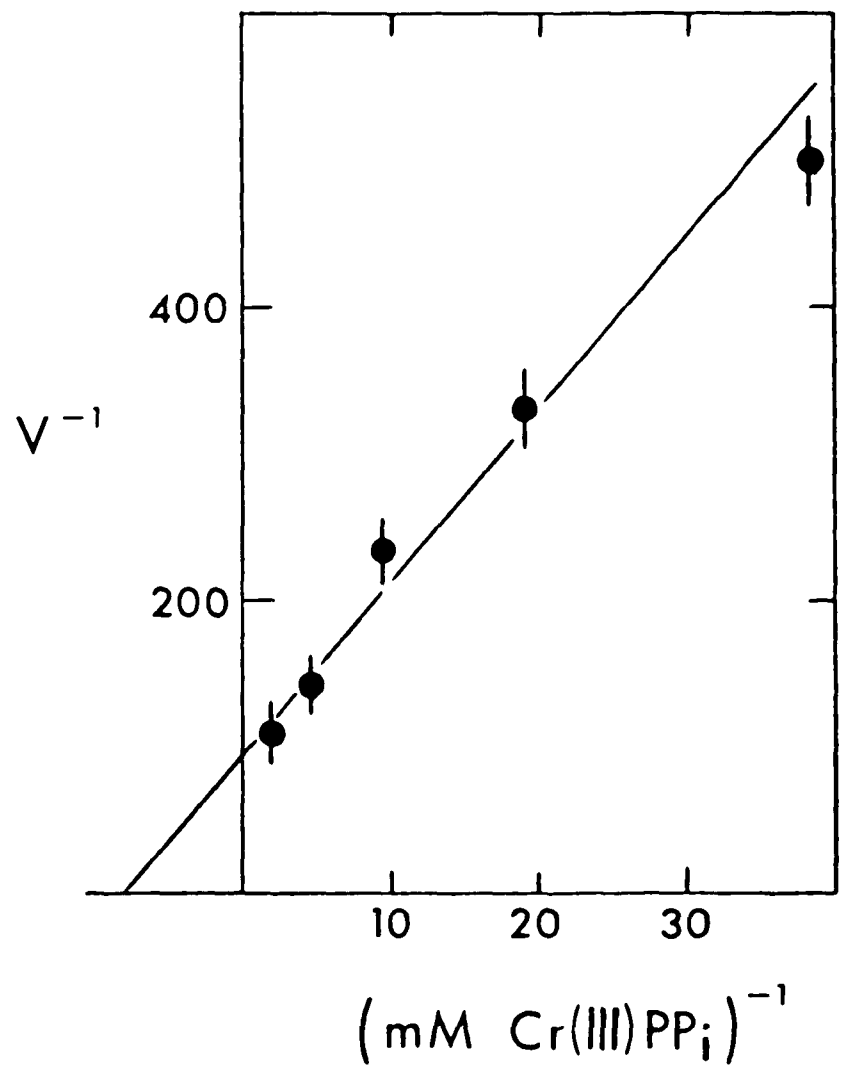
400
200
V^{-1}
10
20
30
$(mM\ Cr(III)PP_i)^{-1}$

tivity of OPRTase are shown in Figures 15A and 15B. As both figures illustrate, changing the Cr(III)PP_i concentration had little effect on the reverse reaction of OPRTase. The slight differences in slope and y-intercept exhibited in Figures 15A and 15B occur because two different enzymic activities were used in each case. However, all other parameters were same, and when these two figures are normalized the results merged. Overall, this result suggests that the true substrate [Mg(II)PP_i] dominates the kinetics of this reaction under these conditions.

Effect of Mg(II)PP_i and Cr(III)PP_i on the forward activity of OPRTase and HGPRTase. The effect of Na(I)PP_i and Cr(III)PP_i on the OPRTase forward reaction in presence of 1mM $MgCl_2$ are shown in Figure 16A and 16B respectively. As is illustrated in these figures, both show mixed-type non-competitive inhibition. The α values were determined from the replots of the slopes and $\frac{1}{Vmax_{app}}$ vs. concentration of Na(I)PP_i (Table 12 and Figure 17A) and vs. concentration of Cr(III)PP_i (Table 12 and Figure 17B). The factor α is the factor by which K_s changes when I occupies the enzyme. These replots were constructed by utilizing equations 14, 15 and 16 below, where I = Na(I)PP_i or Cr(III)PP_i, S = PRibPP, (from Segel, 1975). The α values were 6 and 3.39 respectively. The corresponding K_i values were 60uM for Na(I)PP_i and 620uM for Cr(III)PP_i.

$$\frac{1}{V} = \frac{Ks}{Vmax}\left(1 + \frac{[I]}{K_i}\right)\frac{1}{[S]} + \frac{1}{Vmax}\left(1 + \frac{[I]}{\alpha K_i}\right) \quad (14)$$

$$\text{Slope} \quad \frac{1}{[S]} = \frac{Ks}{K_i\, Vmax}[I] + \frac{Ks}{Vmax} \quad (15)$$

$$\text{y intercept} \quad \frac{1}{Vmax_{app}} = \frac{1}{\alpha K_i\, Vmax}[I] + \frac{1}{Vmax} \quad (16)$$

Figures 15A and 15B

Double reciprocal plots of initial velocities (V) of the OPRTase catalyzed pyrophosphorolysis vs. varied concentration of PP_i at 50uM OMP, 1000uM $MgCl_2$ in 20mM Tris pH 8.0 with two different enzyme preparation. $Cr(III)PP_i$ concentration used in experiment exhibited in Figure 15A were 0uM (open circles), 52uM (solid squares), 208uM (open squares), 520uM (open triangles and 1040uM (solid circles). Similarly in Figure 15B, open circles, open squares, solid circles and open triangles represent 0uM, 523uM, 1045uM and 1568uM $Cr(III)PP_i$ respectively. The value of the intercept for the standard plot (no $Cr(III)PP_i$) in Figure 15A is 19.6 ± 0.4 while in Figure 15B it is 25.5 ± 0.6, yielding a normalizing factor of 1.3 for comparison of these figures.

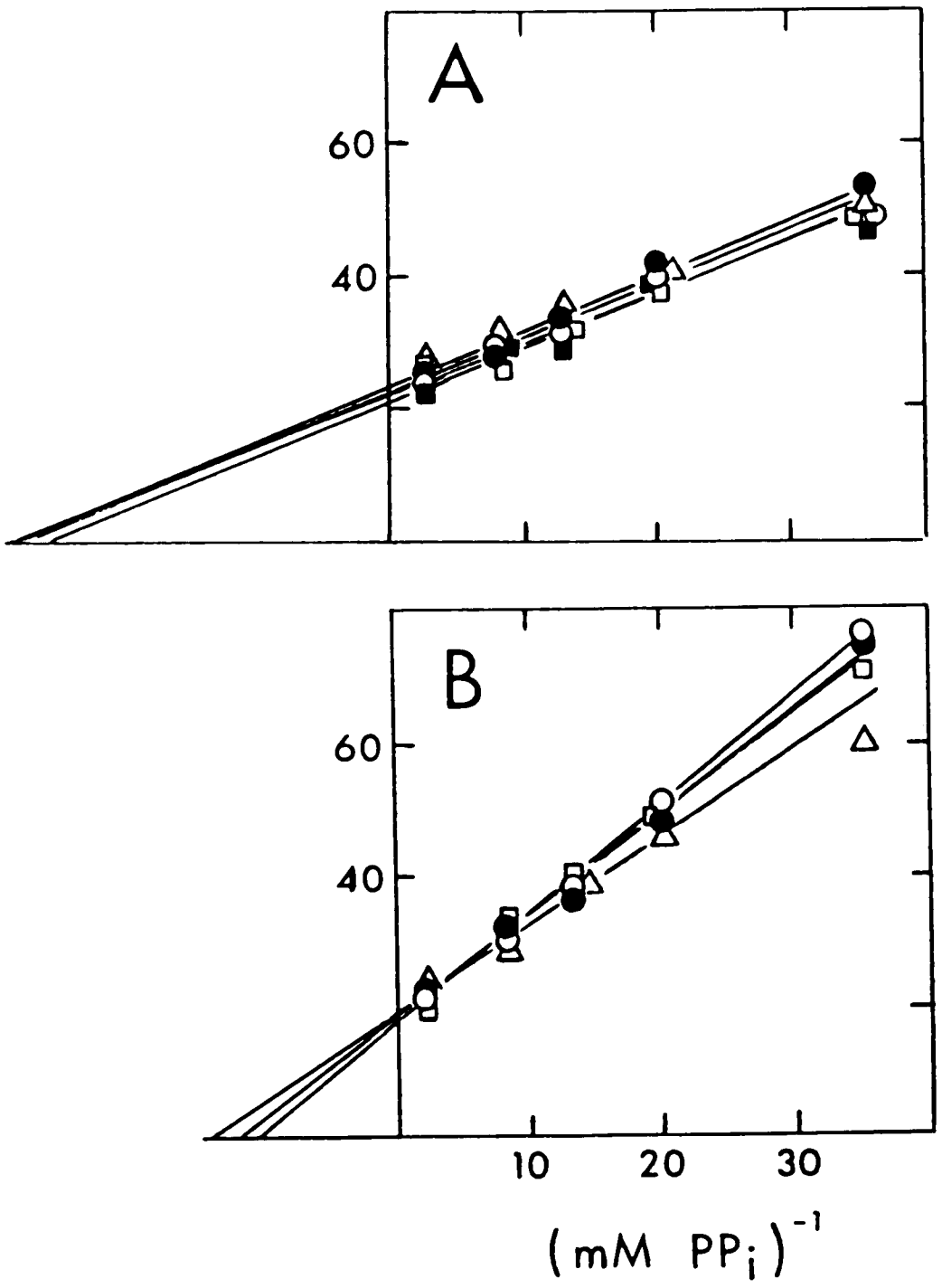
A
60
40
B
60
40
10
20
30
(mM PPi)-1

Figure 16A and 16B

Double reciprocal plots of initial velocities (V) vs. varied concentrations of PRibPP at fixed different concentrations of Na(I)PP_i (16A) and Cr(III)PP_i (16B) for the forward activity of OPRTase. In Figure 16A solid circles represent 0uM, open circles 190uM and semi-solid circles 625uM Na(I)PP_i respectively. In Figure 16B the concentrations of Cr(III)PP_i used were 0uM (solid circles), 260uM (open circles) and 870uM (open triangles). The concentrations of orotate and $MgCl_2$ used in these assays were 150uM and 1000uM respectively.

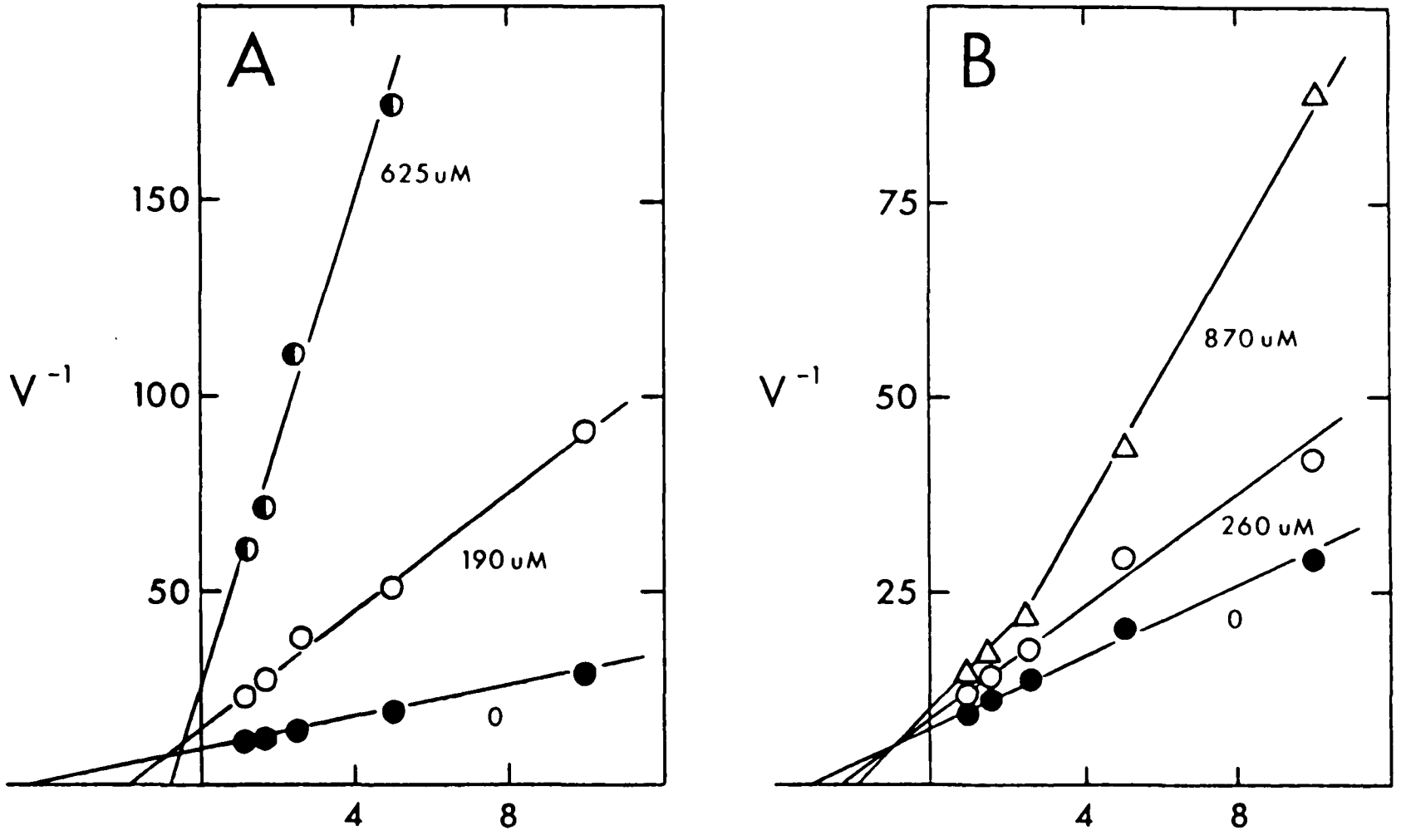
A
B
V⁻¹
150
100
50
75
25
4
8
625 uM
190 uM
0
870 uM
260 uM
0
(μM PRibPP)⁻¹ x 10²

Figures 16C and 16D

Double reciprocal plots of initial velocities (V) for HGPRTase forward activity in presence of 2000uM $MgCl_2$ vs. varied concentration of PRibPP at constant concentration of hypoxanthine (100uM) and different fixed concentrations of Na(I)PP_i (16C) and Cr(III)PP_i (16D), in 100mM Tris pH 7.4. The concentrations of Na(I)PP_i (16C) used were 0mM (solid circles), 1.0mM (open circles), 3.0mM (left hand semi-solid circles), 4.0mM (right hand semi-solid circles) and 6mM (lower bottom solid circles). In Figure 16D, open circles, solid circles and open triangles represent 0mM, 1mM and 6mM Cr(III)PP_i respectively. The effective PRibPP concentration range selected in these studies was 25uM - 200uM.

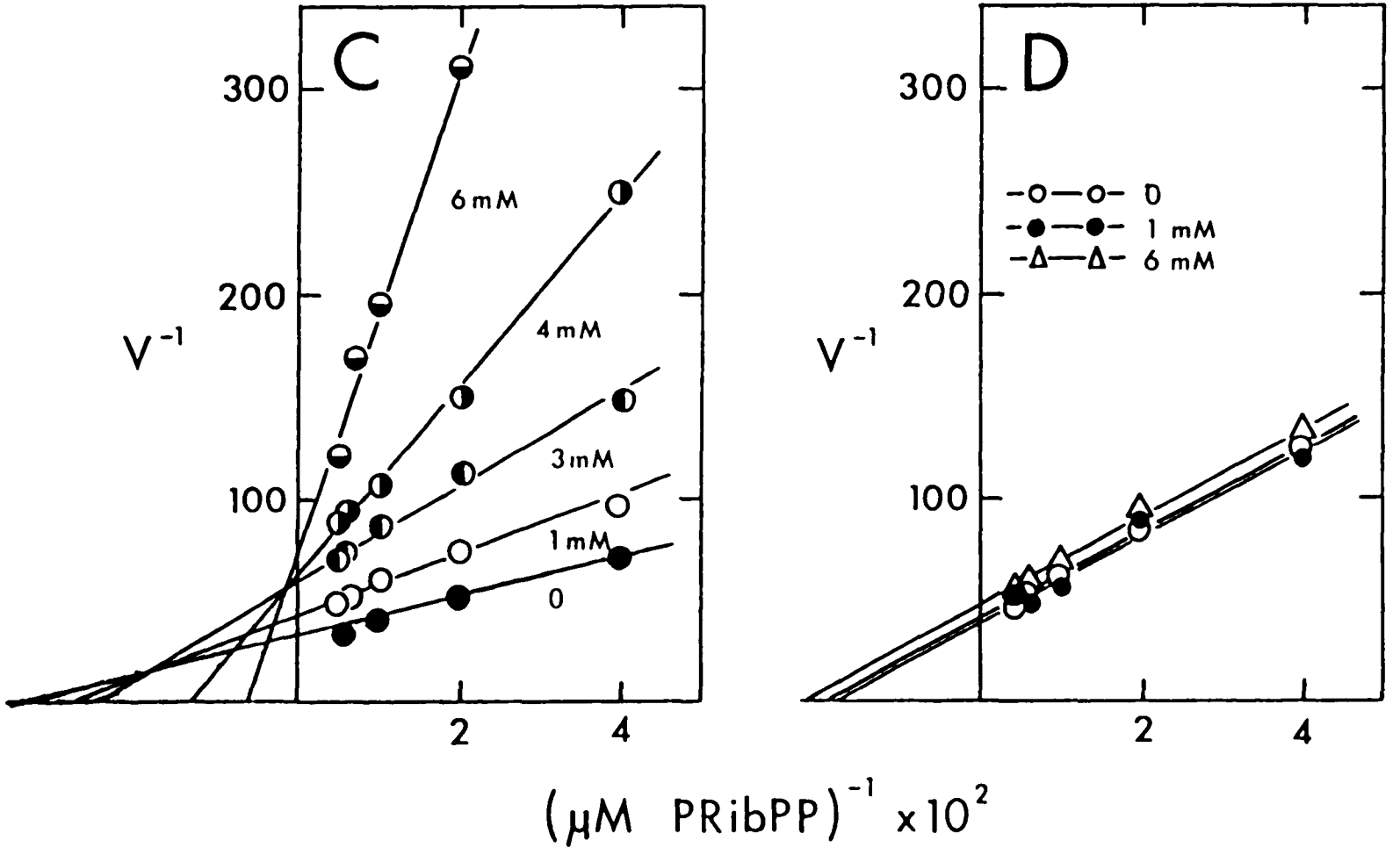
C
D
300
200
100
V^{-1}
6 mM
4 mM
3 mM
1 mM
0
2
4
0
1 mM
6 mM
$(\mu M\ PRibPP)^{-1} \times 10^2$

Table 12

Slope $\frac{1}{PRibPP}$ and $\frac{1}{V}$ axis intercept values as obtained from the double reciprocal plots of initial velocities vs. varied concentrations of PRibPP as depicted in Figures 16A, B and C.

Enzyme	$V^{-1}_{max_{app}}$	Slope	[Na(I)PP_i] uM	[Cr(III)PP_i] uM
OPRTase	9.52	2.08	0	-
	14.29	7.64	190	-
	25.4	31.75	625	-
	7.14	2.33	-	0
	8.33	3.67	-	260
	9.97	5.11	-	870
HGPRTase	31.75	9.52	0	-
	41.27	15.08	1000	-
	58.73	23.41	3000	-

Figures 17A, 17B and 17C

Slope $\frac{1}{PRibPP}$ and $\frac{1}{V}$ axis intercept replots of reciprocal plot data as shown in Figures 16A, 16B, and 16C. In Figure 17A top plot is slope vs. [Na(I)PP_i] where as the bottom plot $\frac{1}{V}$ intercept vs. [Na(I)PP_i] for the OPRTase forward reaction. Figure 17B depicts similar plots for OPRTase but [I] = Cr(III)PP_i]. Figure 17C exhibits the slope vs. [I], [I] = [Na(I)PP_i] and $\frac{1}{V}$ intercept replots for the forward reaction of HGPRTase. From the y and x axis intercept of these plots K_i and α values were calculated for the mixed type inhibition exhibited by Na(I)PP_i and Cr(III)PP_i for OPRTase and by Na(I)PP_i for the HGPRTase forward activities.

A

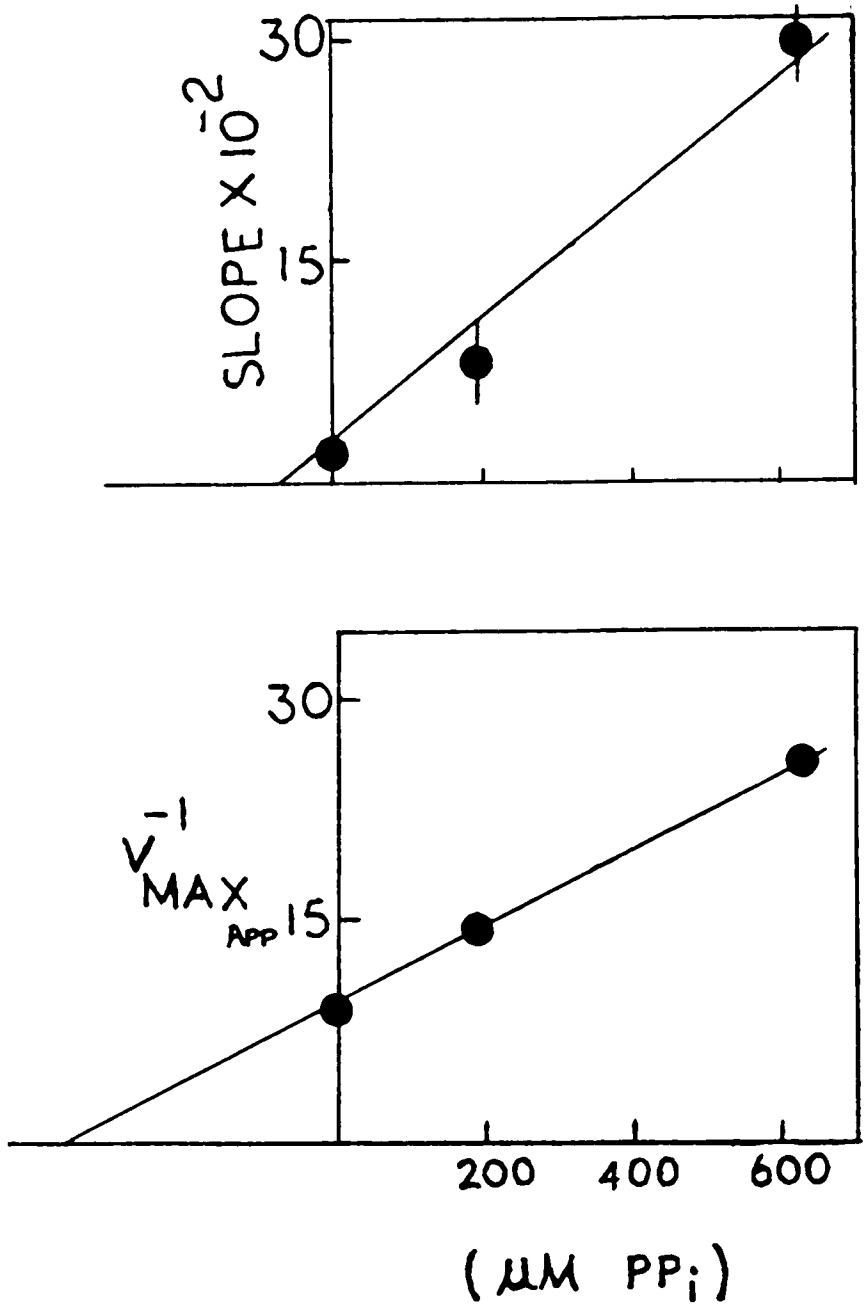

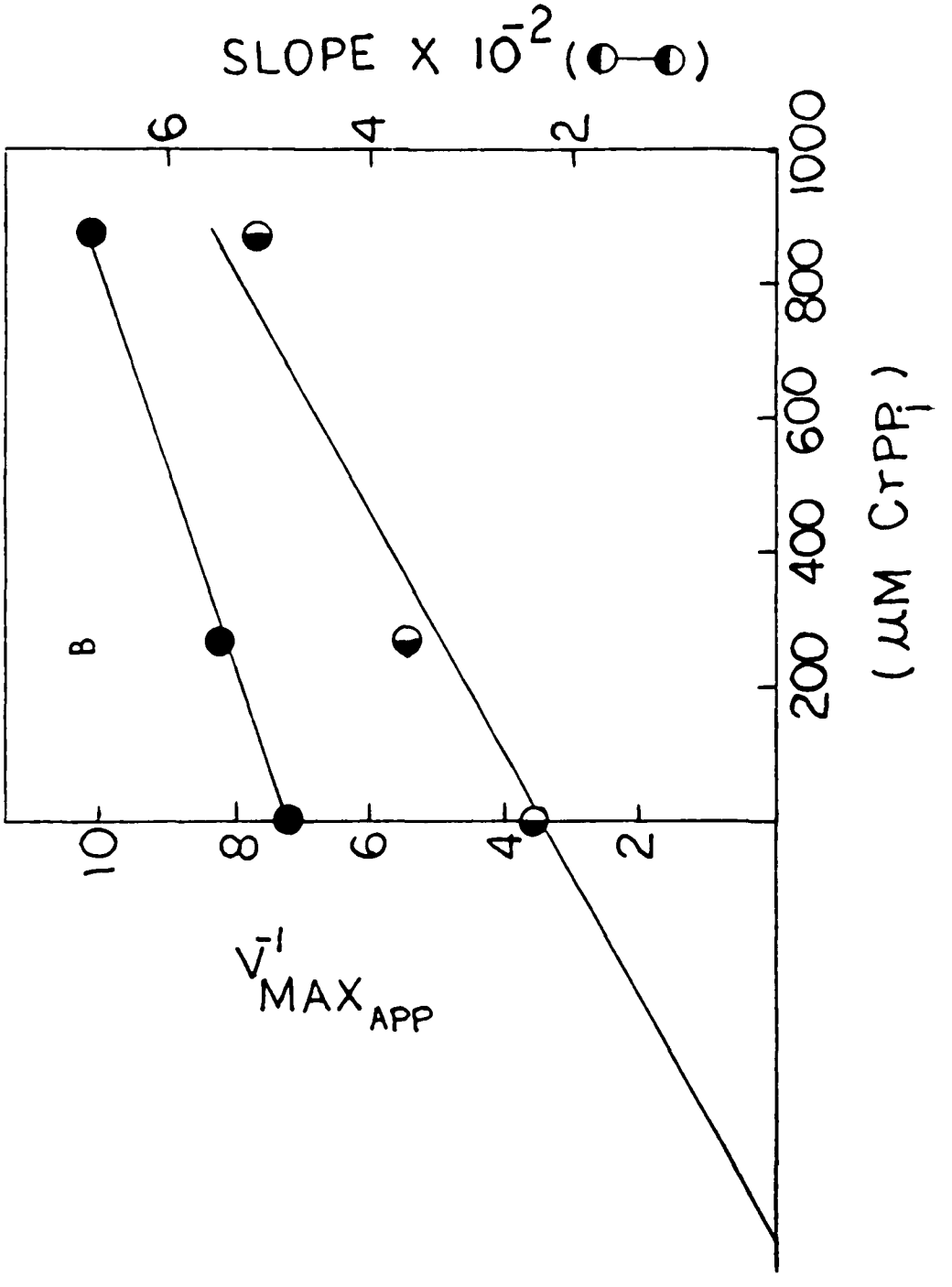
SLOPE X 10^{-2} (●—●)
6
4
2
1000
800
600
400
200
(μM CrPP$_i$)
B
10
8
6
4
2
$V^{-1}_{MAX_{APP}}$

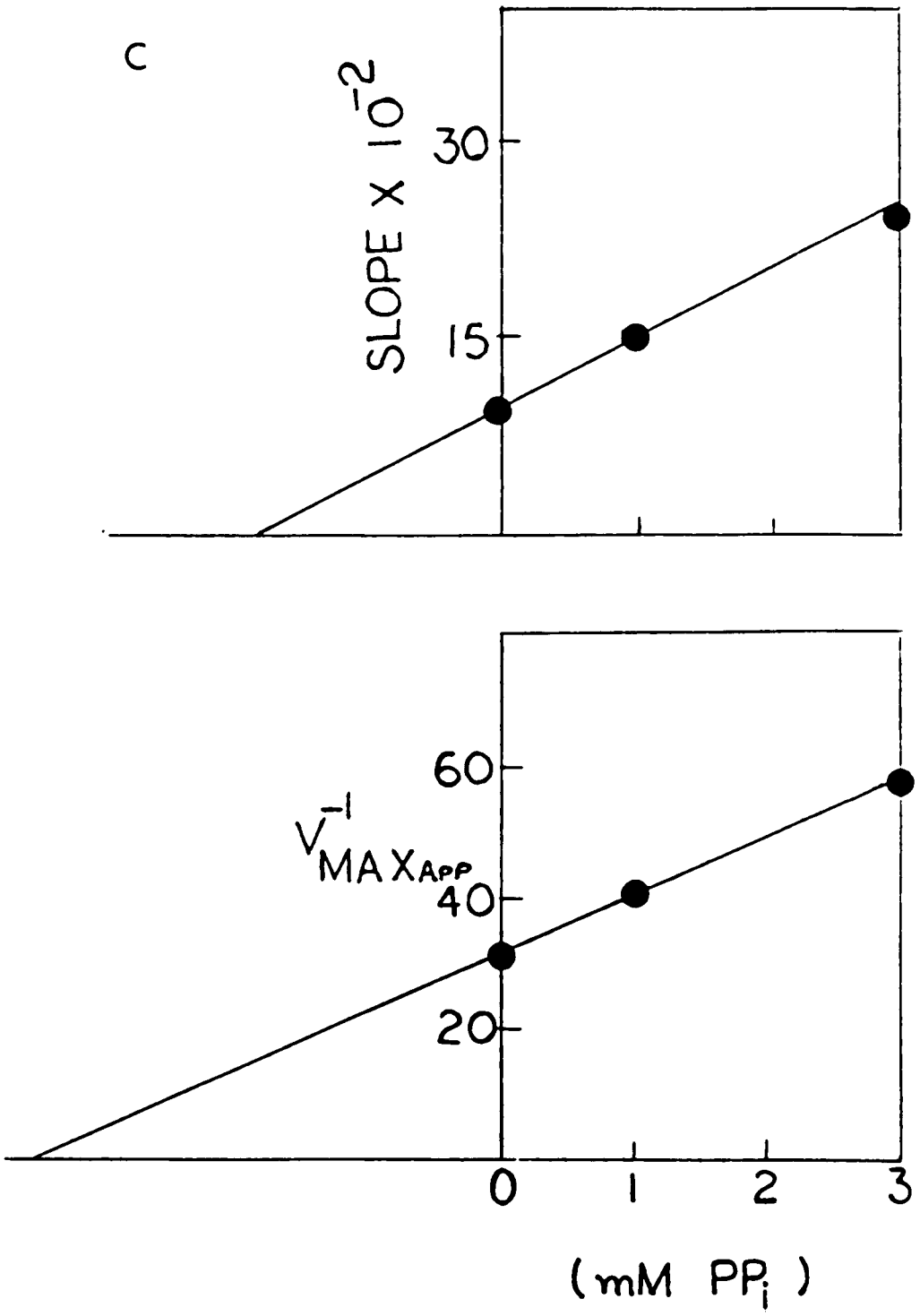
C
SLOPE x 10^{-2}
30
15
$V^{-1}_{MAX_{APP}}$
60
40
20
0
1
2
3
(mM PP_i)

The effect of Na(I)PP_i on the HGPRTase catalyzed forward reaction is shown in Figure 16C. The slopes $\frac{1}{PRibPP}$ and y-intercept values when replotted vs. Na(I)PP_i concentration (up to a limitation value of 3mM) [Figure 17C] yielded a α-value of 1.89 with K_i value of 1.85mM. Cr(III)PP_i as depicted in Figure 16D did not inhibit the HGPRTase forward activity to a significant extent up to 6mM concentration. The pattern generated by the double reciprocal plots of the initial velocities vs. varied concentration of PRibPP at fixed different concentrations of Cr(III)PP_i is of parallel lines indicating whatever little inhibition there is to be uncompetitive.

The reverse pyrophosphorolysis reaction catalyzed by yeast HGPRTase is very unfavorable and could not be successfully characterized by me, and therefore, the effect of Cr(III)PP_i on the reverse reaction of HGPRTase could not be studied.

Attempted Preparation of a Cr(III)PRibPP Complex. As described under Experimental Procedures, the incubation mixture containing PRibPP and chromium chloride was filtered and subjected to Dowex 50W X-2 (H^+ ion form, 100 - 200 mesh) column chromatography. The fractions were checked for ribose and total phosphate contents, along with any inhibitory effect on the OPRTase forward reaction. The fractions with inhibitory effects were pooled and labeled as compound X. Sephadex G-10 chromatography of compound X revealed the new fractions, with this inhibitory effect, to be colorless. Other green-colored fractions were checked for ribose and were found to contain none. These fractions were assumed to be Cr(III)PP_i, since it elutes from Dowex column with the void volume (Merrit, et al., 1981). No further characterization of these green-colored fractions was carried out. The fractions with inhibitory

effect from column G-10 were pooled, concentrated by lyophilization and were subjected to a periodate test. Periodate test were performed because we thought that the inhibitor might be one of the following structures and this test would distinguish them. If compound X would have

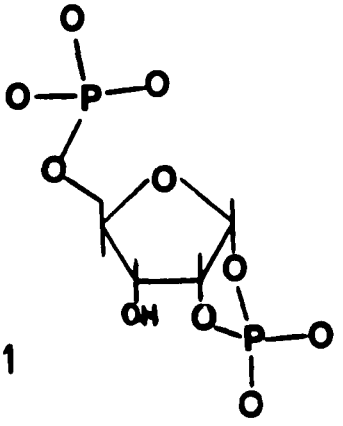

1

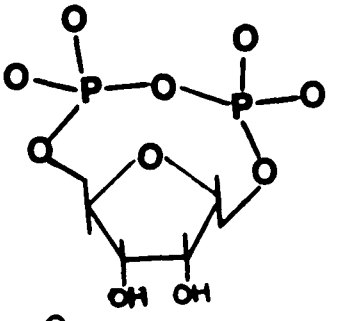

2

structure 1, then it should give a negative periodate test and if compound X was structure 2, then the periodate test would have been positive (Khorana, et al., 1958 and references therein). However, in the second case, a positive result might suggest that phosphoribose is present. Since the periodate test turned out to be strongly positive, we subjected the pooled colorless fractions (no Cr(III) detected) to AG1 X-4 column chromatography and collected 8.0ml fractions. The elution profile is shown in Figure 18. All the fractions were tested for inhibition of OPRTase and then examined for ribose, total phosphate, acid-labile phosphate and inorganic phosphate contents. In this instance, the inhibitory effect was exhibited by the fraction which was negative for both ribose and total phosphate. The repeat check revealed similar results. The Fractions 22-31 which were positive either for ribose and/or phosphate were further characterized by ^{31}P NMR (Figure 19) and for their ribose:PO_4 ratios. The results are tabulated in Table 13. Ribose 1-PO_4, ribose-5'-PO_4 and PRibPP in ammonium formate, pH 5.0,

Figure 18

Elution profile of compound X from AG1 X-4 (formate form) column. The column was equilbrated with 0.1M ammonium formate buffer pH 5.0. Buffer was changed to 0.25M at Fraction 28 and to 0.5M ammonium formate at Fraction 52. Solid circles represent total PO_4 concentration, semi solid circles indicate ribose and open circles identify OPRTase activity.

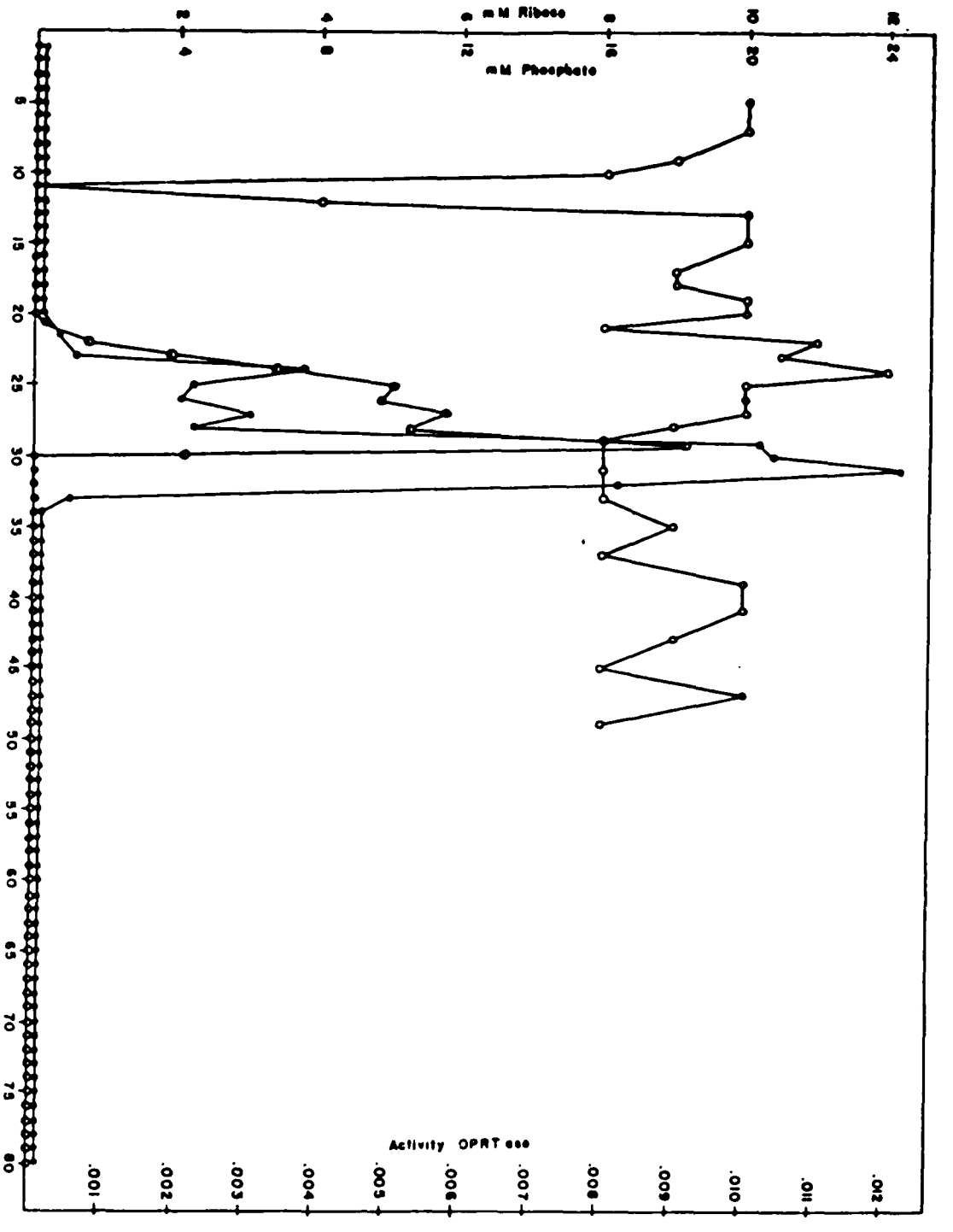
mM Ribose
mM Phosphate
Activity OPRT ase

Figure 19

^{31}P NMR spectra of fractions from AG1 X-4 column. The spectra shown in this figure are those of fractions which were positive for ribose and/or phosphate. 85% orthophosphoric acid in 50% D_2O was used as reference. Ribose-1-phosphate, ribose-5'-PO_4 and PRibPP in 50% D_2O and in ammonium formate buffer pH 5.0 served as standards.

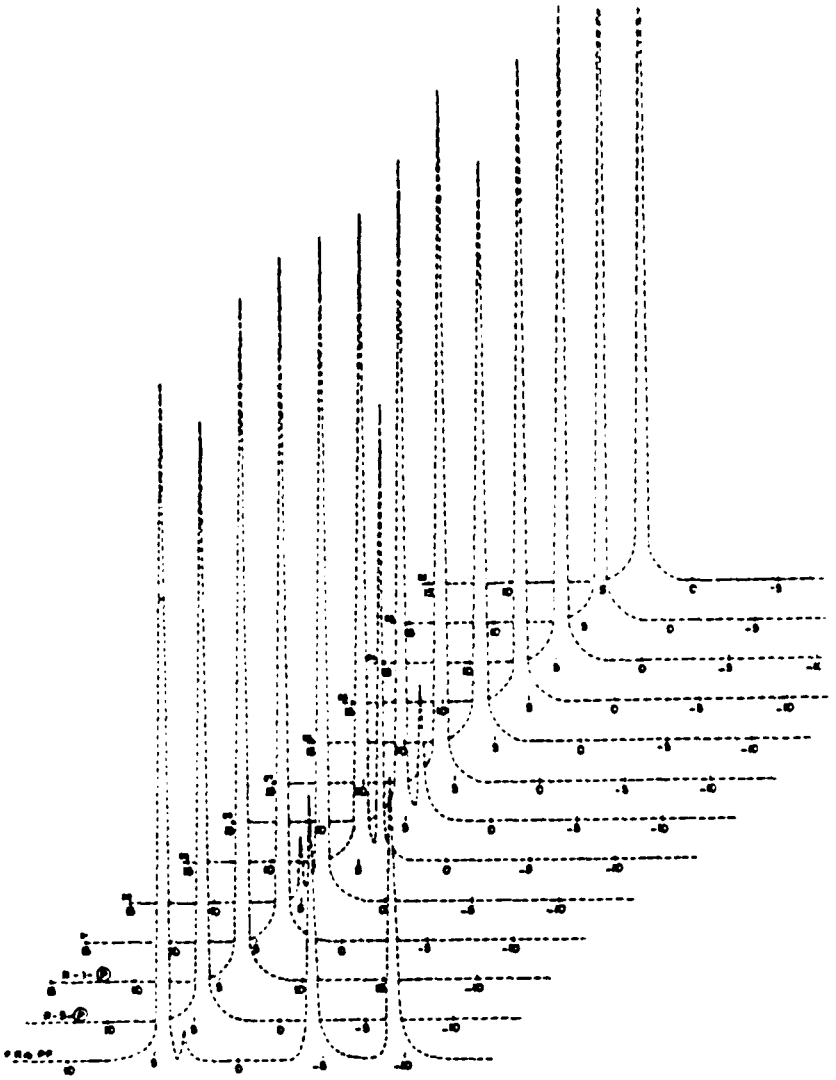

were used as standards for ^{31}P NMR, while 85% H_3PO_4 served as a reference. As shown in Table 13, Fraction #22 is ribose-1-PO_4, Fraction #23 is a mixture of free ribose and ribose-1-PO_4. Fraction #24 exhibited a value of chemical shift that was between that exhibited by ribose-1-P and ribose-5'-PO_4 standards (i.e. 3.55). Since the ratio of ribose to total PO_4 is 1 to 2.3 and because most of the total PO_4 is of an organic nature (non acid hydrolyzable), this fraction was identified as 1, 5 cyclic ribose pyrophosphate, the identification of which was confirmed by a positive periodate test. Fraction #25, 26, and 27 have chemical shifts close to the ribose-5-PO_4 standard. They were identified as ribose-5-PO_4. The absence of significant amounts of acid-labile PO_4 or inorganic PO_4 substantiated this identification. Fraction #28 is mixture of ribose-5-PO_4 and inorganic PO_4. Fraction #29 and 30 are also mixtures of the same, except that the phosphate is present in greater amounts. Since Fraction #31 was negative for ribose but was positive to total phosphate, it was identified as inorganic phosphate. The chemical shift exhibited by this fraction was also used to identify the presence of inorganic PO_4 in Fractions #28-30.

All these products thus identified resemble the alkaline degradation products of PRibPP as reported by Khorana (1958) and Remy, et al., (1955) except that the diphosphate in this case has been identified to be 1-5 ribose cyclic pyrophosphate rather than 1, 5 diphosphate. Our attempt to identify inhibitor compound X from this analysis did not succeed and therefore, it was assumed to be an artifact. A guess was made that cytidine or cytosine might be present since the Dowex column, that I used, had been used previously to purify the arabinoside derivatives of cytosine. When checked for inhibitory effect, both cytidine and cyto-

Table 13: Analysis Summary of Fractions Positive for Ribose or Phosphate or both from AG1 X-4 Chromatography

Fraction #	Ribose (mM)	a*	b**	c***	c - b Acid labile PO_4 (mM)	a-c Organic PO_4 (mM)	Ribose to PO_4 (Total)	^{31}P NMR** ppm
22	0.75	0.75	-	-	-	0.75	1:1	3.22
23	1.95	1.25	-	-	-	1.25	1:0.64	3.3
24	3.3	7.5	-	0.5	0.5	7.0	1:2.3	3.6
25	5.1	4.5	-	-	-	4.5	1:0.88	3.9
26	4.8	4.3	-	0.5	0.5	3.8	1:0.9	4.0
27	5.8	6.3	0.25	0.9	0.65	5.4	1:1.08	4.0
28	5.3	4.5	0.5	1.0	0.5	3.5	1:0.85	3.8 & 2.62
29	9.15	20.5	6.3	8.5	2.2	12.0	1:2.24	3.9 & 2.8
30	2.1	20.8	20.0	20.5	0.5	0.3	1:9.9	4.27 & 2.9
31	-	24.5	21.0	24.5	3.5	-	-	2.9
32	-	16.5	16.5	15.0	-	-	-	-
33	-	1.0	1.25	1.1	-	-	-	-
ribose-1-PO_4***	-	-	-	-	-	-	-	3.2

Table 13 (Continuation)

Fraction #	Ribose (mM)	a*	b**	c***	c-b Acid labile PO_4 (mM)	a-c Organic PO_4 (mM)	Ribose to PO_4 (Total)	^{31}P NMR *+ ppm
ribose-5-PO_4****	-	-	-	-	-	-	-	4.28
PRibPP****	-	-	-	-	-	-	-	4.8 (5)
								-4.8 (β)
								-10.2 (α)

a* = Total PO_4 (mM)

b** = Inorganic PO_4 (mM) c*** = Acid hydrolyzed PO_4 (mM)

*+ ^{31}P Chemical shifts were measured from 85% orthophosphoric acid in 50% D_2O (reference) at 161.8 MHz.

**** The standards used were prepared in 100ml ammonium formate buffer pH 5.0 to provide similar solvent environment.

sine in fact inhibited the OPRTase forward reaction, with cytidine being much more potent than cytosine.

DISCUSSION

Both kinetic and metal activation studies have established that Mg(II) PRibPP is the true substrate in the phosphoribosyl transfer reactions catalyzed by PRTases. Different kinetic mechanisms have been proposed for different PRTases as well as for the same PRTase from different sources. For example, the ping pong mechanism was first proposed by Bell and Koshland (1970) for bacterial ATP phosphoribosyltransferase as a result of their apparent isolation of a labeled enzyme-ribose-5-phosphate intermediate from ^{14}[C] PRibPP. This labeled intermediate was later identified by Parsons and his colleagues (Brashear, et al., 1975) to be an enzyme-product complex and the kinetic mechanism of ATP phosphoribosyltransferase from Salmonella Typhimurium was determined to be Ordered Bi Bi. A ping pong mechanism has been proposed for yeast OPRTase in presence of an optimal concentration of Mg(II) (Victor, et al., 1979). The isotopic exchange studies of Parsons and his colleagues (Goitein, et al., 1978) favored the carbonium ion intermediate as the mechanism by which yeast OPRTase catalyses OMP formation. Similarly in case of HGPRTase, a ping pong mechanism was implicated at first (Ismande, et al., 1961). The source of that HGPRTase activity was red cells. Later studies by Krenitsky and Papaioannou (1969) reconciled all of the data on HGPRTase by proposing that a ping pong mechanism proceeds, when Mg(II) is present at optimal concentration, and that an ordered mechanism proceeds when it is not ($<$ 50uM). Ali and Sloan (1982) proposed an ordered bi bi kinetic mechanism for the yeast HGPRTase catalyzed formation of both IMP and GMP from hypoxanthine and guanine respec-

tively. The different kinetic behavior of various phosphoribosyl transferring enzymes at different divalent metal ion concentrations suggests that more than a single role is played by divalent metal ions in activating these enzymes. Metal activation studies carried out thus far, also have pointed to the fact a 1:1 M(II)-PRibPP complex is the true substrate for these enzymes (Morton and Parsons, 1976; Thompson, et al., 1978; Smithers and O'Sullivan, 1982; Victor, et al., 1979; Ali and Sloan, 1983). Other M(II)-substrate, M(II)-Product and M(II)-E ligations also have been implicated (Victor, et al., 1979; Giacomello and Salerno, 1978; Dodin, et al., 1982). These results suggest that the M(II)-PRibPP complex should be subtly different in its conformation at the active site of different PRTases. This was exactly what we observed when we resolved the conformation of Mn(II)-PRibPP free in solution and when bound to OPRTase and HGPRTase. When Mn(II)-PRibPP is OPRTase bound both the M(II)-to-Proton and M(II)-to-phosphorus distance increase. The model building studies revealed that the 5'-phosphate position may hinder the on-line approach of orotate base at the OPRTase active site. In the case of HGPRTase, however, the 5'-phosphate is positioned away from the ribose in such a manner as to open a path for the on-line approach of base hypoxanthine or guanine. Thus, the resolved conformation of OPRTase bound Mn(II)-PRibPP appears to be consistent with a ping pong mechanism. Here the substrate bound metal upon binding to enzyme is acting to pull the PP_i moiety of PRibPP away. The fact that $Cr(III)PP_i$ is a substrate for the reverse reaction of OPRTase only in the presence of Mg(II) suggested the requirement for a metal ion other than that complexed to PP_i or PRibPP. This requirement for a second divalent metal ion, may thus reflect the need for a second metal to 5-PO_4 binding when

M(II)-PP_i leaves, thus readjusting the pocket to accommodate orotate base. These studies and previous kinetic and metal activation data has led us to propose a mechanism for OPRTase depicted by the transition state in Figure 20 which is consistent with a ping pong kinetic mechanism involving formation of a carbonium ion intermediate. Here Mg(II)-PRibPP binds to the OPRTase active site followed by the release of Mg(PP_i) thereby creating a carbonium ion. The second Mg(II) ion bound to enzyme is positioned to neutralize the newly created negative charge (Figure 20). In the case of HGPRTase, metal-to-phosphorus distances are still suggestive of an interaction between 5'-PO_4 and M(II), however, 5'-PO_4 does not hinder the on-line approach of the base. The metal activation studies of Nagi and Ribet (1977) and those of Ali and Sloan (1983) on yeast HGPRTase have suggested that independent Mg(II) binding to enzyme takes place followed by M(II)-S binding or substrate-M binding. The Cr(III)PP_i did not inhibit the HGPRTase forward activity up to 6mM concentration whereas Mg(II)PP_i did. These results suggested that HGPRTase requires divalent metal ion and that the true substrate in fact is the M(II)-PRibPP. In addition, Cr(III)PP_i may not be allowed to bind at the active site due to steric hindrance. With these findings and the conformation of HGPRTase bound PRibPP elucidated in this study in mind, we propose a mechanism of action for yeast HGPRTase as illustrated by a unique transition state which employs two metal ions (Figure 21) and which is consistent with an ordered bi bi kinetic mechanism as suggested by Ali and Sloan (1982). According to the mechanism M(II)-PRibPP binds to the M-HGPRTase complex, followed by binding of the base. The enzyme bound metal ion may serve to stabilize negative charges of phosphates of PRibPP in conjunction with positively

Figure 20

Proposed transition state for the yeast OPRTase catalyzed reaction.

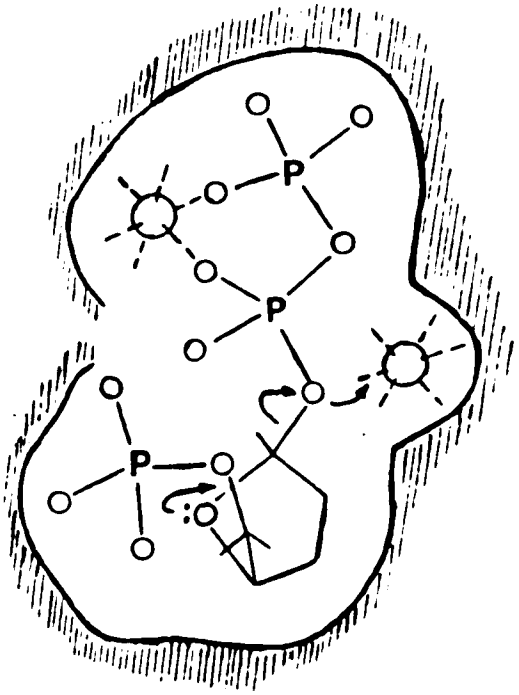
P
P
P

Figure 21

Proposed transition state for the HGPRTase catalyzed reaction.

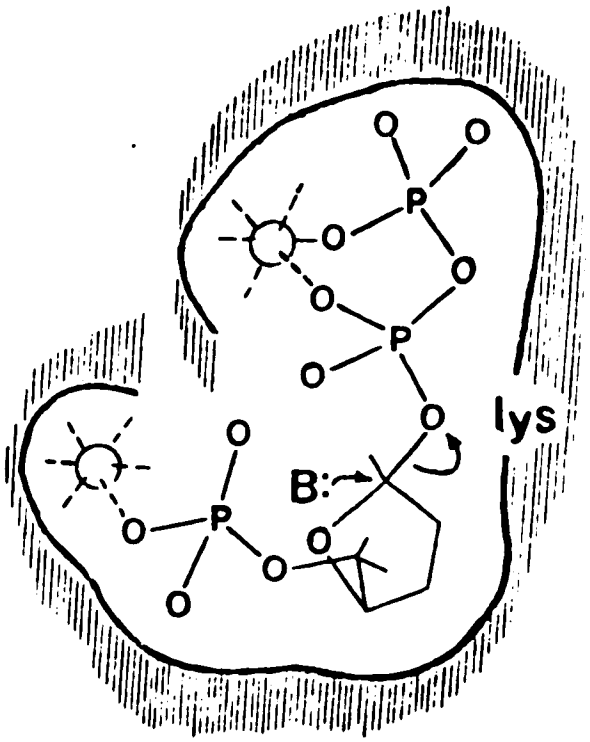
O
O
P
O
O
O
P
O
O
lys
B:
O
P
O
O
O
O

charged amino acids present at the active site. Upon binding of the base, the Mg(II)PP_i leaves followed by IMP release. The mechanism of action proposed here for these two enzymes doesn't exclude other possible mechanisms. However, our present study has revealed surely that the conformation of Mg(II)-PRibPP differs in subtle manners at the active site of these enzymes from the same source which possibly explains why these enzymes differ in their kinetic mechanism. The difference in kinetic mechanism may then dictate the extent of competition for PRibPP among various phosphoribosyl transfer enzyme in vitro as well as in vivo. The present study, therefore, should be extended to other phosphoribosyl transferring enzymes from different sources.

REFERENCES

Ali, L. Z., and Sloan, D. L. (1982) J. Biol. Chem. 257, 1149-1155.

Ali, L. Z., and Sloan, D. L. (1983) Biochemistry 22, 3419-3424.

Altona, C., and Sundaralingam, M. (1973) J. Am. Chem. Soc. 95, 2333-2344.

Ames, B. N., and Dublin, D. T. (1960) J. Biol. Chem. 235, 769-775.

Bagnara, A. S., Letter, A. A., and Henderson, J. F. (1974) Biochim. Biophys. Acta. 374, 259-270.

Bashkin, P., and Sperling, O. (1978) Biochim. Biophys. Acta. 538, 505-511.

Becker, M. A. (1976) Biochim. Biophys. Acta. 435, 132-133.

Becker, M. A. (1976) J. Clin. Invest. 57, 308-318.

Becker, M. A., Raivio, K. O., and Seegmiller, J. E. (1979) Adv. Enzymol. 49, 281-306.

Bell, R. M., and Koshland, D. E., Jr. (1970) Biochem. Biophys. Res. Commun. 38, 539-545..

Berlin, R. D. (1969) Arch. Biochem. Biophys. 134, 120-129.

Blackmore, P. F., and Shuman, E. A. (1982) FEBS lett. 142, 255-259.

Bloch, F. (1946) Phys. Rev. 70, 460-474.

Boer, P., Lipstein, B., de Vries, A., and Sperling, O. (1976) Biochim. Biophys. Acta. 432, 10-17.

Borden, M., Nyhan, W. L., and Bakay, B. (1974) Pediat. Res. 8, 31-36.

Boss, G. R. (1984) J. Biol. Chem. 259, 2936-2941.

Boss, G. R., and Erbe, R. W. (1982) J. Biol. Chem. 257, 4242-4247.

Boss, G. R., and Pilz, R. B. (1985) J. Biol. Chem. 260, 6054-6059.

Brashear, W. T., and Parsons, S. M. (1975) J. Biol. Chem. 250, 6885-6890.

Bressan, R. A., Murray, M. E., Gale, J. M., and Ross, C. W. (1978) Plant Physiol. 61, 442-446.

Brosh, S., Boer, P., Kupfer, B., de Vries, A., and Sperling, O. (1976) J. Clin. Invest. 58, 289-297.

Caskey, C. T., Ashton, D. M., and Wyngaarden, J. B. (1964) J. Biol. Chem. 239, 2570-2579.

Caskey, C. T., and Kruh, G. C. (1979) Cell 16, 1-9.

Chen, P. S. Jr., Toribara, T. Y., and Huber., W. (1965) Anal. Chem. 28, 1756-1758.

Cleland, W. W., Adv. Inorg. Biochem. (1979) 1, 163-190.

Cleland, W. W. (1982) Methods Enzymol. 87, 159-197.

Crowly, G. M. (1964) J. Biol. Chem. 239, 2593-2601.

Delbarre, F., Ausher, C., Amor, B., de Gery, A., Cartier, P., and Hamet, M. (1974) Biomedicine 21, 82.

Dietrich, L. S., Fuller, L., Yero, I. L., and Martinez, L. (1966) J. Biol. Chem. 241, 188-191.

Dodin, G., Lelart, D., and Dubois, J. E. (1982) J. Inorg. Biochem. 16, 201-213.

Dush, M. K., Sikela, J. M., Khan, S. A. and Tischfield, J. A. (1985) Proc. Nat'l. Acad. Sci. U.S.A. 82, 2731-2735.

Eggleston, L. V., and Krebs, N. A. (1974) Biochem. J. 138, 425-435.

Flaks, J. G. (1963) Methods in Enzymol. 6, 144-148.

Foster, A. C., Whetsell, W. O. Jr., Bird, E. D. , and Schwarcz, R. (1985) Brain Research 336, 207-214.

Fox, I. H., and Kelley, W. N. (1971) Ann. Intern. Med. 74, 424-433.

Fox, R. M., Wood, M. H., and O'Sullivan, W. J. (1971) J. Clin. Invest. 50, 1050-1060.

Gershon, S. L., and Fox, I. H., (1974) J. Lab. Clin. Med. 84, 179-186.

Ghangas, G. S., and Milman, G. (1977) Science 196, 1119-1124.

Gholson, R. K., Ueda, I., Ogasawara, N., and Henderson, L. M. (1964) J. Biol. Chem. 239, 1208-1214.

Giacomello, A., and Salerno, C. (1978) J. Biol. Chem. 253, 6038-6044.

Giacomello, A., and Salerno, C. (1979) J. Biol. Chem. 254, 10232-10236.

Goitein, R. K., Chelsky, D., and Parsons, S. M. (1978) J. Biol. Chem. 253, 2963-2971.

Groth, D. P., Young, L. G., and Kenimer, J. G. (1978) Methods Enzymol. 51, 574-580.

Hagen, C. (1973) Biochim. Biophys. Acta, 293, 105-110.

Hanna, L. S., Hess, S. L., and Sloan, D. L. (1983) J. Biol. Chem. 258, 9745-9754.

Hartman, S. C. (1963) J. Biol. Chem. 238, 3024-3035.

Hartman, S. C. (1963) J. Biol. Chem. 238, 3036-3047.

Henderson, E. J., Zalkin, H., and Hwang, L. A., (1970) J. Biol. Chem. 245, 1424-1431.

Henderson, J. F., Brox, L. W., Kelley, W. N., Rosenbloom, F. M., and Seegmiller, J. E. (1968) J. Biol. Chem. 243, 2514-2522.

Hill, D. L. (1970) Biochem. Pharmacol. 19, 545-557.

Hochstadt, J. (1978) Methods Enzymol. 51, 549-558.

Hochstadt, J., and Stadtman, E. R. (1971) J. Biol. Chem. 245, 5294-5303.

Hoffman, D. H., and Sweeney, M. J. (1973) Canc. Res. 33, 1109-1112.

Holden, J. A., and Kelley, W. N. (1978) J. Biol. Chem. 253, 4459-4463.

Hughes, S. H., Wahl, G. M., and Capecchi, M. R. (1975) J. Biol. Chem. 250, 120-126.

Hunt, J. P., Plane, R. A. (1954) J. Am. Chem. Soc. 76, 5960

Ismande, J., Handler, P. (1961) J. Biol. Chem. 236, 525-530.

Ismande, J., Handler, P. (1961) in The Enzymes Vol. 5, 2nd ed. (P. D. Boyer, Editor) 281-304, Academic Press, New York.

Iwai, K., Shibata, K., and Taguchi, H. (1979) Agric. Biol. Chem. 43, 351-355.

Kameda, A. Nihon Univ. J. Med. (1975) 17, 127.

Kaneti, J., Golovinsky, E., Yukhnovsky, I., and Genechev, D. (1970) J. Theor. Biol. 26, 19-27.

Kavipurapu, P. R., and Jones, M. E. (1976) J. Biol. Chem. 251, 5589-5599.

Kelley, W. N., Fox, I. H., and Wyngaarden, J. B. (1970) Biochim. Biophys. Acta. 215, 512-516.

Khorana, G. H., Fernandez, J. F., and Kornberg, A. (1958) J. Biol. Chem. 230, 941-948.

Korn, E. D., Remy, C. N., and Wasiteyko, H. C. (1955) J. Biol. Chem. 217, 875-883.

Kornberg, A., Lieberman, I., and Simms, E. S. (1955a) J. Biol. Chem. 215, 389-402.

Kornberg, A., Lieberman, I., and Simms, E. S. (1955b) J. Biol. Chem. 215, 417-427.

Kosaka, A., Spivey, H. O., and Gholson, R. K. (1977) Arch. Biochem. Biophys. 179, 334-341.

Kowalewski, J., Levy, G. C., Johnson, L. F., and Palmer, L. (1977) J. of Mag. Res. 26, 533-536.

Krenitsky, T. A., and Papaioannou, R. (1969) J. Biol. Chem. 244, 1271-1277.

Krenitsky, T. A., Papaioannou, R., and Ellion, G. B. (1969) J. Biol. Chem. 244, 1263-1270.

Largen, M., and Belser, W. L. (1975) J. Bact. 121, 239-249.

Lesch, M., and Nyhan, W. L. (1964) Am. J. Med. 36, 561-570.

Lin, L. H., Lan, S. J., Richardson, A. H., and Henderson, L. M. (1972) J. Biol. Chem. 247, 8016-8022.

Malayappa, J., Shoemaker, J. D., Horowitz, G. D., Lowry, S. F., and Brennan, M. F. (1985) Metabolism, 34, 325-329.

Mann, D. F., and Byerrum, R. U. (1974) J. Biol. Chem. 249, 6817-6823.

Mantsälä, P., and Zalkin, H. (1984) J. Biol. Chem. 259, 8478. 8484.

McClard, R. W., Black, M. J., Livingston, L. R. and Jones, M. E. (1980) Biochemistry 19, 4699-4706.

Mildvan, A. S. (1974) Ann. Rev. Biochem. 43, 357-399.

Mildvan, A. S., and Cohn, M. (1966) J. Biol. Chem. 241, 1178-1193.

Mildvan, A. S., and Cohn, M. (1970) Adv. Enz. 33, 1-70.

Mildvan, A. S., and Engle, J. (1972) Methods Enzymol. 26, 654-682.

Mildvan, A. S., Grisham, C. M. (1974) Structure and Bonding 20, 1-21.

Mildvan, A. S., and Gupta, R. K. (1978) Methods Enzymol. 49, 322-359.

Mildvan, A. S., Leigh, J. S. Jr., and Cohn, M. (1967) Biochemistry 6, 1805-1818.

Mildvan, A. S., Nowak, T., and Fung, C. H. (1973) Ann. N.Y. Acad. Sci. 2222, 192-210.

Mildvan, A. S., Sloan, D. L., Fung, C. H., Gupta, K. R., and Melamud, E. (1976) J. Biol. Chem. 251, 2431-2434.

Miller, R. L., Adamczyk, D. L., Fyfe, J. A., and Elion, G. B. (1974) Arch. Biochem Biophys. 165, 349-358.

Mills, G. C., Schmalsteig, F. C., Newkirk, K. E., and Goldblum, R. M. (1979) Clin. Chem. 25, 419-424.

Morton, D. P., and Parsons, S. M. (1976) Arch. Biochem. Biophys. 175, 677-686.

Musick, W. D. L. (1981) CRC Crit. Rev. Biochem. 11, 1-34.

Nagy, M., and Ribet, A. M. Eur. J. Biochem. (1977) 77, 77-85.

Niedel, J., and Dietrich, L. S. (1973) J. Biol. Chem. 248, 3500-3505.

Nishizuka, Y., and Hayaishi, O. (1963) J. Biol. Chem. 238, 3369-3377.

Nowak, T., and Mildvan, A. S. (1972) Biochemistry 11, 2819-2828.

Olsen, A. S., and Milman, G. (1974) J. Biol. Chem. 249, 4030-4037.

Olsen, A. S., and Milman, G. (1978) Methods Enzymol. 51, 543-549.

Packman, P. M., and Jakoby, W. B. (1967) J. Biol. Chem. 242, 2075-2079.

Peterson, L. R., and Gupta, K. R. (1979) Biophys. J. 27, 1-14.

Pilz, R. B., Willis, R. C., and Boss, G. R. (1984) J. Biol. Chem. 259, 2927-2935.

Postmas, C., and King, E. (1955) J. Phys. Chem. 59, 1208-1216.

Preiss, J., and Handler, P. (1958) J. Biol. Chem. 233, 493-500.

Raivio, K. O., Lazar, C. S., Krumholz, H. R., and Becker, M. A. (1981) Biochim. Biophys. Acta. 678, 51-57.

Reem, G. H. (1974) J. Biol. Chem. 249, 1696-1703.

Remy, C. N., Remy, W. T., and Buchanan, J. M. (1955) J. Biol. Chem. 217, 885-895.

Richardson, K. K., Fostel, J., and Skopek, T. (1983) Nucleic Acid Research 11, 8809-8816.

Rowe, P. B., and Wyngaarden, J. B. (1968) J. Biol. Chem. 243, 6373-6383.

Satyanarayana, T., and Kaplan, J. G. (1971) Arch. Biochem. Biphys. 142, 40-47.

Schmidt, R., Weigand, H., and Reichert, U. (1979) Eur. J. Biochem. 93, 355-361.

Schultz, G. E. , and Schirmer, R. H. (1974) Nature 250, 142-144.

Seegmiller, J. E. (1976) Adv. Hum. Gen. 6, 75-163.

Seegmiller, J. E., Rosenbloom, F. M., and Kelley, W. N. (1967) Science, 155, 1682-1684.

Segel, I. H. (1975) in Enzyme Kinetics, John Wiley and Sons, pub. New York, 172-174.

Shuster, L., and Abraham, G. (1959) J. Biol. Chem. 234, 129-133.

Slater, J. P., Mildvan, A. S., and Loeb, L. A. (1971) Biochem. Biophys. Res. Comm. 44, 37-43.

Sloan, D. L., and Mildvan, A. S. (1974) Biochemistry, 13, 1711-1718.

Sloan, D. L., and Mildvan, A. S. (1976) J. Biol. Chem. 251, 2412-2420.

Smith L. H., Huguley, C. M., and Bain, J. A. (1972) in The Metabolic Basis for Inherited Disease, 3rd edition (Stanbury, J. B., Wyngaarden, J. B., and Fredrickson, D. S., editors) 1003, Mc Graw Hill, Publ; New York.

Smithers, G. W., and O'Sullivan, W. J. (1979) J. Appl. Biochem. 1, 344-353.

Smithers, G. W., and O'Sullivan, W. J. (1982) J. Biol. Chem. 257, 6164-6170.

Solomon, I. (1955) Phys. Rev. 99, 559-565.

Steyn, L. M., and Harley, E. H. (1984) J. Biol. Chem. 259, 338-342.

Tebar, A. R., Leyva, J. C., Laynez, J., and Ballesteres, A. (1978) Revista Espanola De Fisiologia, 34, 159.

Thomas, C. B., Arnold, W. J., and Kelley, W. N. (1973) J. Biol. Chem. 248, 2529-2535.

Thompson, R. E., Li, E. L., Spivey, H. O., Chandler, J. P., Katz, A. J., and Appleman, J. R. (1978) Bio. Inorg. Chem. 9, 35-45.

Tinkham, M., Weinstein, R., and Kip, A. F. (1951) Phys. Rev. 84, 848-849.

Umezu, K., Amaya, T., Yashimoto, A., and Tomita, K. (1971) J. Biol. Chem. (Tokyo) 70, 249-269.

Van Ackar, K. J., Simmonds, H. A., Potter, C., and Cameron, S. J. (1977) N. Eng. J. Med. 297, 127-132.

Victor, J., Greenberg, L., and Sloan, D. L. (1979a) J. Biol. Chem. 254, 2647-1655.

Victor, J., Leo-Mensah, A., and Sloan, D. L. (1979b) Biochemistry 18, 3597-3604.

Wegman, J., and De Moss, J. A. (1965) J. Biol. Chem. 240, 3781-3788.

Whitfield, Jr. H. A. (1971) J. Biol. Chem. 246, 899-908.

Wild, J. R., and Belser, W. L. (1977) Biochem. Genet. 15, 157-171.

Willis, R. C., Jolly, D. J., Miller, D. A., Plent, M. M., Esty, A. C., Anderson, P. J., Chang, H. C., Jones, O. W., Seegmiller, E. J., and Friedman, T. (1984) J. Biol. Chem. 259, 7842-7849.

Wilson, J. M., Baugher, B. W., Landa, L., and Kelley, W. N. (1981) J. Biol. Chem. 256, 10306-10312.

Wilson, J. M., Baugher, B. W., Mattes, P. M., Daddona, P. E., and Kelley, W. N. (1982) J. Clin. Invest. 69, 706-715.

Wood, M. H., ano O'Sullivan, W. J. (1973) Am. J. Obst. and Gyn. 116, 57-61.

Worthy, T. E., Grobner, W., and Kelley, W. N. (1974) Proc. Nat'l. Acad. Sci. U. S. 71, 3031-3035.

Yeh, G. C., and Phang, J. M. (1983) J. Biol. Chem. 258, 9774-9779.

Yen, R. C. K., Adams, W. B., Lazar, C., and Becker, M. A. (1978) Proc. Nat'l. Acad. Sci. U.S.A. 75, 482-485.

Zubay, G. (1983) in "Biochemistry", Addison-Wesley Pub. New York, 283.

Luz, Z., and Meiboom, S. (1964) J. Chem. Phys. 40, 2686-2692.